DOE/ER/53225--T6

DE93 002531

TASK IIIA: PROGRESS REPORT

Far Infrared Fusion Plasma Diagnostics

FY 1990

Principal Investigator:
N.C. Luhmann, Jr.

Co-Principal Investigator:
W.A. Peebles

SECTION I. PROGRESS REPORT FY90

Task IIIA

I. INTRODUCTION

Over the last several years, reflectometry has grown in importance as a diagnostic for both steady-state density profiles as well as for the investigation of density fluctuations and turbulence. As a diagnostic for density profile measurement, it is generally believed to be well understood in the tokamak environment. However, its use as a fluctuation diagnostic is hampered by a lack of quantitative experimental understanding of its wavenumber sensitivity and spatial resolution. Several researchers[1,2], have theoretically investigated these questions. However, prior to the UCLA laboratory investigation, no group has experimentally investigated these questions. Because of the reflectometer's importance to the world effort in understanding plasma turbulence and transport, UCLA has, over the last year, made its primary Task IIIA effort the resolution of these questions. UCLA has taken the lead in a quantitative experimental understanding of reflectometer data as applied to the measurement of density fluctuations.

In addition to this, work has proceeded on the design, construction, and installation of a reflectometer system on UCLA's CCT tokamak. This effort will allow a comparison between the improved confinement regimes (H-mode) observed on both the DIII-D and CCT machines with the goal of achieving a physics understanding of the phenomena.

Preliminary investigation of a new diagnostic technique to measure density profiles as a function of time has been initiated at UCLA. The technique promises to be a valuable addition to the range of available plasma diagnostics. Work on advanced holographic reflectometry techniques as applied to fluctuation diagnostics has awaited a better understanding of the reflectometer signal itself as discussed above. Technological development work on the necessary sources, detectors, arrays, etc. has proceeded as described in Task IIIB. Efforts to ensure the transfer of the diagnostic developments have continued with particular attention devoted to the preliminary design of a multichannel FIR interferometer for MST.

II. INTERPRETATION OF REFLECTOMETRY

Reflectometry is currently being used to investigate density fluctuations and turbulence in tokamak plasmas (as well as to determine density profiles). However, there are unresolved questions about the spatial resolution and wavenumber sensitivity of this diagnostic which impact the interpretation of the data. Given the growing world wide usage of this diagnostic (JET, DIII-D, TFTR, TEXTOR, ASDEX, etc.) it is vital to provide an unambiguous interpretation of the measurements. This will be of even more importance in the future since this will be an essential diagnostic in devices such as CIT and ITER. These questions are currently being addressed at UCLA using a cylindrical, pulsed filament discharge plasma where ion acoustic waves, launched into the unmagnetized plasma, are studied with a reflectometer system.

An overview of the program results to date are:

1) Experimental apparatus. A cylindrical, pulsed filament discharge plasma device (see Fig. 1) has been configured to study the ion acoustic wave–reflectometer interaction. The device is 88 cm long and 60 cm in diameter and produces a magnetic-field free argon plasma. A typical plasma discharge lasts for 2 msec with a 6 Hz repetition rate, reaching peak densities and electron temperatures of $\sim 3 \times 10^{17}\mathrm{m}^{-3}$ and $\sim$2 eV, respectively. Microwave radiation is launched from the bottom of the chamber with the single horn acting as both launch and receive antennas. The plasma device has good accessibility and is well diagnosed by Langmuir and resonance probes. Two directions of ion acoustic wave launch are available: parallel and perpendicular to the direction of microwave propagation (Fig. 1: grids 1 and 2 respectively). Figure 2(a) shows signals from the reflectometer system and from a Langmuir probe, biased into electron saturation current, for a typical plasma discharge. The Langmuir probe signal first increases as the plasma discharge begins, attains a steady state period of $\sim$1 msec length, then decays as the plasma dies. The reflectometer signal initially acts as an interferometer, passing through several 2π phase changes, until the cutoff density is reached, at which time the signal shows a d.c. response. As the plasma dies away, the initial phase shifts are repeated. Note that an ion acoustic wave was launched at approximately 1520 μsec into the discharge and can be seen on the reflectometer at approximately that time (small blip in reflectometer signal in Fig. 2(a)).

2) The delay between the time of the ion acoustic wave launch and the received reflectometer signal was consistent with the wave propagating down the density gradient at the ion acoustic velocity, $v_s = \sqrt{k_B T_e / m_i}$. Figure 2(b) is a time expansion of Fig. 2(a) showing the reflectometer signal and the launch voltage for the ion acoustic wave. A delay of approximately 50 μsec between the launch time and the perturbation in the reflectometer signal is seen indicating that the ion acoustic wave traveled $\sim$10 cm (for these conditions $v_s \simeq 2 \times 10^5$ cm/sec) before affecting the reflectometer. Figure 2(c) is from a similar discharge but with a lower microwave frequency f_0, thus placing the cutoff region further away from the ion wave launch grid. Consistent with this, the delay time increased from $\sim$50 to $\sim$100 μsec. This is in qualitative agreement with a movement of the critical layer away from the launch grid as f_0 was decreased. The received signal was also found to have the same frequency and number of cycles as the launched wave (see Figs. 2(b-c)). These observations indicated that the signal was highly localized in space. Further evidence of this was obtained by positioning a Langmuir probe such that the perturbation due to the ion wave occurred at the same time as that on the reflectometer. This also conclusively determined the physical position of the reflectometer signal within the plasma. The density profile was obtained using a microwave resonance probe which allowed a determination of the position of the critical density layer. Initial results showed that the reflectometer signal originates before the critical density layer for the microwave frequency used. This is an unexpected result and may be due to errors in the density profile measurement. Work is underway to install an interferometer in order to independently measure the density. Other possible explanations are diffraction and refraction of the microwave beam. This result is very much an area of current research.

3) Ion acoustic waves were also launched perpendicular to the injected microwave beam. The response of the reflectometer depended sensitively on the wavenumber k_{ion} of the ion wave, with the response decreasing as k_{ion} increased (see Fig. 3). This is in qualitative agreement with the picture of the microwave beam being scattered by

the ion wave but can also be explained on the basis of a movement of a density layer (caused by the ion acoustic wave) along with finite reflectometer beam size. A more detailed study of this phenomenon in conjunction with a 2-D numerical code is planned.

4) Initial results from a one dimensional numerical simulation of the reflectometer system were obtained. The code predicts the phase changes induced in the microwave signal by an ion acoustic wave in the plasma. As the code accepts arbitrary plasma density profiles, a large range of parameters, from the laboratory plasma to the DIII-D tokamak, are possible. The magnitude of the phase change was predicted (by the code) to decrease rapidly as k_{ion} increased above $2k_0$, in qualitative agreement with the result expected from a wave scattering picture. Here, k_0 is the vacuum wavenumber of the reflectometer system. Experimentally, the reflectometer response was found to be in qualitative agreement with the code prediction of a diminishing (but nonzero) response for $k_{ion} \succ 2k_0$. A quantitative investigation of this observation is currently underway.

During the coming year, we plan to continue the above investigations as well as initiate the following:

1) By adding another power supply and new filaments, higher plasma densities and density gradients can be obtained. This will allow a study of the gradient sensitivity of the reflectometer and its comparison to theoretical predications.

2) A microwave interferometer to accurately measure the plasma density will be installed.

3) The reflectometer signal depends on both the phase of the returned beam as well as its amplitude. The relative influence of these two effects has not yet been determined. Initially, using a quadrature detector and, subsequently, full heterodyne detection, the dependence on these quantities can be studied in a controlled laboratory experiment.

4) A numerical code is under development at UCLA in conjunction with E.A. Williams of LLNL. Currently, the code is one dimensional and predicts the phase change in the reflectometer signal due to an ion plasma wave with an arbitrary density profile. A quantitative comparison between the laboratory experiment and the numerical calculation will be made. Since the ion acoustic waves are more heavily damped at higher frequencies, the amplitude of the ion wave will be monitored by placing a Langmuir probe in the interaction region. The ion acoustic wave launch voltage will then be adjusted so as to maintain a constant amplitude in that region. Efforts are also underway to expand the code to two dimensions and to include diffraction and refraction effects.

5) Eventually, the laboratory plasma measurements can be extended to include turbulent waves by using a noise excitation source.

6) Comparison between the laboratory plasma and the turbulent plasma of the CCT tokamak at UCLA will begin this summer. This will allow a unique comparison between two very different regimes.

II. CCT

By injecting a radial electric current, the CCT tokamak (Dr. R.J. Taylor, Director) at UCLA achieves an improved confinement regime similar in all measured parameters to the H-mode seen on larger tokamaks around the world. Work is underway to install a reflectometer system on CCT in order to study this H-mode regime and compare to similar regimes on the DIII-D tokamak. The UCLA group is in a unique position to make this comparison since it operates reflectometer systems on both machines. Evidence from DIII-D suggests that the turbulently induced transport is reduced at the L to H-mode transition, possibly due to shear stabilization of the turbulence. Is this the cause or is there another route to improved confinement (H-mode) as may be the case on CCT? If turbulence suppression is the cause of improved confinement, what is it due to and what are its properties (eg. width of suppression region, dependence on parameters, differences between CCT and DIII-D, etc.)? Correlation between the reflectometer signal and Langmuir probes is also planned.

A port/window assembly has been constructed that allows a simultaneous microwave launch and Langmuir probe insertion. A homodyne reflectometer system, utilizing a single antenna for launch and receive, has been designed and tested in the laboratory. Initially, a frequency range of 8 to 12 GHz will be used which will cover the outside edge of the torus, including the H-mode confinement region. A higher frequency range (12-18 GHz) will also be available for future use. A stand-alone data acquisition system, including digitizers and computerized data acquisition and data analysis capability, is under construction. A Langmuir probe system, consisting of probes, probe drive, and the necessary biasing and amplifier electronics, is also being fabricated. It is planned that the reflectometer system will be operational by the end of summer 1990. Both O and X-mode launch will be possible and a detailed comparison of the two types of operation is planned. Finally, the knowledge gained on the laboratory plasma will be used to complement and compare with the turbulent tokamak plasma.

III. ADVANCED REFLECTOMETRY

How do the tokamak density profiles evolve during the L to H-mode transition? How are the density gradients related to the fluctuation levels and to the occurrence of ELM's? Are there modifications to the profiles during periods of high MHD activity? The density profiles also impact the interpretation of the fluctuating reflectometer signal during the L to H-mode transition as well as at other times (during ELM's, Ohmic, L and H-mode away from transition, etc.). There is, therefore, a large amount of interest in knowing the tokamak density profile as a function of time.

At UCLA, we have conceived of a new technique which may make it possible to determine the edge density profile continuously as a function of time. A preliminary study of this method has been initiated at UCLA in conjunction with the UCLA team at DIII-D. It utilizes reflectometer equipment already existing on the DIII-D tokamak. The technique consists of using X-mode system to determine the profiles at several fixed times during the discharge. The O-mode system is then used to interpolate continuously between them, using the X-mode profiles as benchmarks. The method depends on correct alignment of the O-mode system so as to give the low frequency phase shifts associated with the density profile

development. Data have been obtained from the DIII-D reflectometer system, as illustrated in Fig. 4, showing an example of such low frequency phase shifts. A remote controlled mirror is being installed during the machine down time, June-August 1990, which will facilitate this procedure. The required software is currently under development and a preliminary study of the method will be carried out early in the next DIII-D run period.

IV. DIAGNOSTIC SYSTEM AND TECHNOLOGY, DISSEMINATION

We continued our efforts at disseminating the results of our diagnostic system and technology developments to the fusion community. A planning design for an interferometer system for the Wisconsin MST device was produced. Preliminary discussions for possible reflectometers systems for both TFTR and LSX were held. Continued support was provided to MTX in the form of maintaining the corner cube detectors for the 185 μm FIR multichannel interferometer.

Figures 5 and 6 illustrate the proposed experimental arrangement for the MST multichannel FIR interferometer which would jointly be constructed and operated by UCLA and Wisconsin. The support structure and optical system are indicated in Fig. 5. In order to maximize the number of interferometer channels and not create problems with distortion in wall currents, the channels are interleaved toroidally. Optics are therefore mounted on the two sides of a wedged optical table (see Fig. 5) providing a maximum of 11 radially viewing channels. The small spatial offset toroidally is not expected to cause difficulties in interpretation and analysis of data. The location and size of the ports were chosen to coincide with the existing pattern of pumping duct holes in the MST device. In this manner, distortion of wall currents are known to be small from earlier calculations.

A CO_2 pumped, twin frequency FIR laser will be used as the radiation source for the interferometer. A suitable location has been identified close to the device (see Fig. 6). Removable overmoded dielectric waveguide will be used to transport the laser radiation to the optical tables mounted in a vertical plane close to the machine. The UCLA developed laser is capable of operation at a variety of wavelengths. Typical high power lines suitable for interferometry are 118, 185, 398, 432, 743, 985, and 1222 μm. This wavelength range ensures that the interferometry system on MST can be fully optimized for a variety of operating conditions. Calculations of the line integrated phase shifts suggest that a wavelength of $\simeq 500\mu m$ will be suitable for typical plasma conditions existing in MST.

The receiver system will consist of corner cube, quasi-optical Schottky diode mixers designed for optimal operation at $\simeq 500\ \mu m$. These mixers operate at room temperature, are relatively broadband and possess ample sensitivity for use at both longer (1222 μm) and shorter wavelengths (185 μm). A reference IF signal together with the above signals are sent to electronic phase comparators which determine the necessary line integrated phase shifts experienced by the various channels. Standard Abel inversion is then applied to deduce the actual density profile.

Finally, it should be noted that the above system can also be configured in the future to perform Faraday rotation or collective scattering measurements. This would allow important information on the internal magnetic field to be obtained, as well as internal fluctuation data. Interpretation and inversion of the Faraday rotation data represents the greatest challenge for these measurements. UCLA is currently investigating Faraday rotation at the University of Texas (see Task IIIB progress) and the experience gained there will be important when the same diagnostic approach is pursued on MST. Collective scattering

will be limited by port access. Probably the best approach will be to operate at short wavelengths ($< 500\ \mu m$) so that each port will be able to view a larger range of fluctuation wavenumbers. This will also allow correlation of high order MHD activity as well as permitting some degree of spatial resolution along the incident beam.

REFERENCES

1. M.L.V. Pitteway, Proc. R. Soc. 254, (1959) p. 86.

2. J.P. Garcia, et al., 16th European Conference on Controlled Fusion and Plasma Physics, Venezia, 1521 (1989).

TASK IIIA PUBLICATIONS AND PRESENTATIONS FY90

S. Baang, C. Domier, N.C. Luhmann, Jr., W.A. Peebles, T.L. Rhodes, "Spatial Resolution of Microwave/Millimeter Wave Reflectometry," to be published, Review of Scientific Instruments, Oct. 1990.

S Baang, C. Domier, W.A. Peebles, N.C. Luhmann, Jr., "Determination of the Wavenumber Sensitivity and Spatial Resolution of Microwave/Millimeter Wave Reflectometry," 31st Annual APS Meeting Division of Plasma Physics, Anaheim, CA, Nov. 13-17, 1989.

S. Baang, A.E. Chou, C.W. Domier, N.C. Luhmann, Jr., W.A. Peebles, P. Pribyl, T.L. Rhodes, R.J. Taylor, E.A. Williams, CCT Group "Wavenumber Sensitivity and Spatial Resolution of Millimeter Wave Reflectometry," 8th Topical Conf. on High Temperature Plasma Diagnostics, Hyannis, MA, May 6-10, 1990.

S. Baang, A.E. Chou, C.W. Domier, N.C. Luhmann, Jr., W.A. Peebles, P. Pribyl, T.L. Rhodes, R.J. Taylor, E.A. Williams, CCT Group "Wavenumber Sensitivity and Spatial Resolution of Microwave/Millimeter Wave Reflectometry," 17th EPS Conference on Controlled Fusion and Plasma Heating, Amsterdam, The Netherlands, June 25-29, 1990.

S.R. Burns, S. Baang, E.J. Doyle, N.C. Luhmann, Jr., W.A. Peebles, P. Pribyl, T.L. Rhodes, R.J. Taylor, CCT Group "Initial Reflectometer Measurements of Density Fluctuations on the CCT Tokamak," 32nd Annual APS Meeting Division of Plasma Physics, Cinncinati, Ohio, November 12-16, 1990.

S. Baang, A.E. Chou, C.W. Domier, N.C. Luhmann, Jr., W.A. Peebles, T.L. Rhodes, E.A. Williams, "Spatial Resolution of Microwave/Millimeter Wave Reflectometry," 32nd Annual APS Meeting Division of Plasma Physics, Cinncinati, Ohio, November 12-16, 1990.

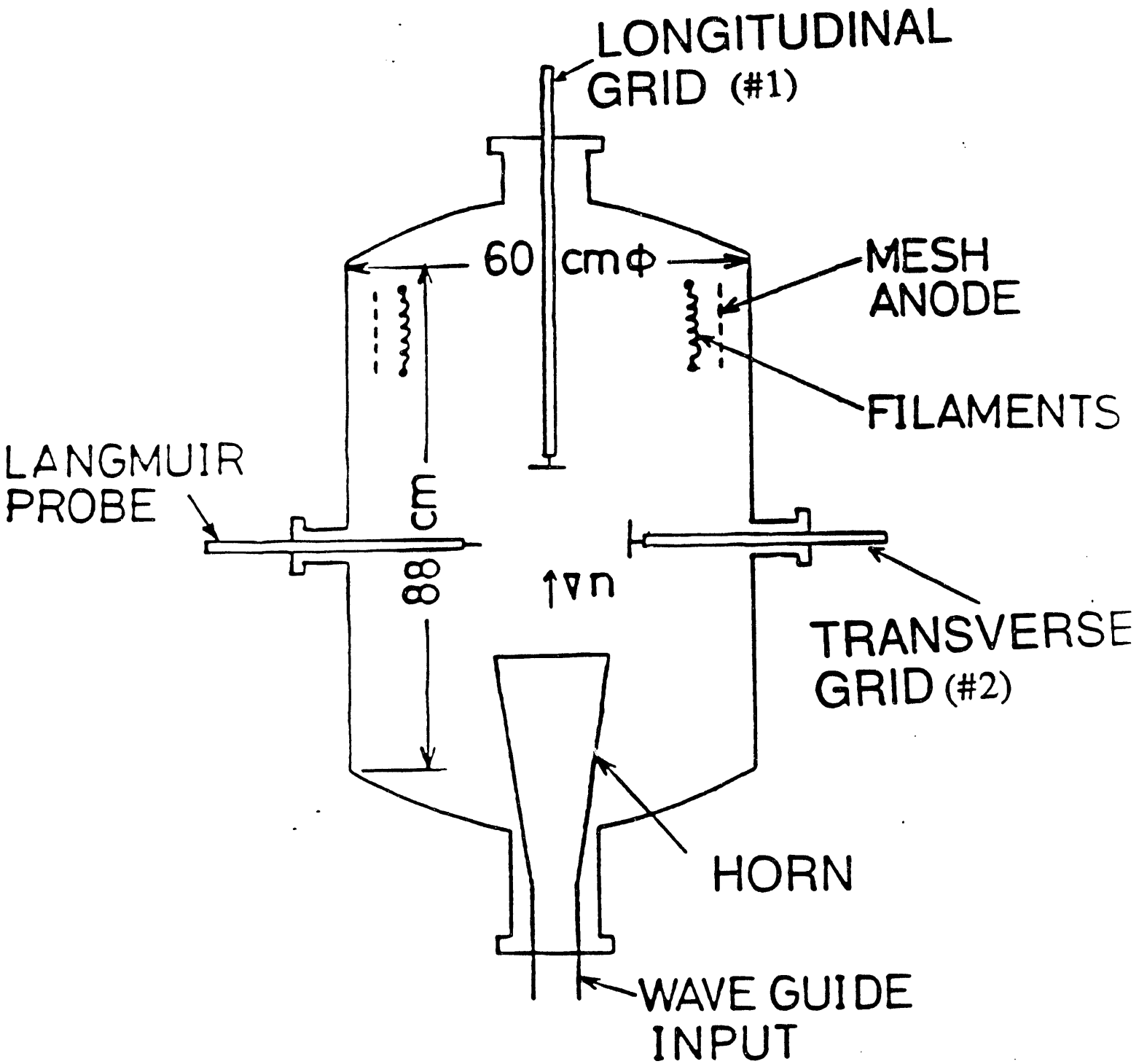

Figure 1. Diagram of experimental setup.

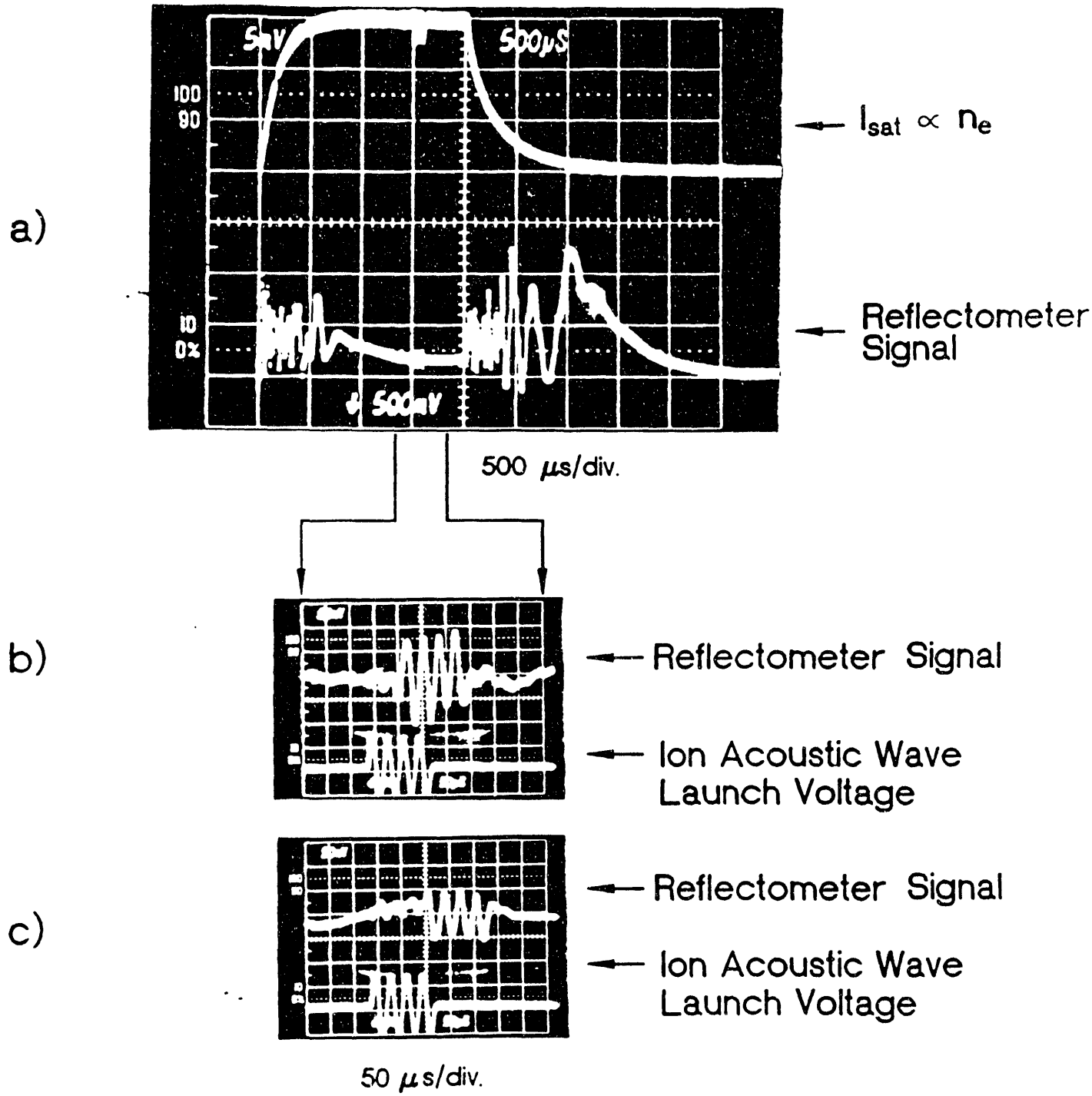

Figure 2. **(a)** Langmuir probe and reflectometer signals over one complete plasma discharge. 500 μsec/div. **(b)** Expanded view of (a) showing time delay between ion acoustic wave launch and reflectometer signal (f_{rf} = 4.6 GHz). 50 μsec/div. **(c)** Same as (b) except frequency of reflectometer is lower (f_{rf} = 3.7 GHz). 50 μsec/div.

a)

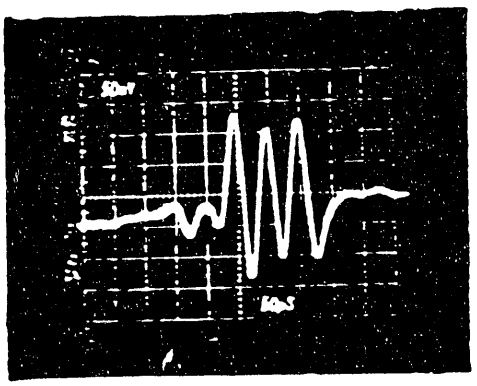

b)

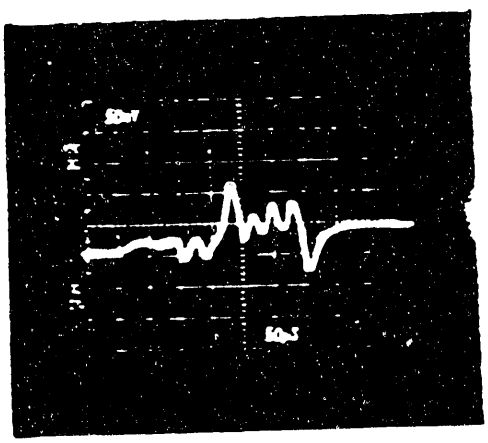

c)

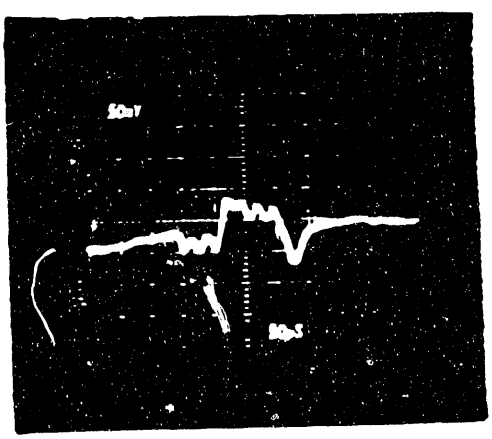

Figure 3. Reflectometer signals for ion acoustic waves launched perpendicular to microwave path. In all three photos f_{rf} = 3.4 GHz while in (**a**) f_{ion} = 20 kHz, (**b**) f_{ion} = 30 kHz, and (**c**) f_{ion} = 40 kHz. The response decreases as $f_{ion}(\propto k_{ion})$ increases. 50 μsec/div.

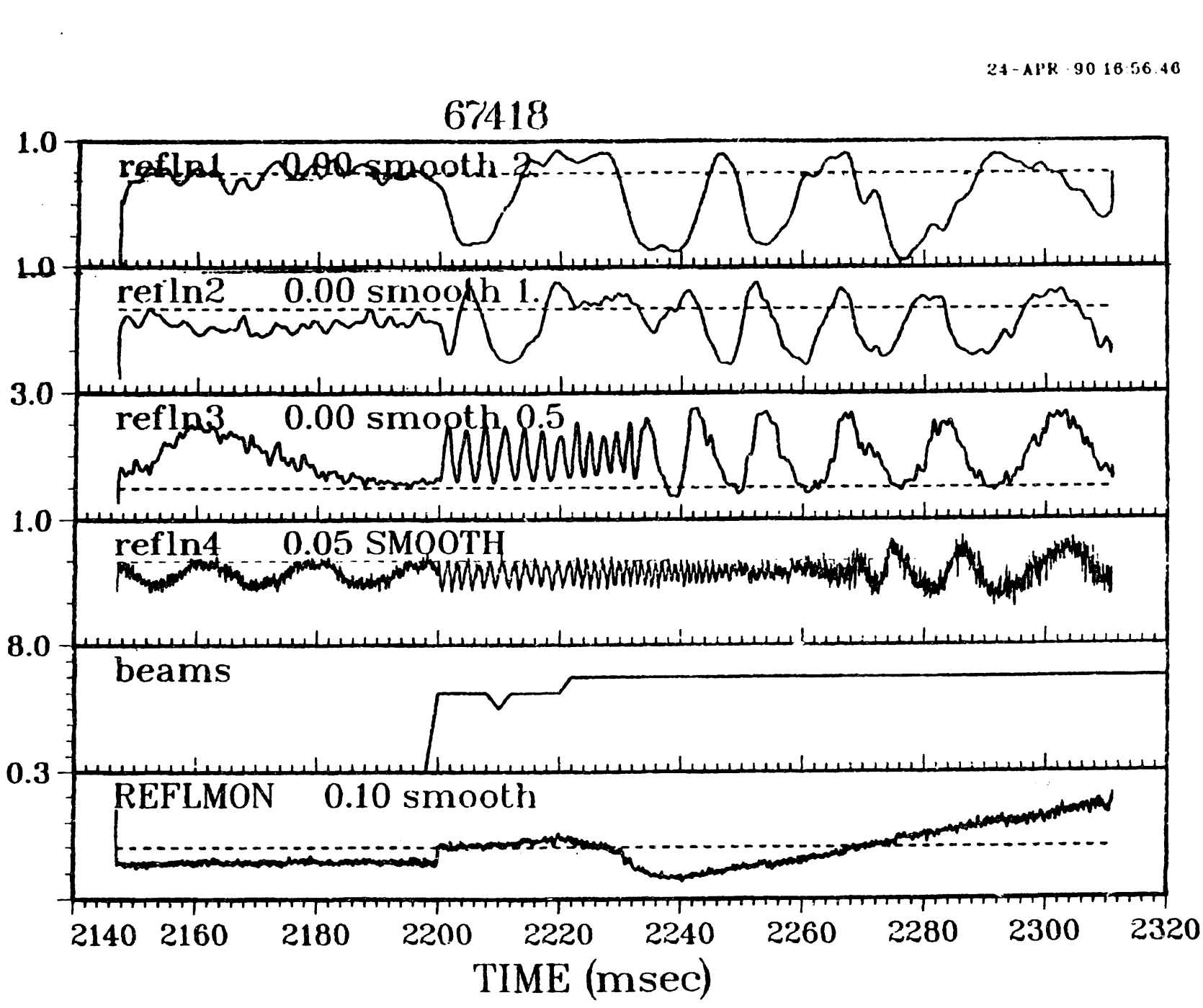

Figure 4. Change in density profiles during neutral beam injection causes low frequency phase shifts in reflectometer data. Four reflectometer channels, neutral beam injection and H_α (REFLMON) are shown.

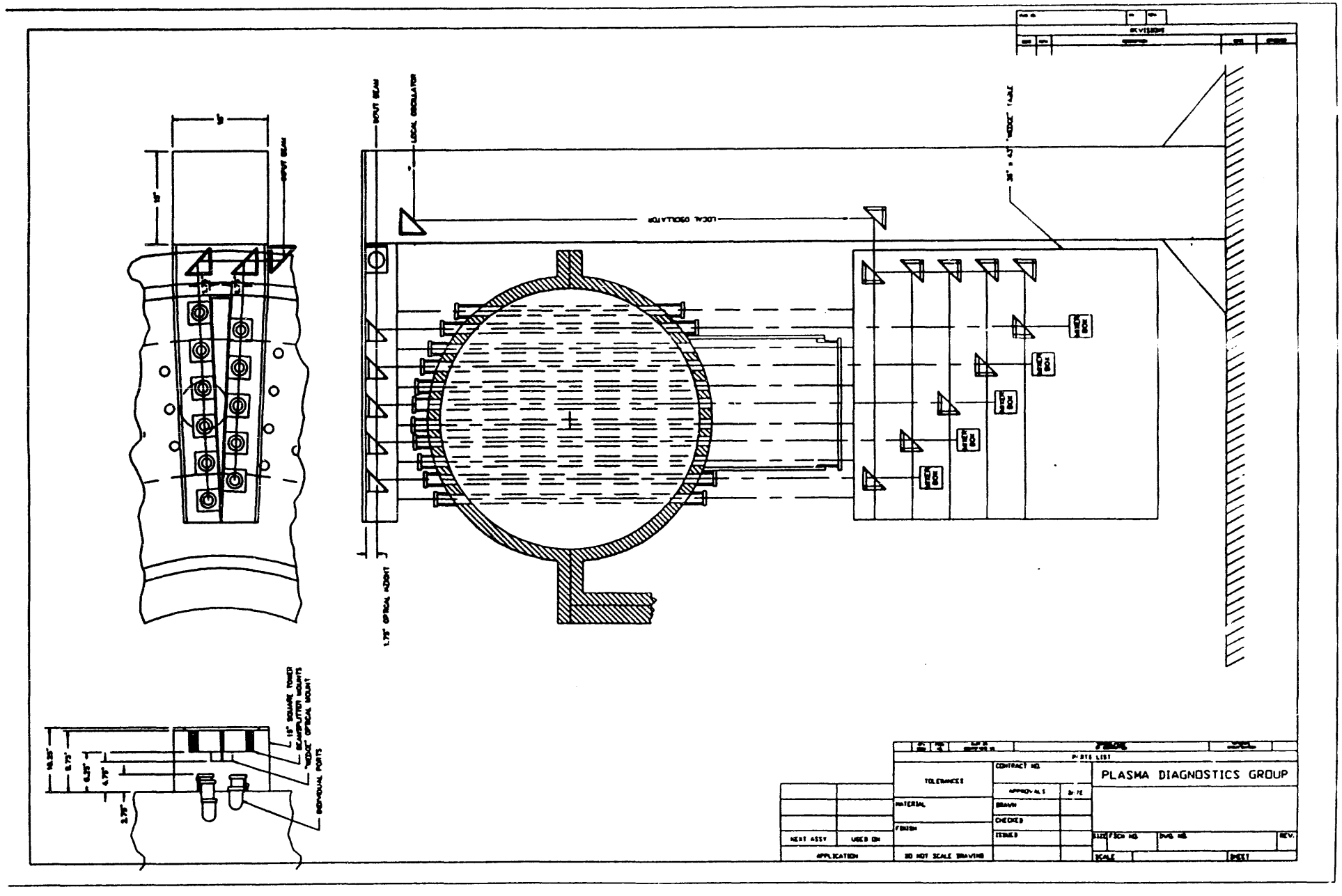

Figure 5. Support structure and optical system for MST interferometer.

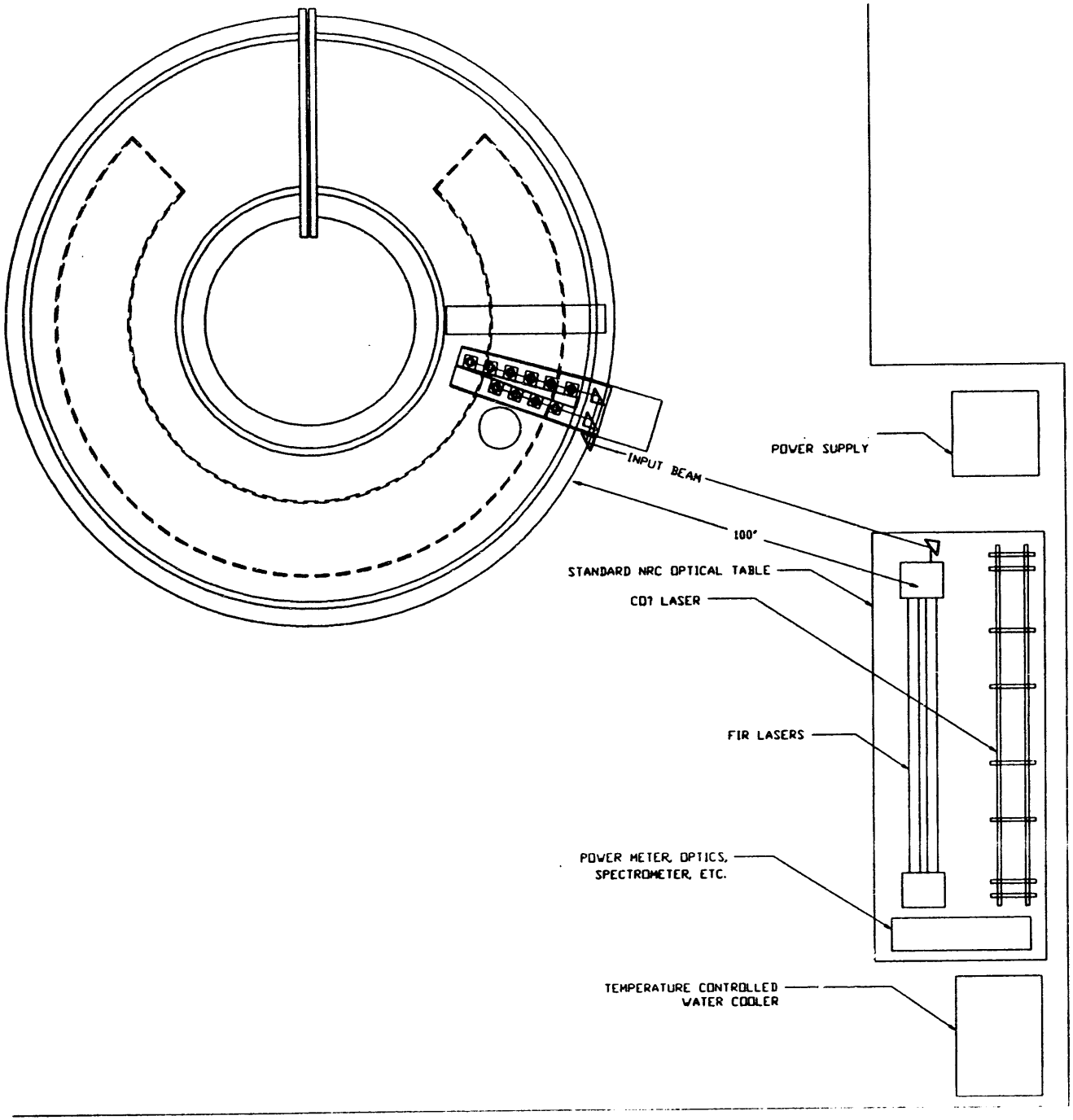

Figure 6. Plan view of proposed MST interferometer illustrating toroidally offset interferometer channels and location of FIR laser system.

TASK IIIB: PROGRESS REPORT

Advanced Plasma Fusion Diagnostics

FY 1990

Principal Investigator:
N.C. Luhmann, Jr.

Co-Principal Investigator:
W.A. Peebles

SECTION I. PROGRESS REPORT FY90

Task IIIB

I. ADVANCED TECHNOLOGY DEVELOPMENT FOR NEXT GENERATION REFLECTOMETER AND HETERODYNE ECE SYSTEMS

During the past few years, the importance of millimeter wave reflectometry has been clearly demonstrated. This has resulted in a spate of systems being installed on devices around the world (JET, DIII-D, TFTR, TEXTOR, ASDEX, ATF, etc.). In a relatively short period of time, these systems have been found to be indispensable in fluctuation studies as well as capable of providing density profiles with excellent spatial resolution. For example, these capabilities are essential in understanding the physics of the L-to-H transition in DIII-D.

The use of reflectometers is anticipated to be even more essential to future devices such as ITER and CIT as well as devices nearing operation such as C-MOD. The limited access and/or higher fields and densities of these plasmas will preclude the use of many techniques which are currently utilized leaving reflectometry as one of the few viable approaches. The problem to be faced, however, is that the required operating frequencies are considerably higher than those currently employed. For example, the DIII-D systems employ sources in the 15-70 GHz range while ITER requires sources in the 70-200 GHz region and CIT and C-MOD up to $\simeq$ 400 GHz. In the case of heterodyne ECE measurements, the high field devices require operating frequencies up to $\simeq$ 1 THz. The difficulty is that commercially available millimeter wave devices and components are essentially only available up to $\simeq$ 94 GHz (the last real military operating band). Therefore, a major focus of the Task IIIB program has been the development of new devices and components which will permit this essential diagnostic to be implemented on these machines. The specific items under active development include quasi-optical monolithic arrays of solid state frequency multipliers, electronic beam steering arrays, and imaging detector arrays. Our progress in a number of these areas is described below. Details can be found in the papers and abstracts listed at the end of this report.

A. Monolithic Frequency Multiplier Arrays

In order to fully utilize the capabilities of reflectometry, sweepable sources will be required at frequencies up to $\simeq$ 400 GHz with heterodyne ECE measurements requiring even higher frequencies ($\simeq$ 1 THz). Unfortunately, conventional solid state sources such as GUNN devices have limited tunability and are restricted to frequencies $\leq$ 90-140 GHz. Electron beam devices such as BWOs operate at higher frequencies, but suffer from narrow sweep bandwidths at the higher frequencies as well as extremely limited lifetime and large size and high voltage requirements.

A common approach to obtaining high frequency is to utilize the nonlinearities of solid state devices for frequency multiplication. This has resulted in output frequencies as high as 1 THz albeit at very limited power levels due to the low power handling capability of the diodes. To provide the required power levels for fusion applications, we have employed spatial power combining of the outputs of large planar arrays of nonlinear frequency multiplication devices.

The concept of a monolithic diode-grid doubler array was previously implemented under Task IIIB in a proof-of-principle experiment with Schottky diode grids fabricated on GaAs wafers[1]. The measurements indicate that the diode grid is a feasible device for generating watt-level powers in the millimeter and submillimeter wave region, and that substantial improvement is possible by increasing the diode breakdown voltage and reducing the series resistance. The theoretical model provides confidence in predictions of achievable CW output power levels of 2.5 W at a frequency of 188 GHz with an edge-cooled grid containing 1000 diodes. Such an array is currently being fabricated.

In an extension of the GaAs Schottky diode doubler array studies, a back- to-back configuration of BIN (barrier-intrinsic-N+) diodes has been developed[3-5] (see Fig. 1(a)) which incorporate a thin (1000 $\AA$) undoped semiconductor layer (I) on a heavily doped layer (N+) serving as a back contact. On top of the undoped layer there is an ultrathin (100 $\AA$) electron-blocking barrier layer (B) in contact with a metal top layer. This blocking layer can be formed by an insulator, a semiconductor with a very wide band gap, or a Mott barrier. The device can be switched rapidly between two capacitance states which correspond to accumulation of electrons at the barrier and depletion of the intrinsic layer, respectively, by the applied bias. This results in a highly nonlinear capacitance-voltage characteristic that is needed for efficient harmonic generation (see Fig. 1(b)). Due to the blocking barrier of the BIN structure, two diodes can be operated back-to-back (see Fig. 1) generating a sharp symmetric spike in the capacitance-voltage curve, which eliminates even harmonics and thus favors tripler and quintupler operation[4,5]. For an optimized input power of 9 mW per diode, a maximum tripling efficiency of 24% at an output frequency of 100 GHz is predicted (see Fig. 2) for the particular GaAs BIN array that has recently been fabricated.

A novel grid structure has been designed for the BIN diode tripler array as shown in Fig. 3[4]. The metal grid consists of a columnar mesh of aluminum strips with Schottky electrodes on each end. The two neighboring Schottky electrodes are designed to provide the back-to-back configuration. There is no need for dc bias lines in the diode-grid design. The grid requires only one metal pattern, which greatly facilitates the fabrication.

We are currently involved in fabricating both doubler arrays (individual diodes) and tripler arrays (back-to-back diodes). We will be initially testing them as multipliers in the 100-200 GHz region. If successful, this will permit us to use them in a system planned for TFTR. This will result in both qualification tests for ITER application as well as physics results. Extensions to the higher frequencies required for C-MOD and CIT continue.

B. Electronic Phase Shifter and Beam Steering Arrays

There is considerable need for an electronic beam steering and focusing capability on the microsecond timescale for the reflectometer systems to be used on the next generation of tokamaks. This capability can be provided by the diode grids. Specifically, the Schottky diode-grid used for the first doubler tests was also used for phase shift measurements[2] with the ultimate goal being an electronic beam steering array. Changing the bias applied to the diode rows changes the diode capacitance, thus controlling the quasi-optical impedance of the diode grid. A different phase shift can be produced for each row by applying a different bias voltage. It has been shown that a complete 360 degree range of phase control could be obtained from a two layer stack of properly designed diode grids (see Fig. 4). Initial proof-of-principle tests were performed on the single diode grids described in the preceding section. In agreement with theory, a phase shift of 70 degrees with a 7 dB loss was obtained at 93 GHz when the bias on the diode grid was changed from -3 V to 1 V in agreement with theory. Using the parameters of the diodes currently under fabrication, we anticipate significant improvement for a full two layer structure. Using a realistic diode resistance of 10 ohms, a reflection loss of 2.5 dB is predicted. Bandwidth, which will be limited by scan angle, should be about 7% for a 45 degree scan angle.

C. Imaging Horn Arrays

The next generation of reflectometers also require sensitive detector/mixer arrays. The approach that is being carried out under our subcontract to Cal Tech is to fabricate monolithic arrays of etched horns and detector elements.

1. Horn Aperture Efficiency

Last year, the work had concentrated on improving the aperture efficiency of the horn array elements. Earlier work[6] demonstrated efficiencies of 44% from horn antenna configurations exhibiting 2 dB of mismatch loss and 1 dB of conduction loss in the horn sidewalls. We have been able to almost eliminate these effects, obtaining aperture efficiencies of 72%[7]. Figure 5 shows our recent results of measured aperture efficiency versus antenna length. The points indicated by stars were obtained from horns whose walls were entirely coated with gold. The points indicated by squares were obtained from horns whose walls were gold coated, except for the region on the edge of the silicon wafer bearing the membrane. The maximum aperture efficiency is 64% for a 0.185λ half-length antenna for the partially coated case. The curve for fully coated horns moves up because resistive loss on the side-walls of the membrane wafer is eliminated, but the aperture efficiency for 0.25λ is lower than partially coated case, due to extra inductive loading produced by the gold near the antenna ends. The maximum observed efficiency is 81% and the repeatable highest efficiency is 72% at a half-length of 0.185λ.

Table 1 gives the breakdown of the losses for the fully coated case at maximum efficiency. The total calculated losses are -0.6 dB, composed of intrinsic pattern loss (taper

loss of the horn), coupling loss to adjacent horns, loss to the cross-polarized component, and impedance mismatch loss between the 50 Ω antenna and the 67 Ω bolometer. The total measured loss is -0.9 dB corresponding to an efficiency of 81%. In the partially coated horns, there is the additional 0.7 dB of resistive loss in the uncoated portion of the horn sidewalls giving a calculated loss of -1.3 dB, compared with the measured -1.9 dB (64%). The maximum theoretical aperture efficiency of the 1 λ square horn is 88%. These results are very encouraging. The efficiencies are competitive with machined horns and are among the highest efficiencies obtained from integrated circuit antennas.

Intrinsic Pattern Loss	0.2 dB
Mismatch Loss	0.1 dB
Cross-Polarization Loss	0.2 dB
Horn-to-Horn Coupling Loss	0.1 dB
Total Calculated Loss	0.6 dB
Total Measured Loss	0.9 dB

Table 1. Horn aperture efficiency losses.

The system coupling efficiency with a lens has also been measured. This is the ratio of the power received by a single horn placed at the focal point to the total power incident on the primary lens. Figure 6 shows a plot of coupling efficiency versus f-number. The highest system coupling efficiency with a lens is 36%, when the f-number is 0.78. We estimate that the loss from reflection and absorption in the lens is 28%, indicating that it should be possible to achieve a system efficiency of 50% with reflecting optics.

2. Diode on Membrane

The frequency response of resistive bolometers is inadequate for most magnetic fusion diagnostic applications. In the long term, we plan to use monolithic Schottky diodes fabricated directly on gallium arsenide membranes. In the short term, we plan to build hybrid circuits made with beam lead diodes mounted on the existing silicon oxynitride membranes. Initial results have been obtained in collaboration with Aerojet. Caltech supplied the arrays and Aerojet personnel bonded the diodes onto the free membrane surface with gold epoxy. Pattern measurements were made by Aerojet and the diode functioned as expected in the video mode.

3. Back-to-Back Horn Antenna Arrays

The crucial question for horn array mixers is the introduction of local oscillator power to each of the horn elements. We have chosen one configuration called the displaced back-to-back horn array. The design (see Fig. 7) consists of a set of forward and backward looking horns sharing the same membrane wafer. The front side is used to receive the signal, and the back side is used for the LO. The incoming signal and LO are fed down monolithic transmission lines on the membrane surface to be combined in a mixer located between the horns.

D. Solid State Grid Oscillator Arrays

To pump the frequency multiplier array, it is convenient to employ a so-called grid oscillator array wherein either two or three terminal devices are arrayed in a planar grid which is incorporated into a quasi-optical cavity resonator. The grid essentially serves as a two dimensional gain medium in this "laser-like" configuration. Most of this work is being carried out by Cal Tech under separate funding.

The grid oscillator concept was first demonstrated using GUNN devices. More recently, 25, 36 and 100 element MESFET grids oscillating at 10, 3 and 5 GHz, respectively, exhibited power-combining and self-locking[8-10]. Currently, a collaboration has been initiated with Rockwell to produce a monolithic array of heterojunction bipolar transistors. It is estimated that up to 50 W can be obtained at $\simeq$ 94 GHz so that this will easily be able to provide pump power for the nonlinear frequency multiplier arrays.

UCLA efforts in the grid oscillator array have been to investigate the feasibility of employing arrays of resonant tunneling devices to directly serve as reflectometer oscillator sources. The results of these design studies have been extremely encouraging with projected operating frequencies up to $\simeq$ 1 THz. An additional advantage is that the fabrication steps are essentially identical to those utilized for our diode grid frequency multipliers and phase shifters.

II. HIGH POWER CO_2/FIR LASER DEVELOPMENT FOR MULTICHANNEL SCATTERING AND INTERFEROMETRY/POLARIMETRY

The operation of interferometry, polarimetry and collective scattering systems can potentially be significantly improved through recent development work at UCLA. Work has concentrated on two different, yet complementary, approaches to increasing the available power from such lasers. This is essential for the 2-D scattering and interferometry systems to be employed on TEXT upgrade.

A. Development of 350 W CO_2 Pump Laser

The existing CO_2 pump laser grew out of a collaboration with Apollo Lasers, and a former UCLA graduate student, Alain Semet. The split discharge design eliminates the need for Brewster windows, as well as glass-blown laser tubes. The laser typically produces 135 W output powers and is extremely stable. Details regarding this laser can be found in Refs. 11-13.

Recent design work has concentrated on doubling the discharge length of the existing laser by basically folding the laser cavity. This is illustrated in Fig. 8 where the existing and new laser designs are illustrated. The new design will be structurally a single unit, utilizing turning mirrors to reduce the overall length. Physically, the laser will be identical in length but extended vertically by $\sim$ 8 inches.

The laser is expected to produce $\sim$ 350 W operating continuously. This should at least double the output power of the FIR laser at all wavelengths, while producing negligible deterioration in frequency and power stability. The system will immediately find application at TEXT, where increased power is necessary for the 2-D interferometer/scattering system presently under construction.

B. Metallic-Waveguide Far-infrared Laser

Optically pumped FIR lasers generally employ overmoded dielectric waveguide in their cavities. Such waveguide supports EH_{11} modes that couple effectively to Gaussian modes in free space. At frequencies exceeding $\sim$ 400 GHz, attenuation is very low in such waveguides and so their use is ideal for the majority of wavelengths employed in optically pumped FIR lasers. However, at wavelengths $\sim$ 1 mm (300 GHz) the losses in such waveguide can be substantial and consideration has therefore been given to the use of lower loss metallic waveguides at these frequencies.

Generally, the use of cylindrical, smooth metallic guides has been shown to produce higher output powers accompanied by non-Gaussian like modes often possessing random polarization. Recent work at UCLA has shown that when the distance between the output coupler and the guide is changed, the coupling losses between the two play an important role in determining resonator modes. Adjustment of the position of the FIR coupler has produced a linearly polarized, quasi-Gaussian mode with output powers $\sim$ 3 times those obtained with dielectric waveguide. This improvement in output power has motivated the next phase in development in collaboration with General Atomics.

In order to achieve EH_{11} mode operation routinely in metallic, overmoded guide, it is necessary to groove the interior of the cylindrical guide periodically at a spacing $< \lambda/2$. This results in EH_{11} modes having the lowest insertion loss in such guide. General Atomics have developed the necessary fabrication techniques for such waveguide within their gyrotron heating program. John Doane (General Atomics), an expert in the design of such systems, has agreed to help UCLA in this effort and General Atomics have agreed to supply the necessary waveguide for test at 245 GHz. It is expected that output powers will, at least, triple, while mode quality and polarization properties should remain Gaussian and plane polarized.

C. FIR Ring Laser Development

The twin frequency optically pumped far-infrared laser system developed at UCLA (see Fig. 8) for plasma diagnostics applications has been extremely successful in practice. Apart from its use on TEXT, such a system is being used on DIII-D, at FOM in the Netherlands, one is being planned for MST and another is under consideration for use at the Los Alamos National Laboratory, and the CO_2 pump laser itself is being used at the University of Sydney in Australia. However, there are circumstances under which feedback of the radiation into the laser resonator cavity can adversely affect the stability of the FIR output power and its frequency. This frequency and/or power variation can cause problems in the tracking and frequency resolution for heterodyne detection systems which rely on extremely stable operation of the sources. With the linear cavity design currently in use, feedback from an experiment (i.e. the DII-D scattering system) enters the cavity and pulls the absolute frequency of the laser. If the frequency is pulled by only one part in 9^6, the heterodyne scattered signal is lost in the frequency pulled sidebands. To a lesser extent, this laser system also experiences instabilities when CO_2 laser radiation feeds back from the FIR cavity into the CO_2 laser, pulling its frequency and power (which is followed in the FIR laser). The effects of feedback on both lasers can be entirely eliminated by use of a ring laser cavity, which is shown in Fig. 9. For certain operating conditions (inhomogeneous broadening in the FIR medium), the FIR feedback radiation is not resonant with the same subset of particles being pumped, so the frequency pulling is eliminated. Also, it is impossible for the CO_2 radiation to reflect back on itself once it has entered the ring cavity. Under some operating conditions, the FIR ring laser should demonstrate unidirectional operation as the geometry allows asymmetric pumping of the velocity distribution. Thus, the cavity mode selects only molecules having a specific axial velocity to participate in the inversion and a preferred direction is established.

Given the need for a feedback stable FIR laser and the possible ring laser solution, a program to investigate its potential has been established. After an initial ring laser of modest dimensions (2.5 cm diameter waveguide cavity 2.2 m long) was operated with reasonable power levels at wavelengths of 118 μm and 393 μm, another ring laser with dimensions suitable for use in plasma diagnostics has been built and operated. Improved operation in Methanol at 118 μm and in formic acid at 393, 419, and 432 μm has been achieved along with an output of 2 mW in isotopic methyl fluoride ($C^{13}H_3F$) at 1.22 mm (245 GHz). The laser line at 245 GHz has been combined in a Schottky diode mixer with a high harmonic of an ultra stable source so the absolute laser frequency can be monitored under a variety of conditions. Under the influence of strong feedback, the laser frequency for linear and ring configurations has been measured and shown to be improved for the ring cavity (see Fig. 10). In addition, several unexplained features in the gain profile for the two directions have been observed which may be related to a Lamb dip or standing wave or traveling wave gain asymmetries. Thus, advances in laser research may result from the ring laser program, as well as a more stable source for plasma diagnostics.

III. POLARIMETRY MEASUREMENTS OF CURRENT PROFILE

As mentioned in last year's progress report, the purpose of the present work is not only to establish a routine polarimetric measurement of the current density profile on TEXT, but also to extend the measurement to higher densities and fields. Therefore, the major emphasis has been on the investigation of the possibility of measuring both the Faraday rotation and elliptization of the incident electromagnetic wave in order to more accurately compensate for the expected large elliptization at submillimeter wavelength on device such as C-MOD, MTX and CIT. We have proposed and tested two detection schemes for polarimetry which are different from that of Soltwisch (on TEXTOR) in using a small wire spacing polarizer as beam combiner.

Here, we will oriefly summarize the proposed systems. The schematic of the two interferometer/polarimetry systems is shown in Fig. 11. Parabolic cylindrical mirrors are used to expand the probe and reference beam in one dimension to view the entire plasma cross section. The two beams are combined and detected using a linear array of corner cube GaAs Schottky barrier diode mixers. In the first detection scheme, the polarization change due to the plasma yields two output signals whose amplitude ratio is given by

$$R = \sqrt{\frac{(1+\epsilon_p^2) - (1-\epsilon_p^2)\sin 2\psi_p}{(1+\epsilon_p^2) + (1-\epsilon_p^2)\sin 2\psi_p}}$$

$$\simeq \cot(\psi_p + \frac{\pi}{4}) \qquad \text{when } \epsilon_p \ll 1$$

Here, ψ_p is the Faraday and ϵ_p is the wave elliptization. In addition, there is a phase difference between equivalent detectors given by

$$\Delta\phi = \tan^{-1}[\epsilon_p \tan(\psi_p + \frac{\pi}{4})] - tan^{-1}[\epsilon_p \tan(\psi_p - \frac{\pi}{4})]$$

In the second detection scheme, a polarization transforming reflector (PTR) is used as a quarter-wave polarizer to rotate the polarization direction of the probe beam by 45° and quadrature phase-sensitive detection technique is used to measure the Faraday rotation and elliptization simultaneously, which are given as follows

$$R\cos\Delta\phi = \tan\psi_p \frac{1-\epsilon_p^2}{1+\epsilon_p^2\tan^2\psi_p}$$

$$\simeq \tan\psi_p \qquad \text{when } \epsilon_p \ll 1$$

$$R\sin\Delta\phi = \frac{\epsilon_p}{\cos^2\psi_p[1+\epsilon_p^2\tan^2\psi_p]}$$

$$\simeq \epsilon_p \qquad \text{when } \psi_p \ll 1$$

In principle, therefore, measurement of the amplitude ratio and phase difference, or quadrature output from the phase-sensitive detection system, allows one to independently evaluate ψ_p and ϵ_p. It should be noted that compared to the Soltwisch method the Faraday rotation measurement with both our techniques is very insensitive to the

elliptization. Also, the accuracy of ψ_p from our second technique is the same as that of Soltwisch, and better than our first method.

In order to be able to perform meaningful measurement of the current density profile on a number of devices with our polarimetry/interferometry systems, these proposed systems need to be carefully assessed and demonstrated through prototype laboratory experiments. Therefore, during the past year, extensive laboratory experimental studies have been performed to assess the feasibility of measuring both the Faraday rotation and elliptization simultaneously. First, we have tested the principle of the proposed elliptization measurement, as shown in Fig. 12, where a quartz plate was used to introduce a known elliptization and rotation to the incident beam. The experimental results are shown in Figs. 13 and 14, where the phase difference $\Delta\phi$ and the quadrature output are plotted as a function of the quartz rotation angle and compared with theoretical prediction. The results with both schemes show excellent agreement between theory and experiment.

In addition, because the accuracy of measuring Faraday rotation and elliptization with our methods is highly dependent on that of the signal amplitude, techniques must be established to overcome unfavorable effects, such as the mixer's nonlinear response and beam deflection due to plasma refraction. Therefore, we have measured the mixer response to the input FIR power by using rotating wire polarizer to introduce a known change of input power, and have found that in some regions of operation the mixer response is linear (within 2%), as shown in Fig. 15. Furthermore, we have the modified the small parabolic mirror and beam combiner, and tested their capability of compensating for beam deflection by rotating a mirror to simulate the effect. The experimental results show that for a well-aligned system, the output amplitude ratio of two equivalent mixers can be kept constant (within $\pm$ 5%) when the beam deflection angle is smaller than or equal to $\pm 1°$. These tests provide confidence that we will be able to improve the accuracy of the measurement.

In order to demonstrate the feasibility of improving the accuracy of the measurement of ψ_p with these compensation techniques, a modified 5 channel test system was constructed and installed on TEXT to perform measurements of the central-q value and also the current density profile by scanning the entire system from shot to shot. The Faraday rotation data are shown in Figs. 16 and 17. It was found that there remain a number of unresolved effects that may limit the accuracy of measurements. They are as follows: (1) mixer dc and RF bias shifts cause the mixer to operate in the nonlinear region; (2) system alignment on TEXT is not as good as that in the laboratory experiment; (3) FIR radiation reflected by the plasma and optics enter the FIR cavity and cause the output power and frequency to become unstable. The effects mentioned above need to be checked and overcome through laboratory experiments prior to use of our system in current profile measurements on TEXT.

Therefore, in the coming year the major effort will be directed towards accurate current density profile and central q measurements on TEXT. The goals in the coming year are as follows.

1. Identify the obstacles that limit the accuracy of the measurement and establish techniques to overcome them.

2. Modify the system, optics and electronics to ensure that the system works reliably.

3. Demonstrate the possibility of accurately measuring both the Faraday rotation and elliptization simultaneously with our detection schemes.

IV. ECRF WAVE SCATTERING

After construction and laboratory tests of a 185 GHz low noise heterodyne receiver, the system was installed on DIII-D to enable scattering from ECRH waves. The receiver was used with the FIR laser operating at 245 GHz to detect the frequency down-shifted radiation scattered by the electrostatic component of a 60 GHz wave. The DIII-D tokamak employs X-mode ECRH with up to 1.7 MW available from 10 gyrotrons. It was hoped that severe problems of poor accessibility limiting the scattering geometry to far-forward scattering and a large separation between the X-mode launch waveguides and the scattering system could be overcome by the extreme sensitivity of the receiver system. In the initial tests, no scattered radiation from the laser could be detected; however, strong third harmonic electron cyclotron emission from the plasma interior was detected. The excellent signal-to-noise ratio of this signal suggested the use of the technology for highly sensitive radiometric measurements of ECE. Initial design and tests of a crossed waveguide harmonic mixer to detect the broadband ECE from DIII-D show promise for the investigation of heat pulse propagation, time resolved temperature profiles, and possibly temperature fluctuations. Longer term development will involve a scattering system for the 110 GHz waves.

V. ADVANCED HOLOGRAPHIC REFLECTOMETRY

The advanced holographic reflectometry development has thus far involved a study of related techniques in other fields. An example is the hologram matrix radar which has been employed in the microwave region to measure the thickness of ice caps or mine beds and in the acoustic region for profiling the tissue layers of an organ[14,15]. This technique determines the distance by the spatial distribution of the amplitude and phase of the scattered wave rather than by the lapse of time as in conventional radars. We have now located two graduate students with excellent microwave antenna and circuits backgrounds who will be developing the laboratory experiments.

REFERENCES

(1) C. F. Jou, W.W. Lam, H. Chen, K. Stolt, N.C. Luhmann, Jr., and D.B. Rutledge, "Millimeter-Wave Monolithic Schottky Diode-Grid Frequency Doublers," IEEE Trans. on Microwave Theory and Tech., 36, No. 11, pp. 1507-1514, 1988.

(2) W.W. Lam, C.F. Jou, H. Chen, K. Stolt, N.C. Luhmann, Jr., and D.B. Rutledge, "Millimeter-Wave Monolithic Schottky Diode-Grid Phase Shifters," IEEE Trans. on Microwave Theory and Tech., 36, No. 5, pp. 902-907, 1987.

(3) U. Lieneweg, B. R. Hancock, and J. Maserjian, "Barrier-Intrinsic-N+ (BIN) Diodes for Near-Millimeter Wave Generation," 12th Intl. Conf. Infrared and Millimeter Waves, Tech. Dig., pp. 6-7, 1987.

(4) R.J. Hwu, C.F. Jou, N.C. Luhmann, Jr., W.W. Lam, D.B. Rutledge, B. Hancock, U. Lieneweg, and J. Maserjian, "Watt-Level Millimeter-Wave Monolithic Diode-Grid Frequency Multipliers," Rev. of Scientific Instruments, 59, No. 8, pp. 1577-1579, 1988.

(5) R.J. Hwu, C.F. Jou, W.W. Lam, U. Lieneweg, N.C. Luhmann, and D.B. Rutledge, "Watt-Level Millimeter-Wave Monolithic Diode-Grid Frequency Multipliers," 1988 IEEE MTT-S Digest, pp. 533-538, 1988.

(6) G.M. Rebeiz, D. P. Kasilingam, Y. Guo, P.A. Stimson, and D.B. Rutledge, "Monolithic millimeter-wave two-dimensional horn imaging arrays," accepted for publication to the *IEEE Trans. on Antennas and Propagate.*, June, 1988.

(7) Yong Guo, Karen Lee, P.A. Stimson, Kent Potter and D.B. Rutledge, "Aperture Efficiency of Chemically Etched Horns at 93 GHz", Proceedings of *IEEE AP-S International Symposium*, May 7-11, 1990, Dallas, Texas.

(8) Z.B. Popovic and D.B. Rutledge, "Diode-Grid Oscillators," 1988 IEEE Antennas and Propagation Symposium, June 1988.

(9) Z.B. Popovic, M. Kim, and D.B. Rutledge, "Grid Oscillators," International J. of Infrared and Millimeter Waves, 9, No. 7, pp. 647-654, 1988.

(10) Z.B. Popovic, R.M. Weikle, M. Kim, K.A. Potter, D.B. Rutledge, "Bar-Grid Oscillators," IEEE Trans. on Microwave Theory and Tech., 38, No. 3, pp. 225-230, 1990.

(11) T. Lehecka, R. Savage, Jr., R. Dworak, W.A. Peebles, N.C. Luhmann, Jr., A. Semet, "High Power, Twin Frequency FIR Lasers for Plasma Diagnostic Applications," Rev. Sci. Instrum., 57, (8), pp. 1986-88, 1986.

(12) W.A. Peebles, R.L. Savage, Jr., D.L. Brower, S.K. Kim, T. Lehecka, J. Howard, E.J. Doyle, N.C. Luhmann, Jr., "Plasma Diagnostic Applications on the TEXT Tokamak Using a High Power, Twin Frequency Optically Pumped Far-Infrared Laser," Int. J. of Infrared and mm-Waves, Vol. 8, No. 11, pg. 1355-1363, 1987.

(13) T. Lehecka, W.A. Peebles, R.L. Savage, Jr., N.C. Luhmann, Jr., "A High-Power CH^3F Laser for Plasma Diagnostics," IEEE J. on Quantum Electronics, QE-24, No. 1, pp. 5-7 (1988).

(14) K. Izuka, H. Ogura, J.L. Yen, V.K. Nguyen and J.R. Weedmark, "A Hologram Matrix Radar," Proc. of IEEE, 64, pp 1493-1504, (1976).

(15) K. Izuka, "Review of Hologram Matrix Radars," SPIE, Vol. 231, 1980 International Optical Computing Conference, pp. 179-187 (1980).

TASK IIIB PUBLICATIONS AND PRESENTATIONS FY90

1. R.J. Hwu, L.P. Sadwick, N.C. Luhmann, Jr., and D.B. Rutledge, "Theoretical Design and Optimization Consideration of The Barrier-Intrinsic-N^+ Millimeter-Wave Frequency Multipliers Based on DC and Low Frequency Characteristics," submitted to IEEE Trans. of Electron Devices, 1990.

2. R.J. Hwu, L. Sjogren, N.C. Luhmann, Jr., Z.B. Popovic, R.W. Weikel, M. Kim, and D.B. Rutledge, "Millimeter and Submillimeter Wave Technology Developments for the Next Generation of Fusion Devices," Review of Scientific Instruments, 61, No. 10, 1990.

3. P. Huang, N.C. Luhmann, Jr., D.S. Pan, "A New Method of Determination of the I-V Characteristics of Negative Differential Conductance Devices by Microwave Reflection Coefficient Measurements," submitted to IEEE Electron Device Letters, 1990.

4. D.B. Rutledge, "Aperture Efficiency of Integrated-Circuit Horn Antennas," 1st International Symposium on Terahertz Technology, Ann Arbor, Michigan, March, 1990.

5. Yong Guo, Karen Lee, Philip Stimson, Kent A. Potter, and David B. Rutledge, "Aperture Efficiency of Chemically Etched Horns at 93 GHz," The International Antenna and Propagation Symposium, Dallas, Texas, May, 1990.

6. Gabriel M. Rebeiz, Curtis C. Ling, and David B. Rutledge, "Large Area Bolometers for Millimeter-Wave Power Calibration," Int. J. Infrared and Millimeter Waves, 10, pp. 931-936, 1989.

7. Y. Guo, K. Lee, P. Stimson, K. Potter, and D. Rutledge, "Aperture Efficiency of Integrated-Circuit Horn Antennas," to be published in Microwave and Optics Letters.

8. K. Lee, Y. Guo, P. Stimson, K. Potter, and D. Rutledge, "Thin-Film Power-Density Meter for Millimeter Wavelengths," to be published in the IEEE Transactions on Antennas and Propagation.

9. R.J. Hwu, L. Sjogren, N.C. Luhmann, Jr., Z. Popović, Robert Weikle, Moonil Kim, and D.B. Rutledge, "Millimeter and Submillimeter Wave Technology Developments for the Next Generation of Fusion Devices," submitted for publication to the Review of Scientific Instruments.

10. David Rutledge, "Millimeter-Wave Imaging Devices," The Second Sendai International Conference, Sendai, Japan, September, 1990.

11. N.C. Luhmann, Jr., "Millimeter Wave Plasma Diagnostics," Invited Presentation The Second Sendai International Conference, Sendai, Japan, September, 1990.

12. Hwu, R.J., L.P. Sadwich, N.C. Luhmann, Jr., D.B. Rutledge, M. Sokolich, B. Hancock, "Quasi-Optical Watt-Level Millimeter-Wave Monolithic Solid-State Diode-Grid Frequency Multipliers," 1989 IEEE MTT-S Digest, CH2725, pp. 1069-1072, 1989.

13. R.J. Hwu, C.F. Jou, N.C. Luhmann, Jr., M. Kim, W.W. Lam, Z.B. Popovic, D.B. Rutledge, "Array Concepts for Solid State and Vacuum Microelectronics Millimeter Wave Generation," IEEE Trans. on Electron Devices, 36, No. 11, pp. 2645-2650, 1989.

14. P. Stimson, Yong Guo, Karen Lee, and D. Rutledge, "Advances in Monolithic Horn-Antenna Imaging Arrays," 13th Annual Antenna Applications Symposium, Robert Allerton Park, IL, September, 1989.

15. Koji Mizuno and David Rutledge, "Multi-Element Quasi-Optical Devices–A New Trend in Millimeter and Submillimeter Wave Electron Devices," 14th International Conference on Infrared and Millimeter Waves, Wurzburg, Germany, October 1989.

16. R.J. Hwu, X.H. Qin, W.S. Wu, L.B. Sjogren, N.C. Luhmann, Jr., D.B. Rutledge, B. Hancock, U. Lieneweg, and J. Maserjian, "Development of Monolithic Solid-State Diode-Grid Frequency Multiplier Arrays," 15th International Conference on Infrared and Millimeter Waves, 1990.

17. L.B. Sjogren, N.C. Luhmann, Jr., R.J. Hwu, W. Wu, X.H. Qin, M. Kim, D.B. Rutledge, Z.B. Popovic, B. Weikle, W.W. Lam, B. Hancock, U. Lieneweg, J. Maserjian, "Development of a Monolithic 94 GHz Quasi-Optical 360 Degree Phase Shifter," 15th International Conference on Infrared and Millimeter Waves, 1990.

18. Y. Jiang, J.H. Lee, S. Burns, N.C. Luhmann, Jr., W.A. Peebles, C.L. Rettig, "Use of Metallic Waveguide to Improve Performance of Far-Infrared Lasers for Fusion Plasma Diagnostics," 32nd Annual APS Meeting Division of Plasma Physics, Cincinati, Ohio, November 12-16, 1990.

19. W.A. Peebles, D.L. Brower, S. Burns, N.C. Luhmann, Jr., C.X. Yu, "UCLA FIR Diagnostic Systems on TEXT and Developments for TEXT Upgrade," 8th Topical Conference on High Temperature Plasma Diagnostics, Hyannis, MA May 6-10, 1990.

20. R.J. Hwu, N.C. Luhmann, Jr., D.B. Rutledge, "Millimeter and Submillimeter Wave Technology Developments for the Next Generation," 8th Topical Conf. on High Temperature Plasma Diagnostics, Hyannis, MA, May 6-10, 1990.

21. C.X. Yu, M. Nagatsu, W.A. Peebles, D.L. Brower, K. Kawahata, W.L. Li, N.C. Luhmann, Jr., "Polarimetric Measurement of the Current Density Profile in TEXT," 8th Topical Conf. on High Temperature Plasma Diagnostics, Hyannis, MA, May 6-10, 1990.

22. Y. Jiang, C.L. Rettig, S. Burns, J.H. Lee, N.C. Luhmann, Jr., W.A. Peebles, "Recent Developments in Optically Pumped Far-Infrared Lasers for Plasma Diagnostics," 8th Topical Conf. on High Temperature Plasma Diagnostics, Hyannis, MA, May 6-10, 1990.

23. R.J. Hwu, N.C. Luhmann, Jr., L.B. Sjogren, X.H. Qin, W. Wu, D.B. Rutledge, B. Hancock, and U. Lieneweg, "Watt Level Quasi-Optical Monolothic Frequency Multiplier Development," 1st International Symposium on Space Terahertz Technology, Ann Arbor, Michigan, March 5-6, 1990.

24. C.X. Yu, M. Nagatsu, W.A. Peebles, D.L. Brower, N.C. Luhmann, Jr., W.L. Li, TEXT Group, "Current Density Profile Measurements Via Polarimetry on TEXT," 31st Annual APS Meeting Division of Plasma Physics, Anaheim, CA Nov. 13-17, 1989.

25. R.J. Hwu, N.C. Luhmann, Jr., L. Sadwick, D. Rutledge, "Millimeter Wave Solid State Source Array Development for Millimeter and Submillimeter Wave Reflectometry and Scattering," 31st Annual APS Meeting Division of Plasma Physics, Anaheim, CA, Nov. 13-17, 1989.

26. D.W. Sprehn, C.L. Rettig, N.C. Luhmann, Jr., W.A. Peebles, R. Zimmerman, "Source Technology Development for FIR Scattering," 31st Annual APS Meeting Division of Plasma Physics, Anaheim, CA, Nov. 13-17, 1989.

27. W.A. Peebles, S. Baang, D.L. Brower, K. Burrell, E.J. Doyle, S. Kim, T. Lehecka, W.L. Li, N.C. Luhmann, Jr., M. Matsumoto, M. Nagatsu, R. Philipona, C. Rettig, C.X. Yu, DIII-D Group, TEXT Group, "UCLA Diagnostic Systems and Fluctuation and Transport Measurements on the DIII-D and TEXT Tokamaks," 4th International Symposium on Laser-Aided Plasma Diagnostics, Fukuoka, Japan, November 20-23, 1989.

28. R.J. Hwu, L.P. Sadwick, N.C. Luhmann, Jr., D.B. Rutledge, and M. Sokolich, "Monolithic Integration of Varactor Diodes on III-V Compound Semiconductors for Watt-Level Frequency Multiplication at Millimeter-Wave Region," International Conference on Semiconductor and Integrated Circuit Technology, Beijing, China, October 22-28, 1989.

29. R.J. Hwu, N.C. Luhmann, Jr., D.B. Rutledge, D. Streit, B. Hancock, and U. Lieneweg, "Microwave and Millimeter-Wave Frequency Multiplier Arrays," 14th International Conference on Infrared and Millimeter Waves, Wurtzburg, Germany, October 2-6, 1989.

30. R.J. Hwu, C.F. Jou, N.C. Luhmann, Jr., M. Kim, W.W. Lam, Z.B. Popovic, D.B. Rutledge, "Array Concepts for Solid State and Vacuum Microelectronics Millimeter Wave Generation," 2nd International Vacuum Microelectronics Conference, Bath, England, July 23, 1989.

31. R.J. Hwu, L.P. Sadwick, N.C. Luhmann, Jr., D.B. Rutledge, and M. Sokolich, "Highly Efficient Frequency Triplers in the Millimeter Wave Region-Incorporating A Back-To-Back Configuration of Two Varactor Diodes," International Conference on Millimeter Wave and Far-Infrared Technology, Beijing, China, June 19-23, 1989.

32. W.A. Peebles, T. Lehecka, D.L. Brower, S. Kim, M. Nagatsu, N.C. Luhmann, Jr., "The Application of Stable, High Power, Twin Frequency, Optically Pumped Far-Infrared Lasers to Fusion Plasma Diagnostics," International Conference on Millimeter Wave and Far-Infrared Technology, Beijing, China, June 19-23, 1989.

33. R.J. Hwu, L.P. Sadwick, N.C. Luhmann, Jr., D.B. Rutledge, and M. Sokolich, "Theoretical and Experimental Investigation of Watt-Level Wafer Scale Integration Microwave and Millimeter-Wave GaAs and AlGaAs Frequency Multipliers," 47th Device Research Conference, Boston, Mass., June 18-21, 1989.

34. R.J. Hwu, N.C. Luhmann, Jr., B. Hancock, M. Sokolich, D.B. Rutledge, L.P. Sadwick, "Quasi-Optical Watt-Level Millimeter-Wave Monolithic Solid-State Diode-Grid Frequency Multipliers," 1989 IEEE Microwave and Millimeter Wave Monolithic Circuits Symposium, Long Beach, CA, June 12-13, 1989.

FIGURE CAPTIONS

Figure 1. Two back-to-back connected GaAs BIN diodes.

Figure 2. Predicted tripling efficiency versus input power at various input frequencies for the experimental GaAs BIN diode grid.

Figure 3. BIN diode tripler array.

Figure 4. Schematic of two layer phase shifter and diode grid layout.

Figure 5. Aperture efficiency versus dipole length.

Figure 6. Coupling efficiency versus f-number.

Figure 7. Displaced back-to-back horn array.

Figure 8. Schematic of linear and folded CO_2 laser configurations.

Figure 9. Outline sketch of CO_2/FIR laser system developed at UCLA for use in plasma diagnostics experiments.

Figure 10. Far-infrared ring laser diagram.

Figure 11. Plots of the absolute frequency pulling of the FIR laser in linear (upper) and ring (lower) configurations under the influence of strong feedback which sweeps the gain. Note different spans.

Figure 12. Schematic of the multichannel far-infrared interferometry/polarimetry system.

Figure 13. Experimental arrangement utilized for the elliptization measurement.

Figure 14. (a) Experimental results illustrating the phase difference between two equivalent mixer outputs versus the quartz rotation angle and (b) theoretical prediction curve.

Figure 15. (a) Experimental results showing the quadrature output of locking amplifier versus the quartz rotation angle (b) theoretical prediction curve.

Figure 16. Mixer response calibration.

Figure 17. Faraday rotation measurements on TEXT.

Figure 18. Faraday rotation measurements on TEXT.

EFFICIENT FREQUENCY TRIPLER USING BACK-TO-BACK DIODE CONFIGURATION

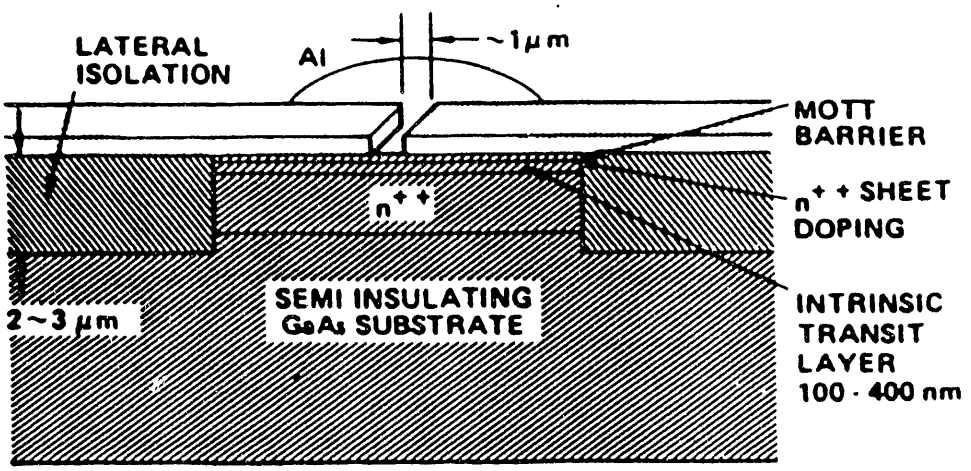

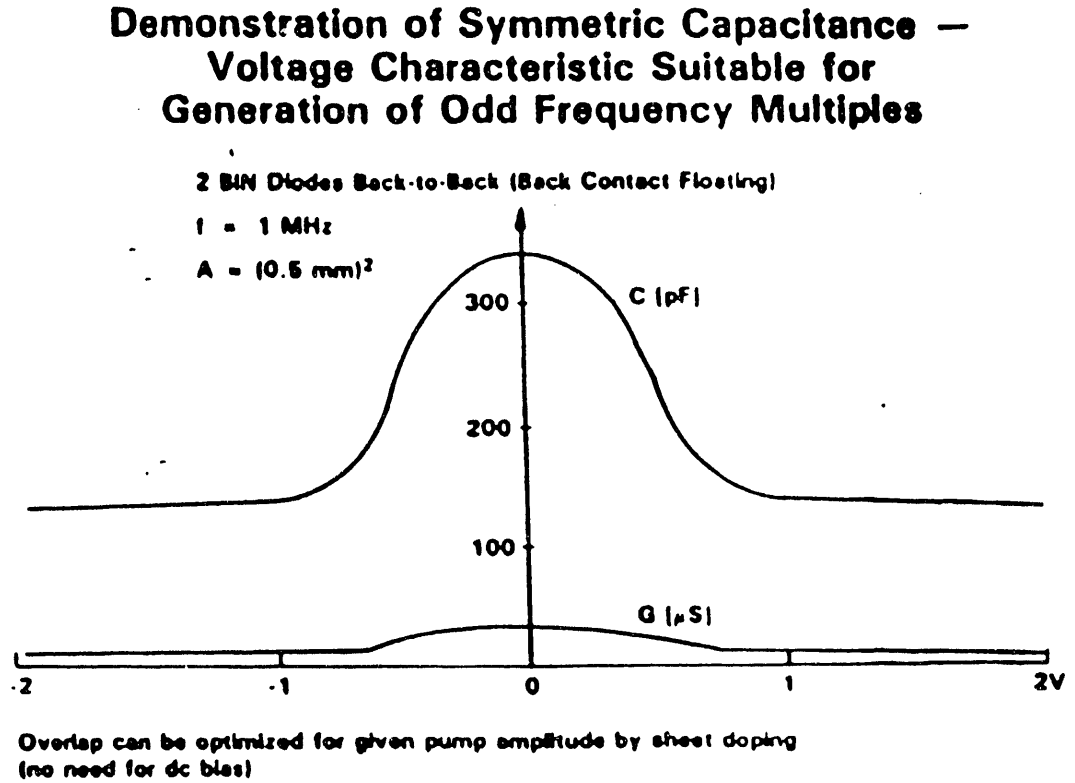

Figure 1. Two back-to-back connected GaAs BIN diodes.

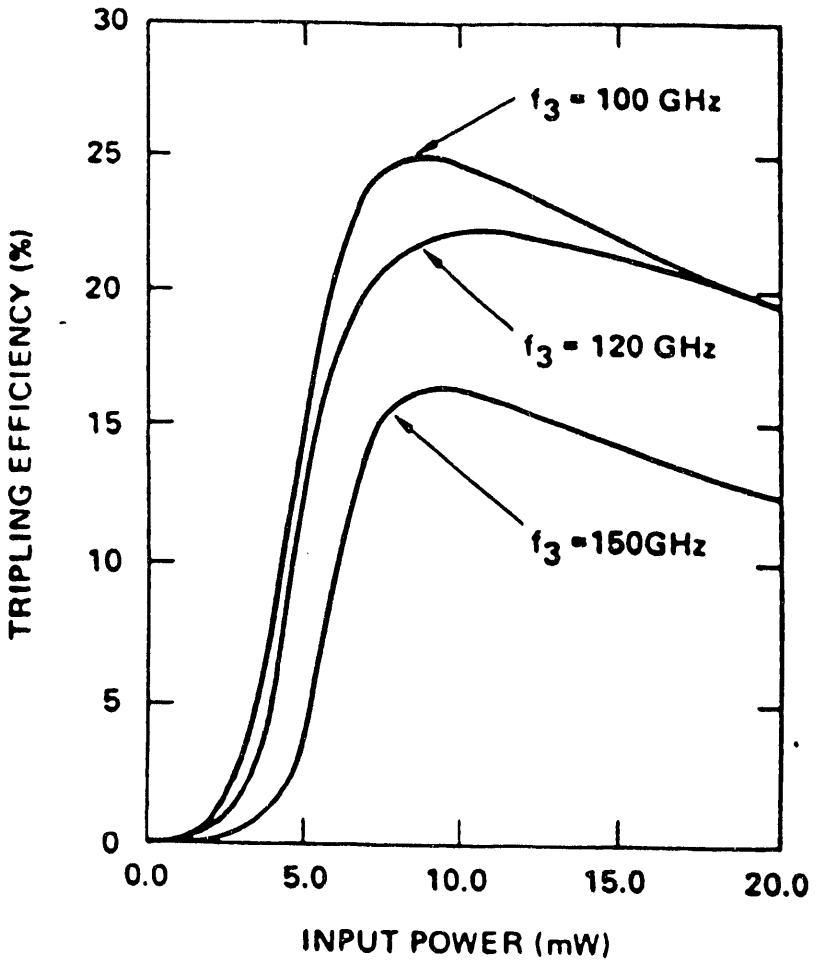

Figure 2. Predicted tripling efficiency versus input power at various input frequencies for the experimental GaAs BIN diode grid.

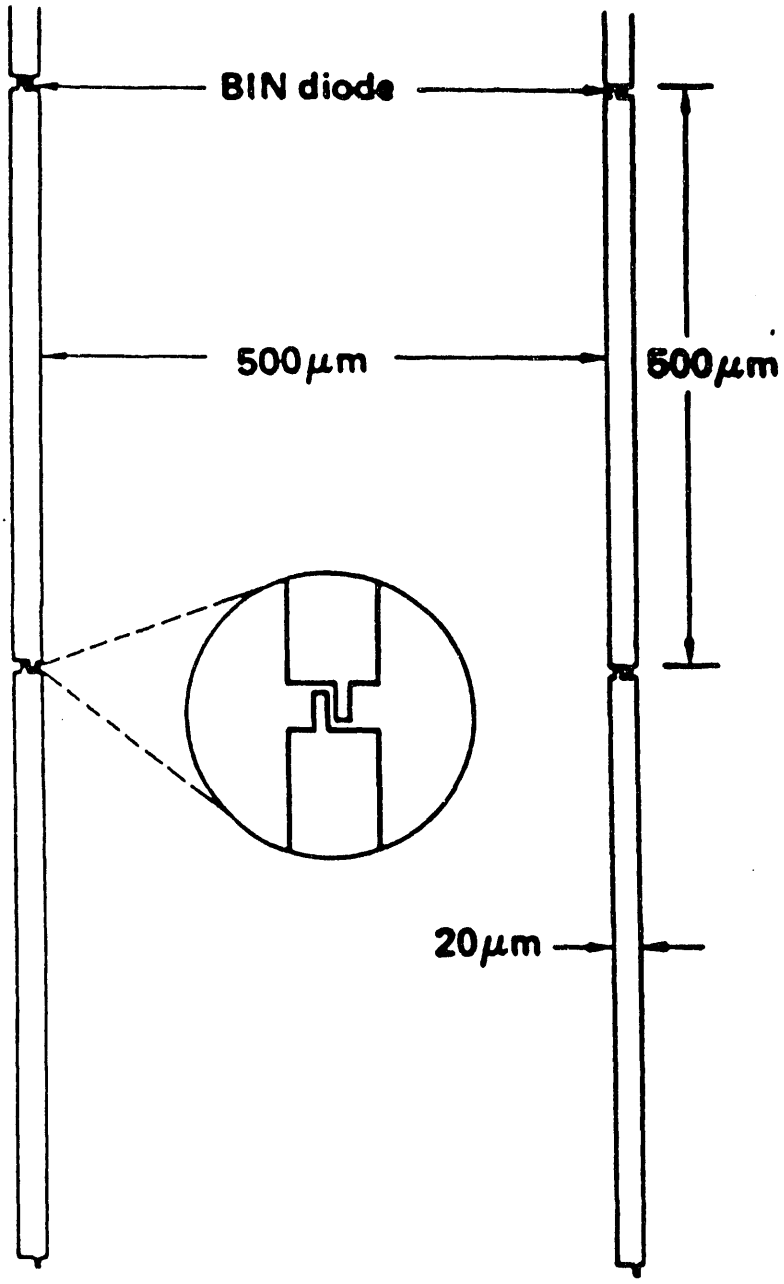

Figure 3. BIN diode tripler array.

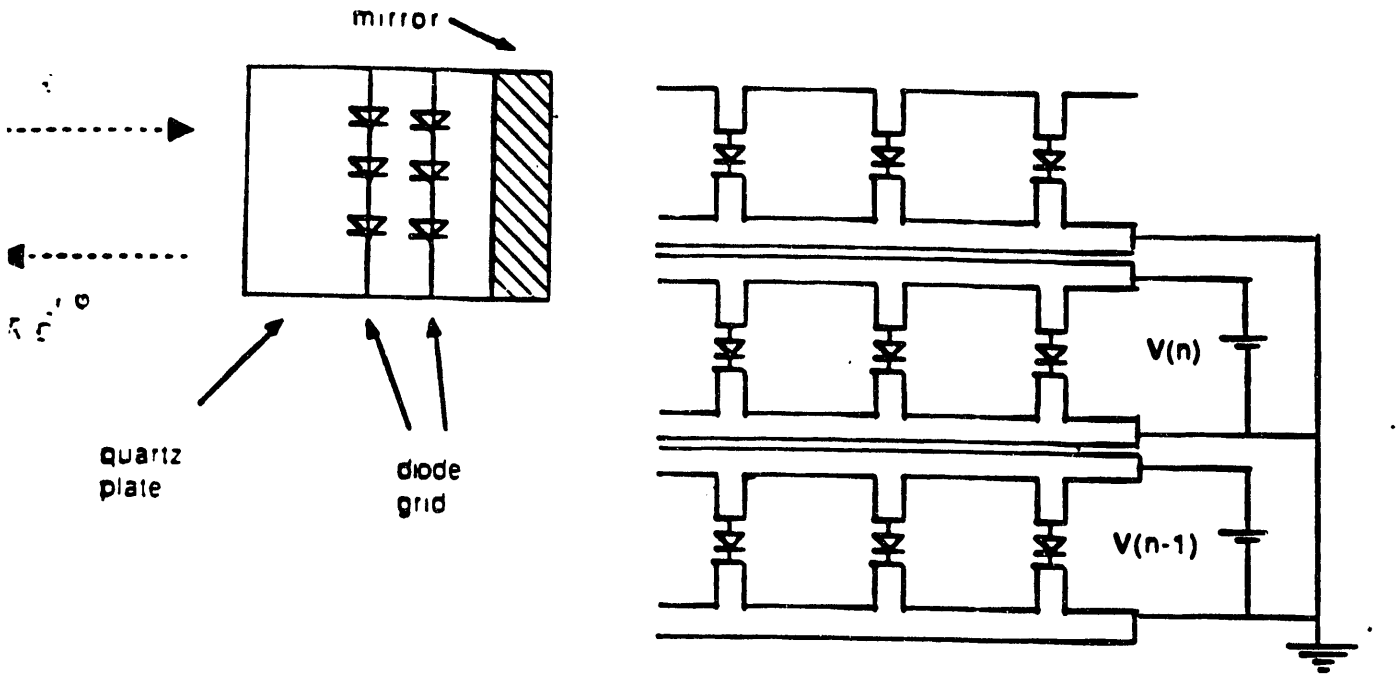

Amplitude

Phase

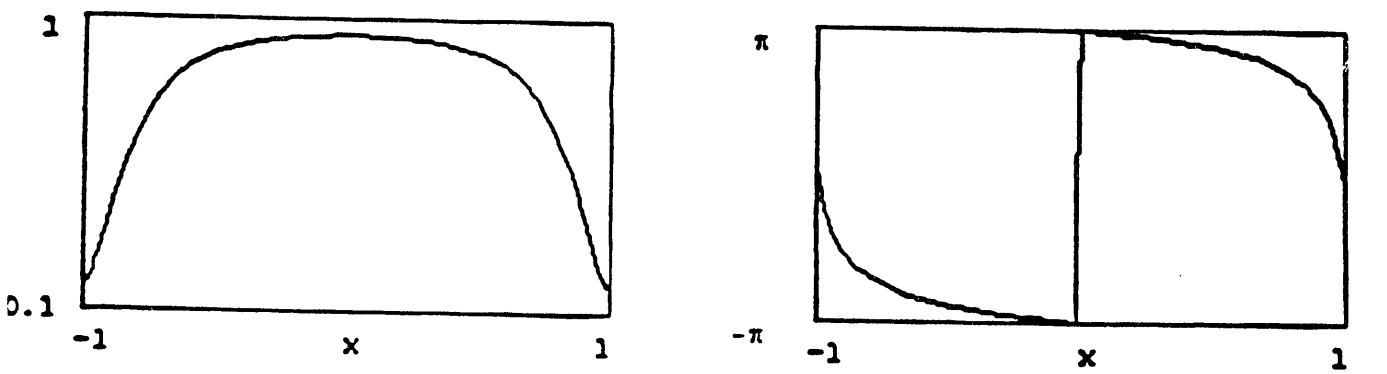

without cover plate (Rdiode=10 ohm)

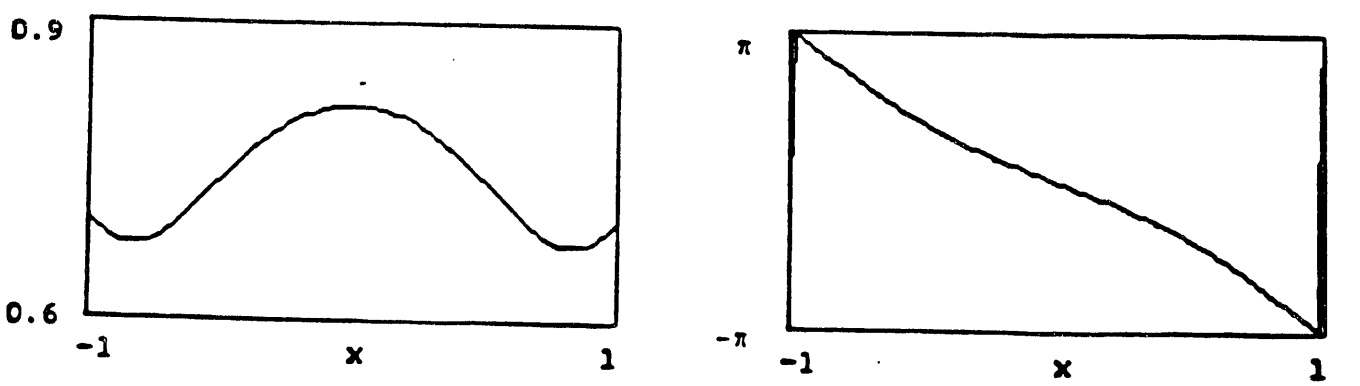

with cover plate (Rdiode=10 ohm)

x = normalized diode grid reactance

Figure 4. Schematic of two layer phase shifter and diode grid layout.

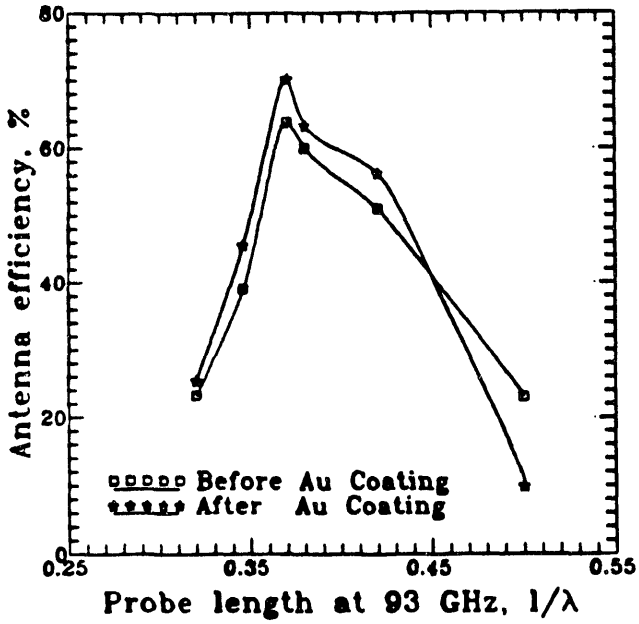

Figure 5. Aperture efficiency versus dipole length.

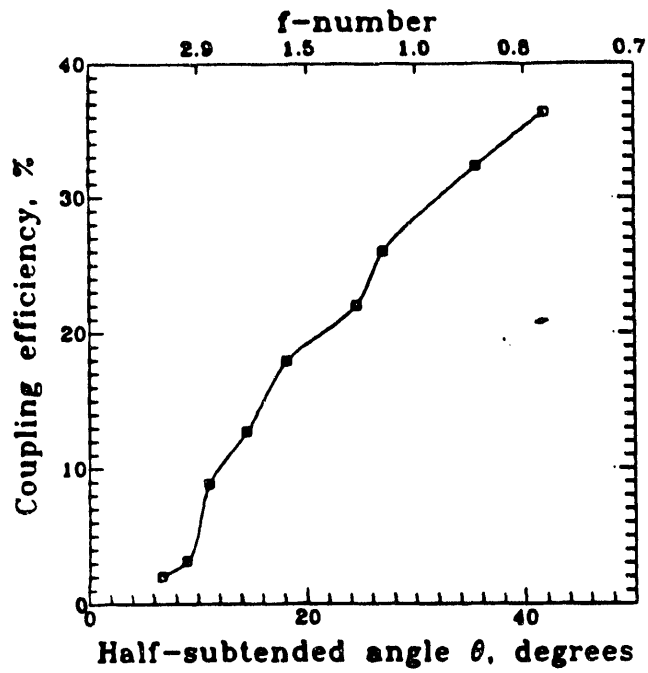

Figure 6. Coupling efficiency versus f-number.

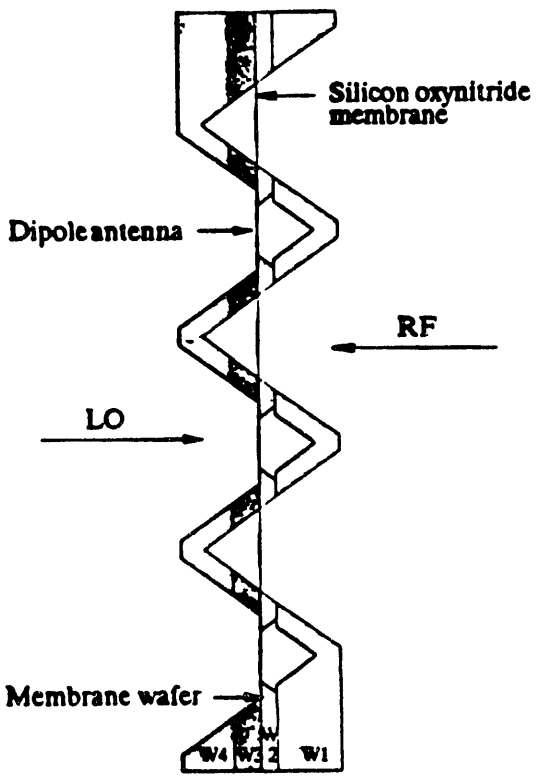

Figure 7. Displaced back-to-back horn array.

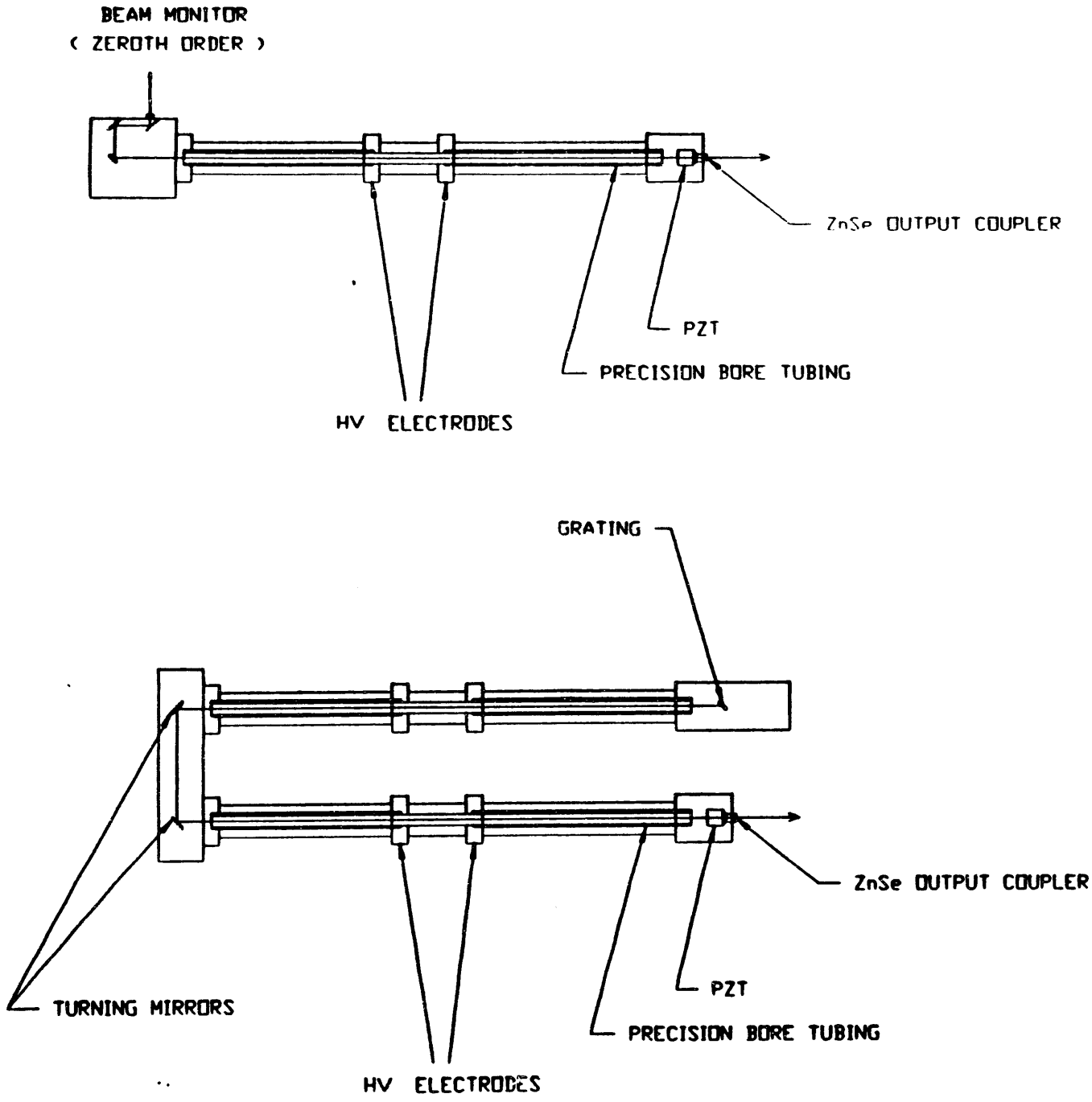

Figure 8. Schematic of linear and folded CO_2 laser configurations.

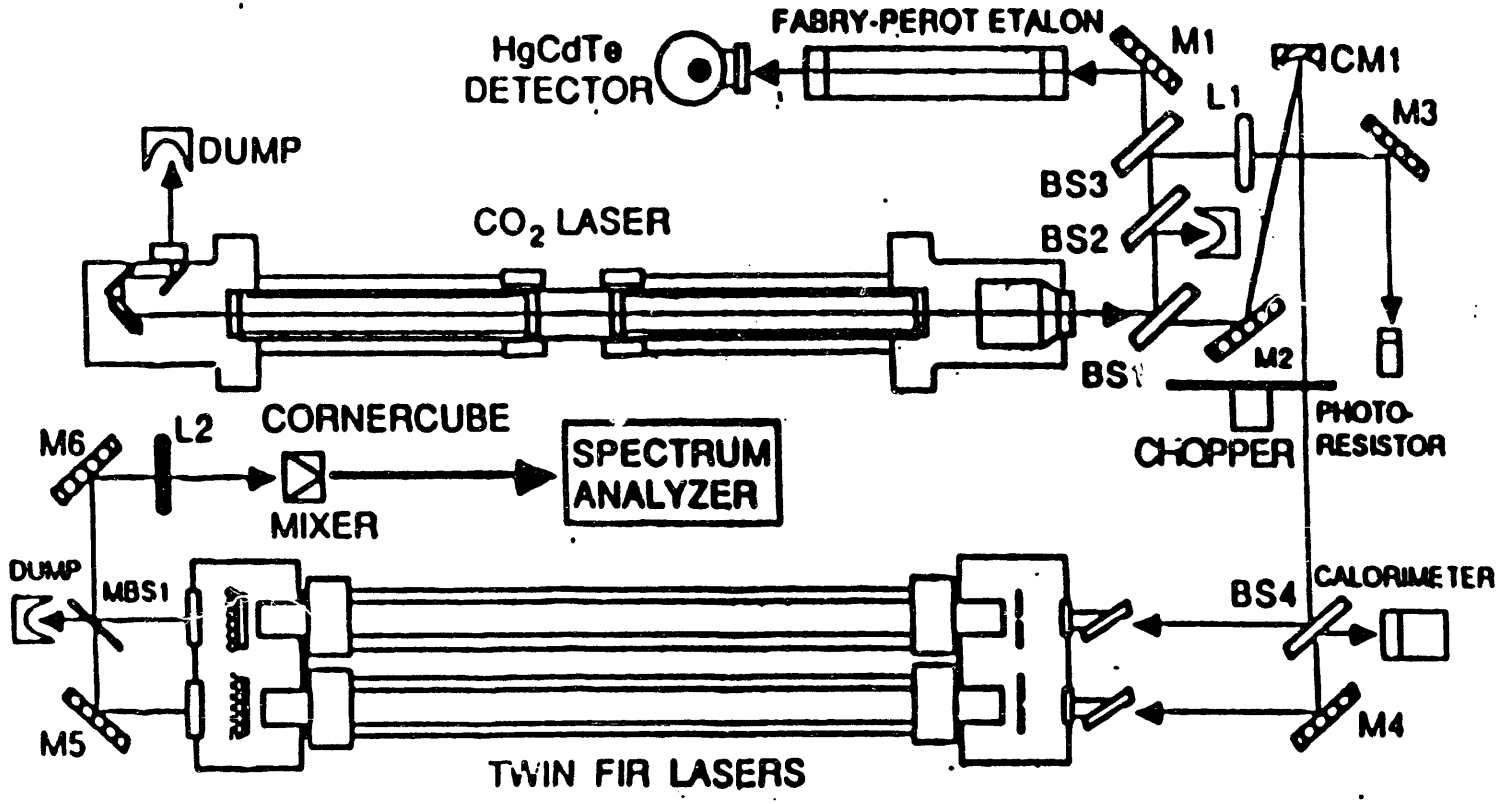

Figure 9. Outline sketch of CO_2/FIR laser system developed at UCLA for use in plasma diagnostics experiments.

Far-Infrared Ring Laser Diagram

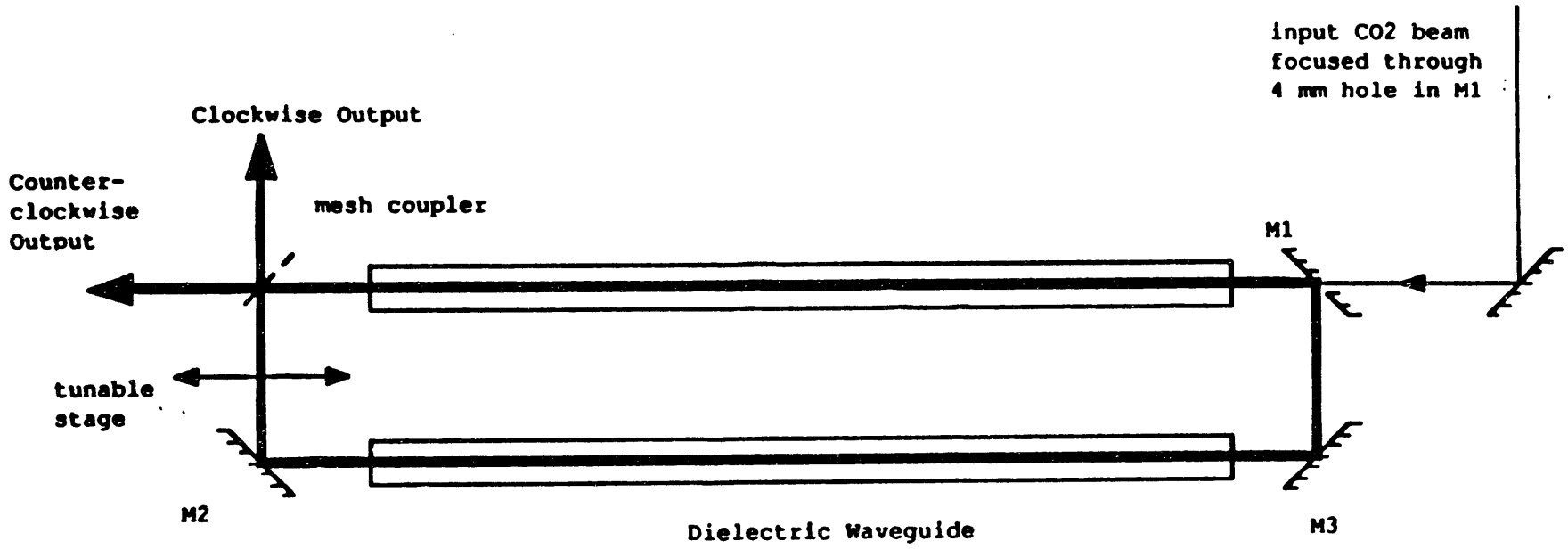

Figure 10. Far-infrared ring laser diagram.

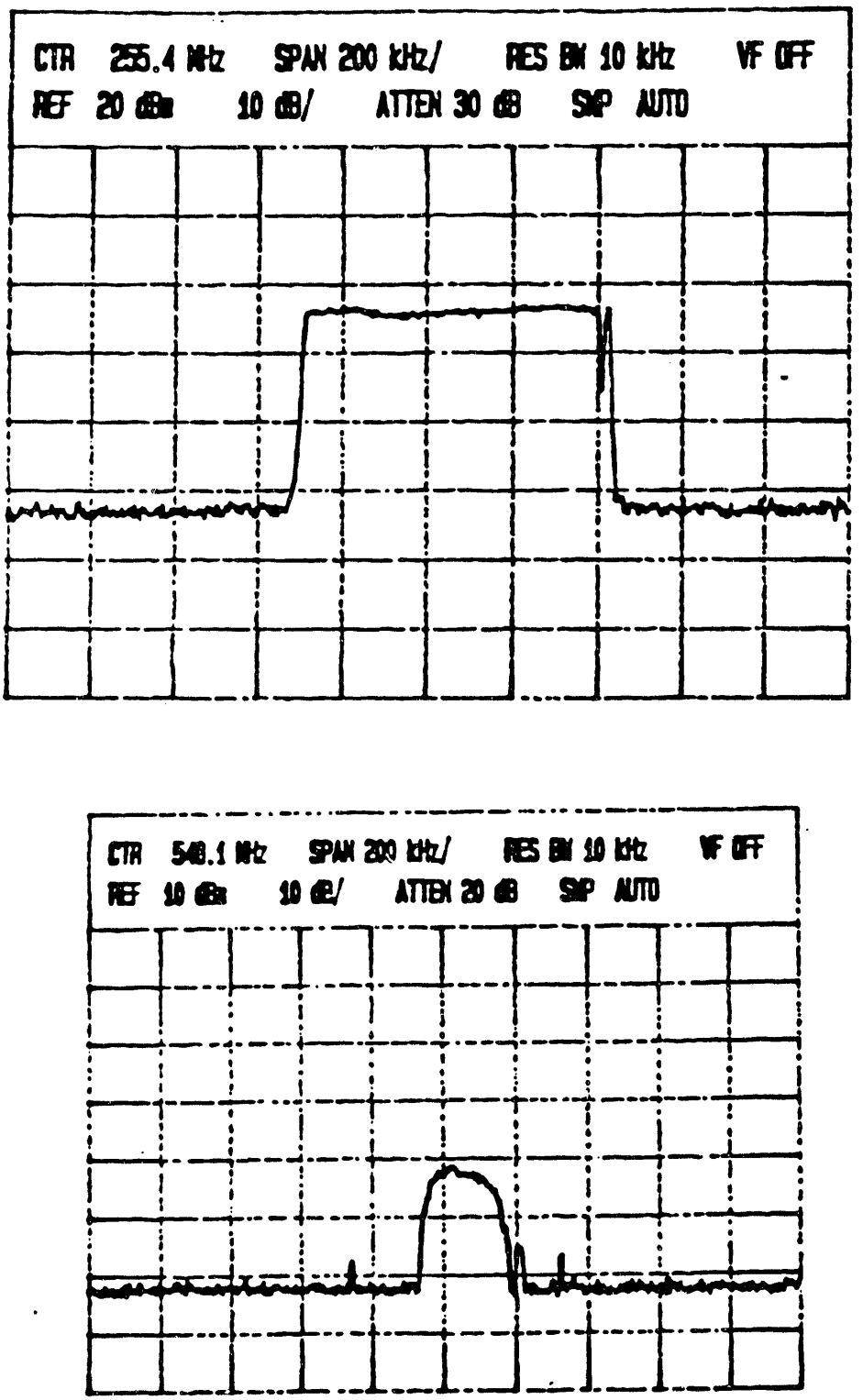

Figure 11. Plots of the absolute frequency pulling of the FIR laser in linear (upper) and ring (lower) configurations under the influence of strong feedback which sweeps the gain.

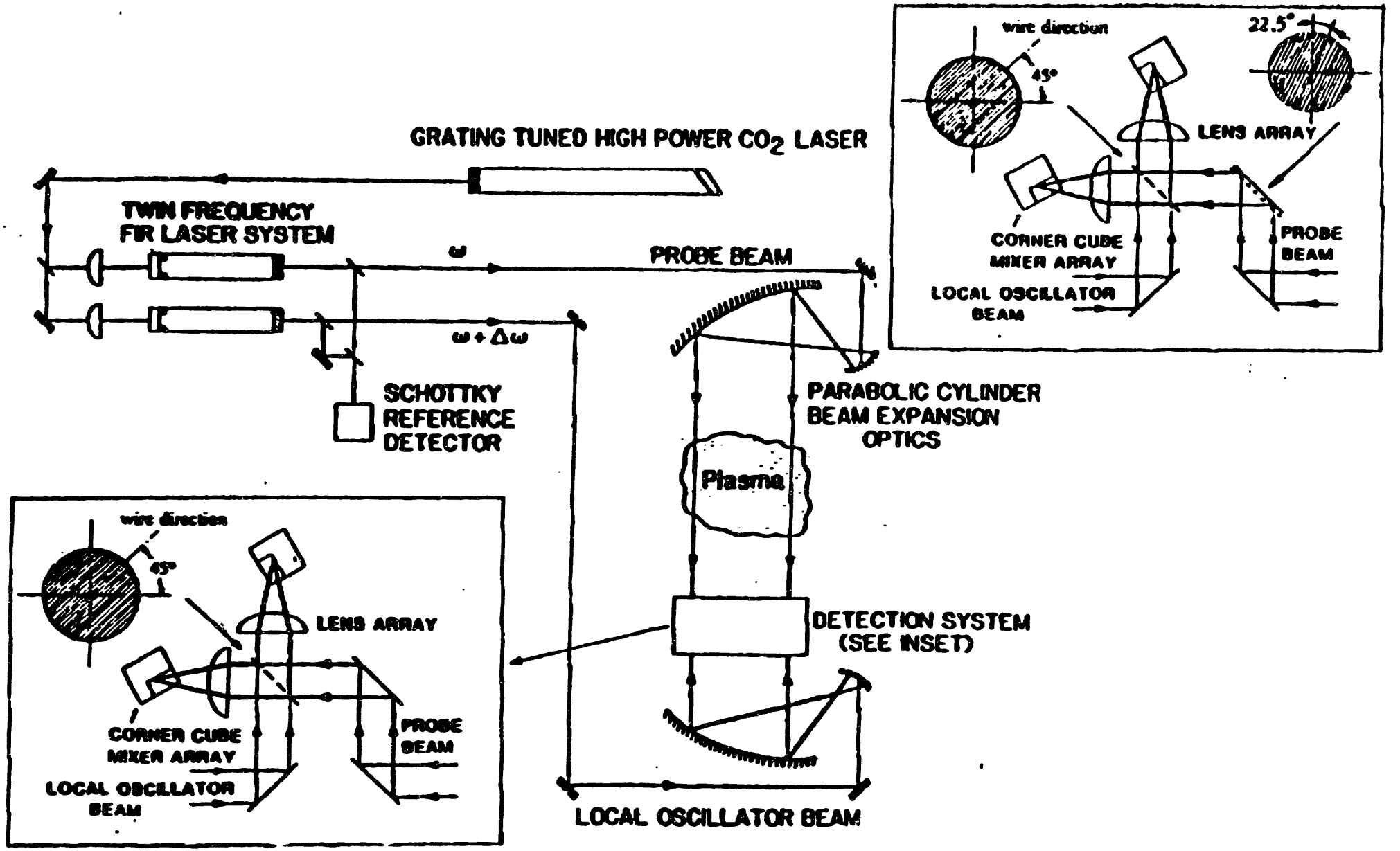

Figure 12. Schematic of the multichannel far-infrared interferometry/polarimetry system.

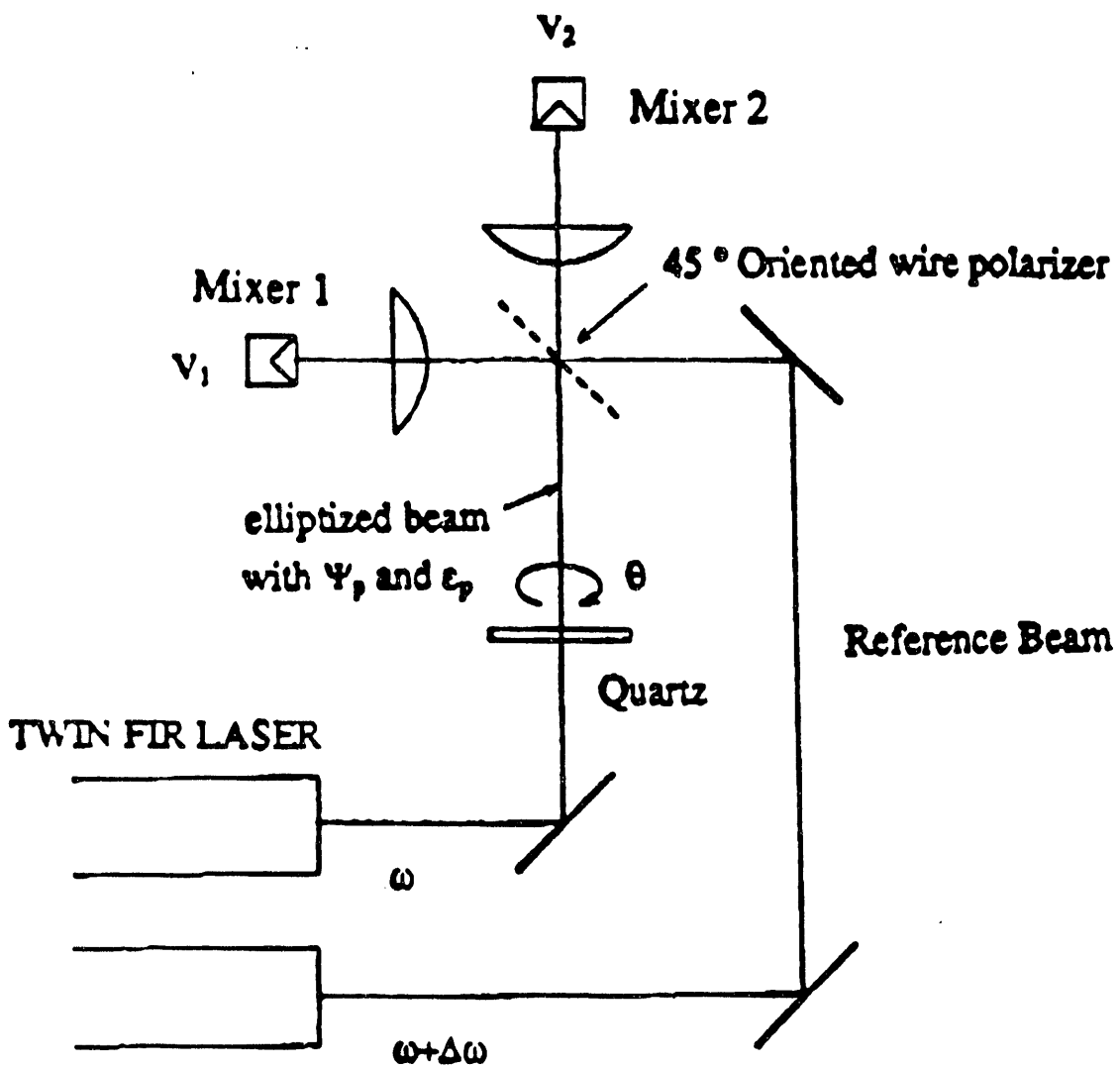

$\lambda = 432\ \mu m$ (HCOOH)

$\Delta\omega/2\pi \sim 750$ kHz

Figure 13. Experimental arrangement utilized for the elliptization measurement.

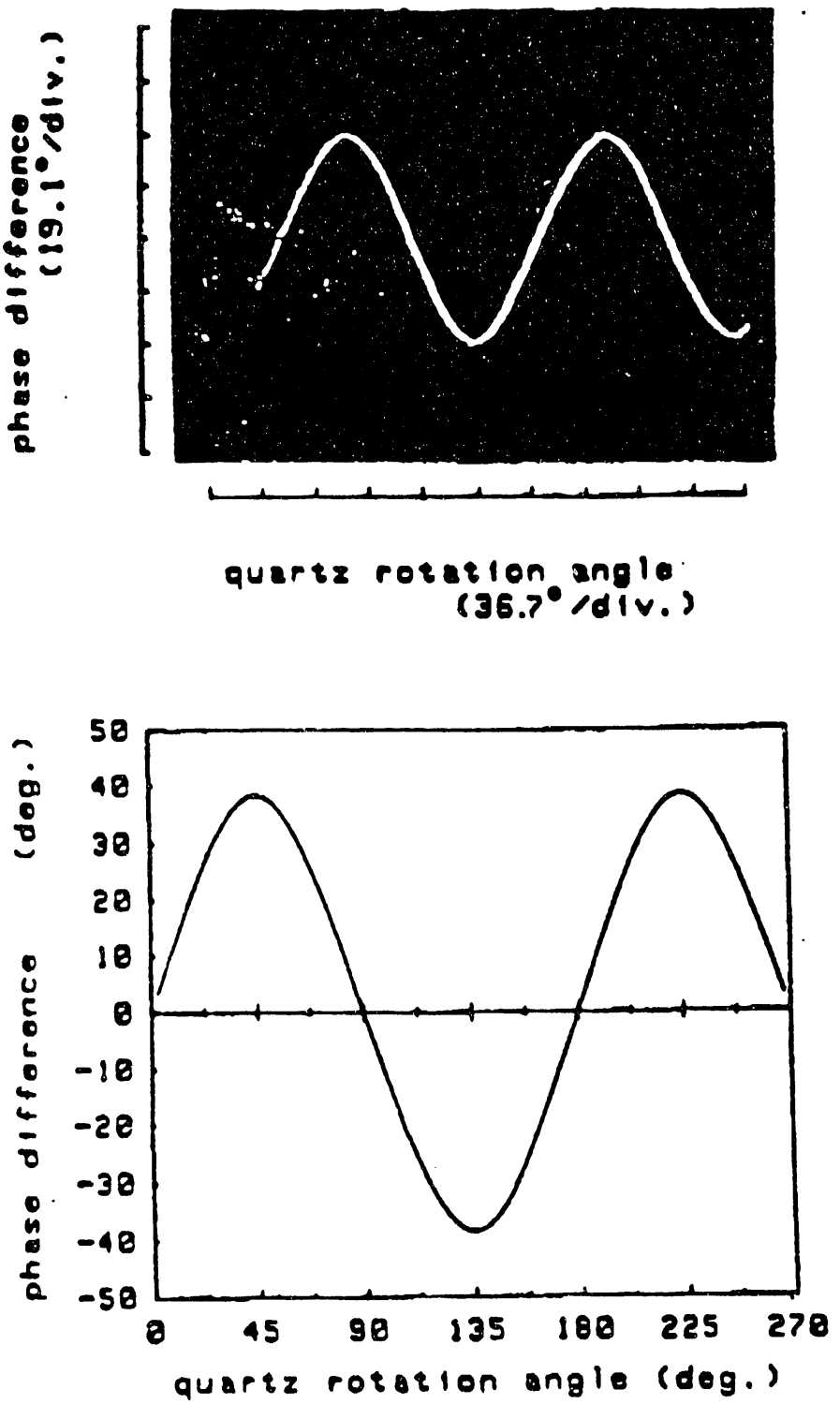

Figure 14. (a) Experimental results illustrating the phase difference between two equivalent mixer outputs versus the quartz rotation angle and (b) theoretical prediction curve.

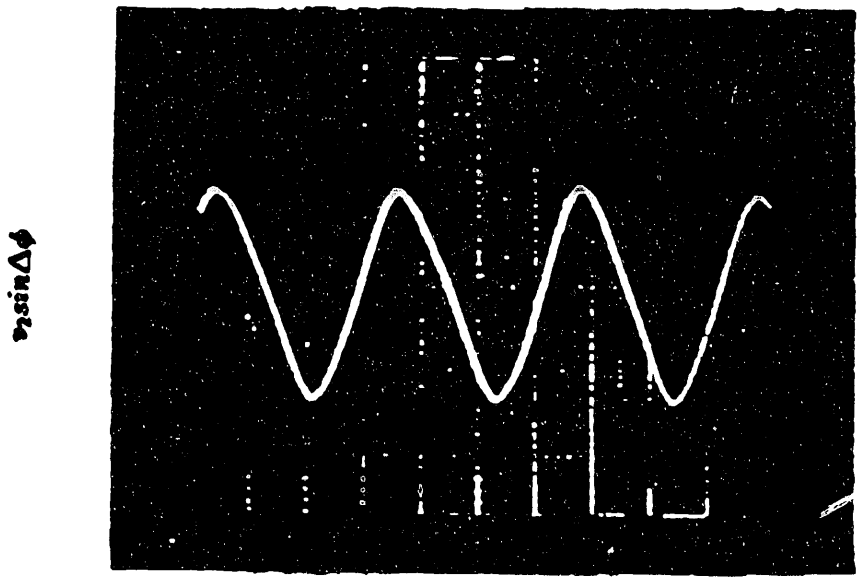

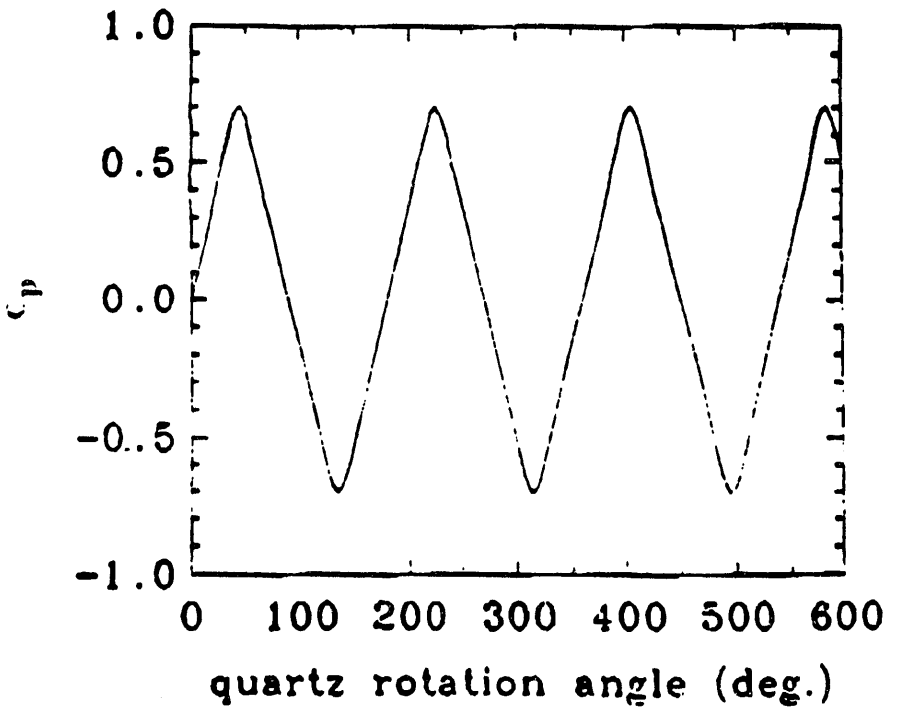

Figure 15. (a) Experimental results showing the quadrature output of locking amplifier versus the quartz rotation angle (b) theoretical prediction curve.

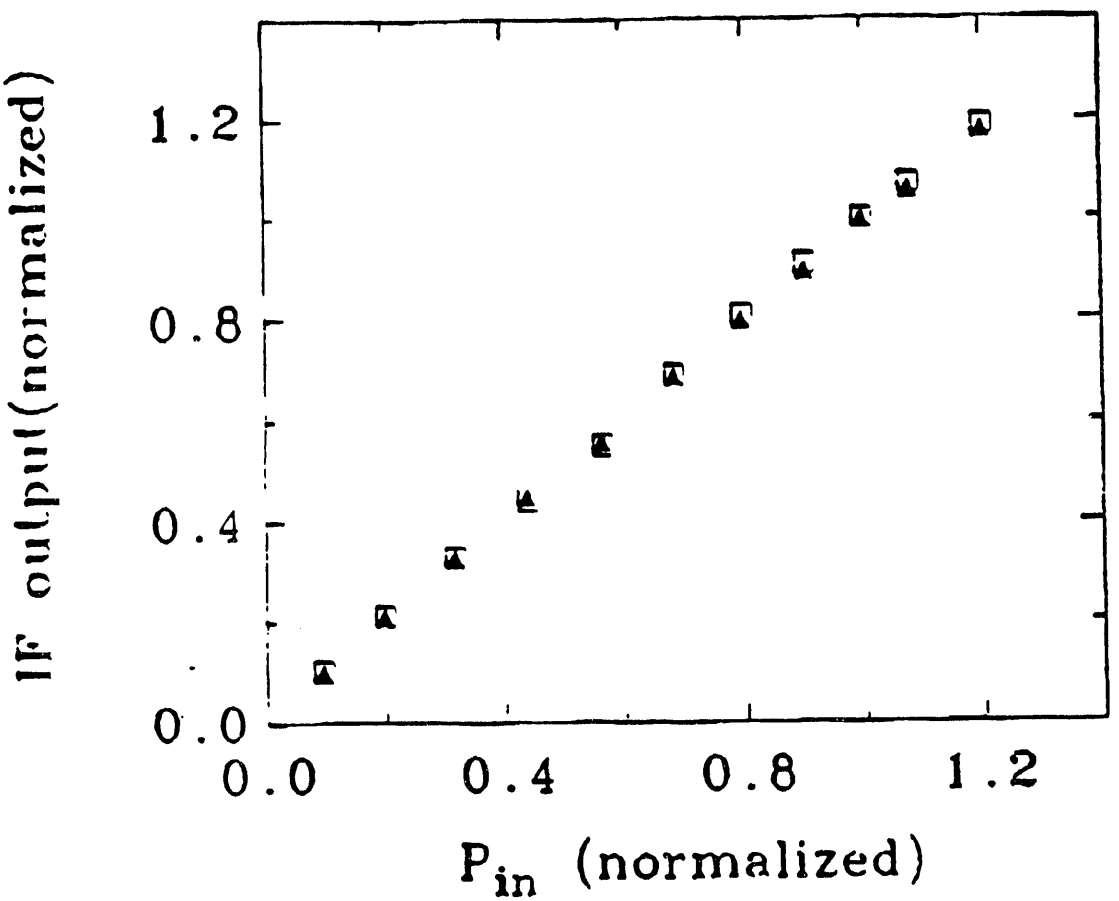

Figure 16. Mixer response calibration.

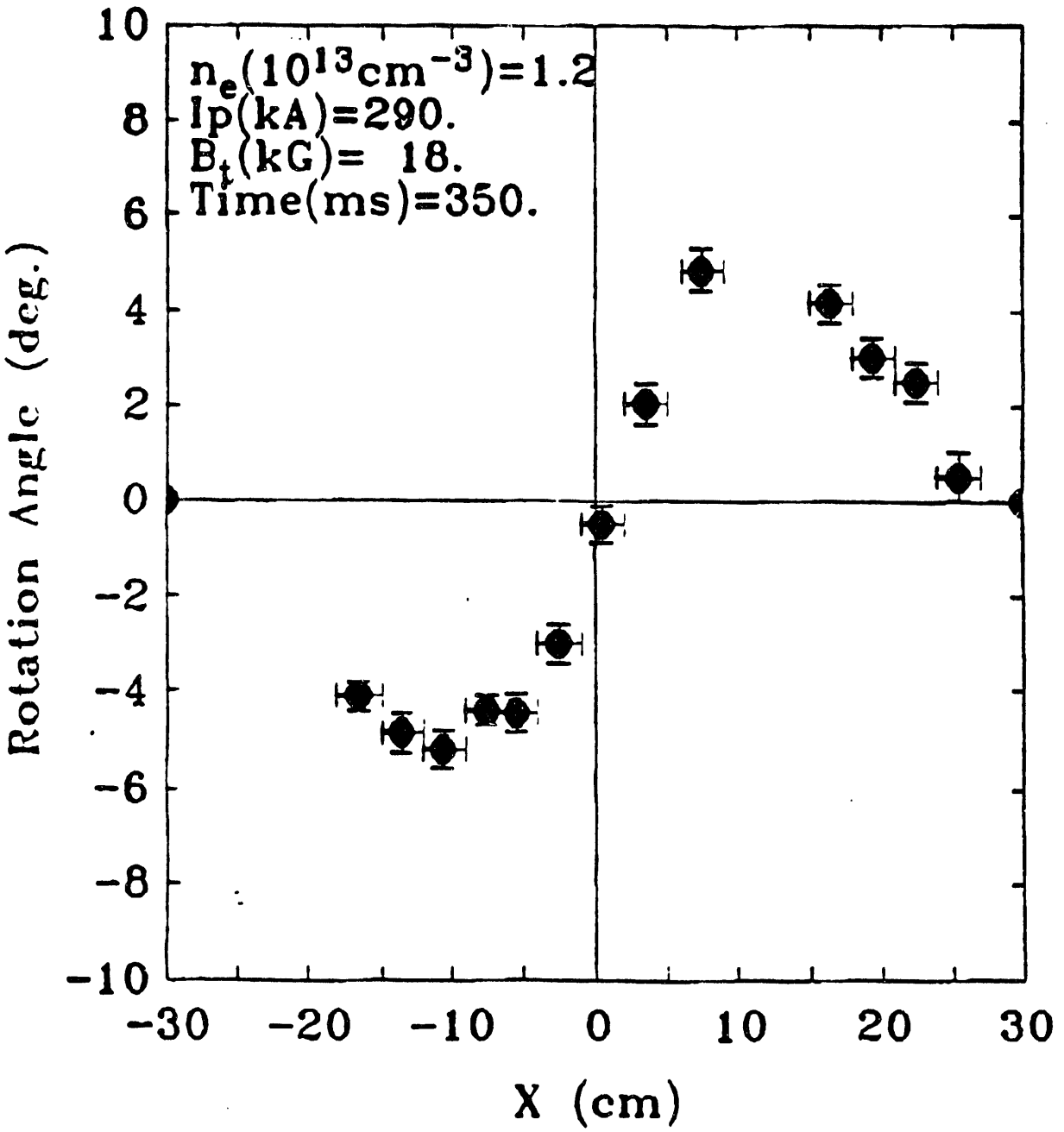

Figure 17. Faraday rotation measurements on TEXT.

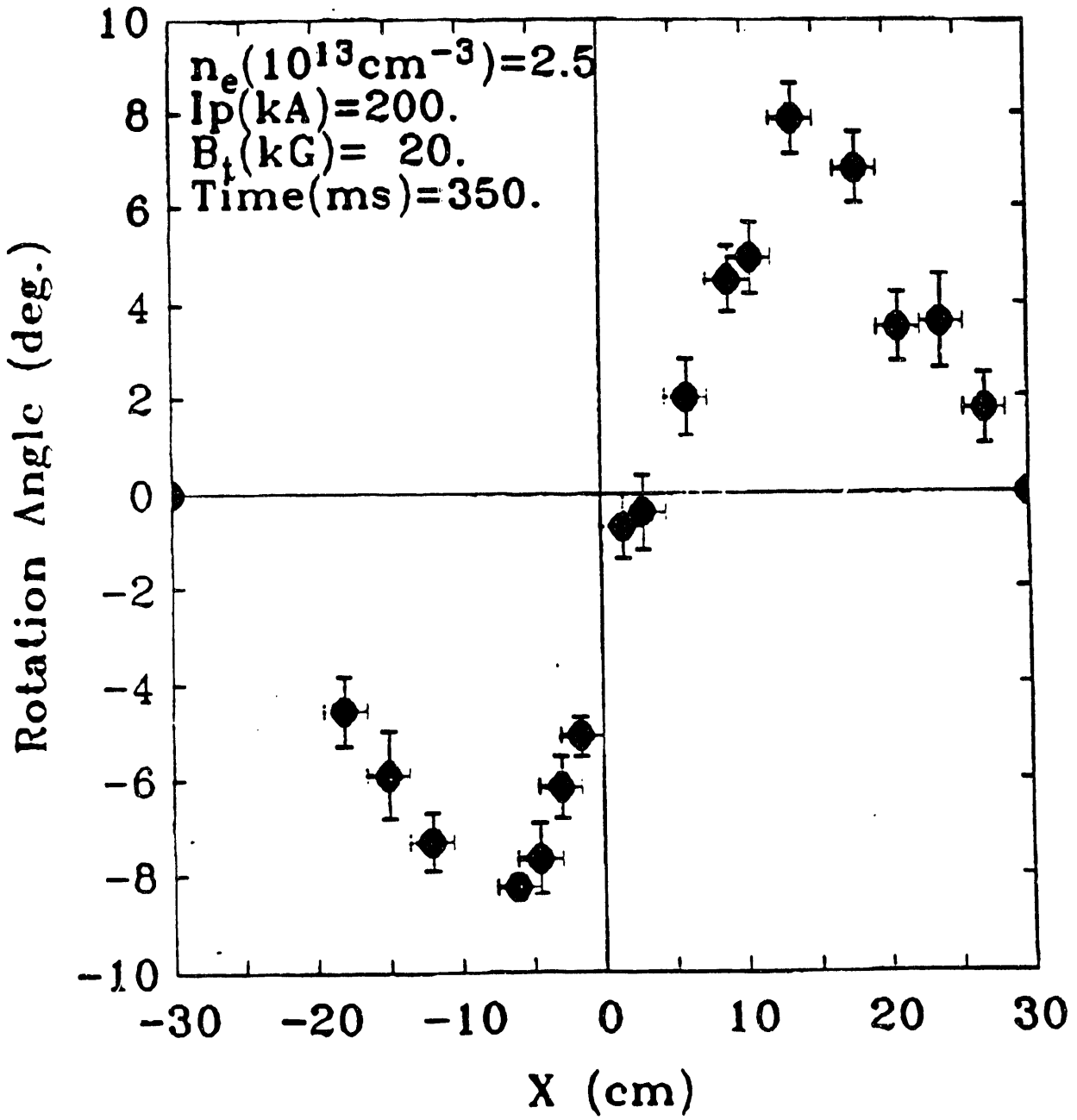

Figure 18. Faraday rotation measurements on TEXT.

TASK VIIA: PROGRESS REPORT

Transport Studies on the TEXT Tokamak Using FIR Scattering/Interferometry and Reflectometry

FY 1990

Principal Investigator:
W.A. Peebles

Co-Principal Investigator:
N.C. Luhmann, Jr.

SECTION I. PROGRESS REPORT FY90

Task VIIA

The research efforts described below have been performed in support of the overall TEXT Research Program. They naturally fall into two categories. First, research activities pursued primarily by UCLA with the support of TEXT program staff (e.g. "Experimental Evidence for Coupling of Plasma Particle and Heat Transport in the TEXT Tokamak," PRL 65, 337-340 1990). Second, research activities where UCLA has been providing a supportive role for research projects initiated by TEXT staff (e.g. "Electron Thermal Confinement Studies with Applied Resonant Fields on TEXT," Nuclear Fusion 29, 547-562 1989).

The contributions in both categories have been broadbased and relevant to the mandate of the Transport Task Force Initiative of the DOE. The reference list at the end of this Section indicates the major contributions over the last year. These numerous contributions to the TEXT Program involved a major UCLA commitment (three full time staff at TEXT), requiring hardware maintenance and operation, data acquisition and analysis, as well as generation of publications.

As mentioned above the UCLA FIRSIS (Far-Infrared Scattering-Interferometry System) on TEXT has been involved in several areas of magnetic confinement fusion research over the past year which are particularly relevant to the mandate of the Transport Task Force Initiative of the DOE. These include the study of

A. electrostatic drift wave turbulence and transport,

B. ion-pressure-gradient-driven turbulence and transport,

C. spatial localization of fluctuation measurements,

D. MHD physics and relation to turbulence and transport

- (i) Mirnov oscillations
- (ii) sawtooth phenomena
- (iii) disruptions

E. density profile parameterization and tomography, and

electron cyclotron resonance heating effects on

- (i) electron density profiles
- (ii) microturbulence

Each of the above areas of research will now be briefly reviewed. Details may be found in the references listed at the end of this section.

A. Electrostatic Drift-Wave Turbulence and Transport

Efforts to relate measurements of broadband electrostatic turbulence to heat and particle transport in the TEXT tokamak have shown that fluctuations can indeed account for the measured transport when the mean wavevector is $\bar{k}$ = 2-3 cm^{-1}. These results are described in a paper by R.V. Bravenec et al.[1] and will be presented as invited talks at the IAEA-1990 meeting by R.L. Hickok[2] and the APS-DPP 1990 meeting by D.W. Ross. This work involves a detailed comparison of the UCLA FIR scattering data with the RPI HIBP data and the Texas Langmuir probe measurements. In addition, the UCLA interferometer measurements were essential for the modulated gas feed experiments.

B. Ion-Pressure-Gradient-Driven Turbulence and Transport

An active ion feature (i.e. turbulence propagating in the ion diamagnetic drift direction) in the density fluctuation spectra has been identified in high density gas-fueled discharges on TEXT via FIR scattering and can be suppressed by hydrogen pellet injection. Transport models indicate that this mode can account for the high-density saturation of the global energy confinement time observed in tokamaks. These results are detailed in recent papers by D.L. Brower et al.[3] and W.L. Rowan et al.[4].

C. Spatial Localization of Density Fluctuation Measurements

The spatial localization of the density fluctuation measurements represents a crucial issue when relating microturbulence observations to transport. During the past year, this has been addressed by using an externally applied resonant field (see papers by D.L. Brower et al.[5] and W.A. Peebles et al.[6]) and correlations between multiple scattering volumes (see W.A. Peebles et al., IAEA-1990[7]). The latter technique determines the correlation of signals from overlapping scattering volumes at the same wavevector. By moving one scattering volume with respect to the other, the decorrelation of the signals versus distance offers information on the spatial distribution of fluctuations.

D. MHD Physics and Relation to Turbulence and Transport

(i) Mirnov Oscillations: Both naturally occurring (S. McCool et al.[8], J. Chen et al., APS-DPP-1990) and externally imposed (S. McCool et al.[9]) magnetic island structures have been studied in the past year. Mirnov oscillations are observed to modify the plasma potential profile which in turn has dramatic implications for the fluctuation spectra and amplitude. By imposing the applied resonant field (EML), a strong shear in the poloidal rotation velocity is induced which results in the stabilization of the density fluctuations. This type of phenomena can be directly related to the rotation increase and confinement improvement observed at the L-to H-mode transition (C.X. Yu et al., APS-DPP-1990).

(ii) Sawtooth Phenomena: Experimental evidence for the coupling of plasma particle diffusion and heat flow was recently published in papers by D.L. Brower et al. in Physical Review Letters[10] and the EPS-90, Amsterdam Proceedings[11]. These results were also discussed at the TTF-Hilton Head meeting and will appear in the Transient Transport Session Summary by T. Simonen et al.[12]. Particle transport has also been measured by employing oscillating gas puffing (OGP) techniques. Here, the relation between heat and particle transport appears to be different. These results are discussed in publications by K. Gentle et al., EPS-89[13], EPS-90[14], and will also appear in APS-DPP-90 posters by K. Gentle et al. and B. Richards et al.

(iii) Disruptions: A major new result during the past year pertains to the physics of high-density limit disruptions in tokamaks and the long-time ($5 \times \tau_E$) precursors observed in the density fluctuations, heat transport and particle transport. Understanding disruptions and devising schemes to avoid them is an area of research especially relevant to the next generation devices such as CIT and ITER. Preliminary results and analysis will be presented at the IAEA-90 meeting[7] and a full report is currently in progress.

E. Density Profile Parameterization and Tomography

In a paper by W.L. Li et al.,[16] Gaussian and parabolic functional fits with three free parameters are made to the measured profiles and compared. Scaling of the equilibrium density profile shape with plasma current, toroidal magnetic field and density profile shape with plasma current, toroidal magnetic field and density is clearly observed. By performing a regression analysis on each free parameter for the functional fit, one can construct a set of analytical relations describing the TEXT density profile for steady-state ohmic discharges. In addition, a new tomographic approach which takes into account diffraction from density irregularities was investigated. The relevance for multichannel interferometry measurements was demonstrated numerically and the technique applied to the inversion of TEXT multichannel interferometer data as described in a paper by J. Howard et al.[17].

F. Effects of Electron Cyclotron Resonance Heating

The UCLA FIR interferometer system was employed to study the effects of ECRH on the density profile and density fluctuations with the results described in papers by D. Sing et al., EPS-90, Amsterdam[18] and B. Richards et al.[19]. Typically, one observes a small increase in the density fluctuation level despite large changes in $T_e(r)$ suggesting that ∇T_e is not an important driving term for the microturbulence in these discharges.[18] OGP measurements of the particle diffusion coefficient during ECRH indicate a marginal increase towards the edge[19].

FY90 PUBLICATIONS AND PRESENTATIONS

1. Bravenec, R.V., D.W. Ross, P.M. Schoch, D.L. Brower, J.W. Heard, R.L. Hickok, P.W. Terry, A.J. Wootton, X.Z. Yang, "Quasilinear Transport Inferred From Density Fluctuation Spectra," submitted to Nuclear Fusion, April 1990.

2. Hickok, R.L., P.M. Schoch, T.P. Crowley, J.W. Heard, K.W. Gentle, D.W. Ross, R.V. Bravenec, A.J. Wootton, B. Richards, W.L. Rowan, D.L. Brower, W.L. Li, N.C. Luhmann, Jr., W.A. Peebles, C.X. Yu, "Turbulent Fluctuations and Transport in TEXT," 13th International Conf. on Plasma Physics and Controlled Nuclear Fusion Research, Washington, D.C. 1-6 October 1990.

3. Brower, D.L., M.H. Redi, W.M. Tang, R.V. Bravenec, R.D. Durst, S. Fan, Y.X. He, S.K. Kim, N.C. Luhmann, Jr., S.C. McCool, A.G. Meigs, M. Nagatsu, A. Ouroua, W.A. Peebles, P.E. Phillips, T.L. Rhodes, B. Richards, C.P. Ritz, W.L. Rowan, A.J. Wootton, "Experimental Evidence for Ion-Pressure-Gradient-Driven Turbulence in TEXT," Nuclear Fusion 29, 1247-1254 (1989).

4. Rowan, W.L., R.V. Bravenec, J.C. Wiley, R.D. Bengtson, R.D. Durst, K.W. Gentle, S.C. McCool, A.G. Meigs, W.H. Miner, A. Ouroua, P.E. Phillips, B. Richards, T.L. Rhodes, D.W. Ross, E.J. Synakowski, A.J. Wootton, M.E. Austin, R.F. Gandy, D.L. Brower, S.K. Kim, N.C. Luhmann, Jr., W.A. Peebles, J.Y. Chen, Z.M. Zhang, P.M. Schoch, R.L. Hickok, K.W. Wenzel, X.Z. Yang, "Transport With Pellet Fueling in the Texas Experimental Tokamak," Nuclear Fusion 30, 903-918 (1990).

5. Brower, D.L., C.X. Yu, S.J. Zhao, W.A. Peebles, N.C. Luhmann, Jr., X.Z. Yang, P.M. Schoch, R.L. Hickok, "Spatial Resolution of FIR Scattering Measurements on TEXT," Rev. Sci. Instrum. 61, (1990).

6. Peebles, W.A., S. Baang, D.L. Brower, K. Burrell, E.J. Doyle, R.J. Groebner, T. Lehecka, N.C. Luhmann, Jr., H. Matsumoto, R. Philipona, C. Rettig, T.L. Rhodes, C.X. Yu, "Fluctuation Measurements in the DIII-D and TEXT Tokamaks via Collective Scattering and Reflectometry," Rev. Sci. Instrum. 61, (1990).

7. Peebles, W.A., D.L. Brower, N.L. Bretz, and the UCLA, DIII-D, TEXT and TFTR Groups, "Collective Scattering Studies of Microturbulence in DIII-D, TEXT and TFTR," 13th International Conference on Plasma Physics and Controlled Nuclear Fusion Research, Washington, D.C., 1-6 October 1990.

8. McCool, S.C., J.Y. Chen, A.J. Wootton, R.D. Bengtson, D.L. Brower, W.A. Craven, M.S. Foster, R.L. Hickok, H. Lin, C.P. Ritz, P.M. Schoch, B.A. Smith, X.Z. Yang, C.X. Yu, "The Effect of Magnetic Perturbations on the Edge Transport in TEXT," Journal of Nuclear Materials, 1990.

9. McCool, S.C., A.J. Wootton, A.Y. Aydemir, R.D. Bengtson, J.A. Boedo, R.V. Bravenec, D.L. Brower, J.S. deGrassie, T.E. Evans, S.P. Fan, J.C. Forster, M.S. Foster, K.W. Gentle Y.X. He, R.L. Hickok, G.L. Jackson, S.K. Kim, M. Kotschenreuther, N.C. Luhmann, Jr., W.H. Miner, N. Ohyabu, D.M. Patterson, W.A. Peebles, P.E. Phillips, T.L. Rhodes, B. Richards, C.P. Ritz, D.W. Ross, W.L. Rowan, P.M. Schoch, B.A. Smith, J.C. Wiley, S.B. Zheng, "Electron Thermal Confinement Studies with Applied Resonant Fields on TEXT," Nuclear Fusion 29, 547-562 (1989).

10. Brower, D.L., S.K. Kim, K.W. Wenzel, M.E. Austin, M.S. Foster, R.F. Gandy, W.L. Lin, N.C. Luhmann, Jr., S.C. McCool, M. Nagatsu, W.A. Peebles, C.P. Ritz, C.X. Yu, "Experimental Evidence for Coupling of Plasma Particle and Heat Transport in the TEXT Tokamak," Phys. Rev. Lett. 65, 337-340 (1990).

11. Brower, D.L., C.X. Yu, S.K. Kim, K.W. Wenzel, M.E. Austin, M.S. Foster, R.F. Gandy, W.L. Li, N.C. Luhmann, Jr., S.C. McCool, M. Nagatsu, W.A. Peebles, C.P. Ritz, B.A. Smith, Z.M. Zhang, "Coupling of Plasma Particle Diffusion and Heat Flow in TEXT," Proc. of 17th European Conf. on Controlled Fusion and Plasma Heating, Amsterdam, The Netherlands, June 1990.

12. Simonen, T.C., D.L. Brower, P. Efthimion, J.C. deHaas, E. Fredrickson, K.W. Gentle, E.B. Hooper, E. Marmar, R. Stambaugh, "Plasma Transport Studies Using Transient Techniques," Plasma Physics and Controlled Fusion.

13. Gentle, K.W., B. Richards, D.L. Brower, M.E. Austin, G. Cima, N.C. Luhmann, Jr., W.A. Peebles, P.E. Phillips, W.L. Rowan, A.J. Wootton, "Effect of ECH on Particle Transport in the TEXT Tokamak," Proc. of Sixteenth European Conf. on Controlled Fusion and Plasma Physics (Venice, Italy), Europhysics Conf. Abstracts 13B, Part 1, 159-162 (1989).

14. Gentle, K.W., M.E. Austin, D.L. Brower, G. Castle, G. Cima, R. Gandy, W.L. Li, N.C. Luhmann, Jr., S.C. McCool, D.M. Patterson, W.A. Peebles, P.E. Phillips, B. Richards, W.L. Rowan, P.M. Schoch, B.A. Smith, D.C. Sing, A.J. Wootton, C.X. Yu, "Particle and Heat Transport from TEXT Perturbation Experiments," Proc. of 17th European Conference on Controlled Fusion and Plasma Heating, Amsterdam, The Netherlands, June 1990.

15. Li, W.L., D.L. Brower, S.K. Kim, M. Nagatsu, C.X. Yu, W.A. Peebles, N.C. Luhmann, Jr., S.C. McCool, R.V. Bravenec, X.Z. Yang, Z.M. Zhang, "Plasma Parameter Dependences of the Electron Density Profile in TEXT," Rev. Sci. Instrum. 61, 1990.

16. Howard, J., W.A. Peebles, D.L. Brower, S.K. Kim, N.C. Luhmann, Jr., "Application of Diffraction Tomography to Plasma Density Measurements," Rev. Sci. Intrum. 61, (1990).

17. Sing, D.C., J. Schultz, B. Richards, M.E. Austin, D.L. Brower, J.Y. Chen, G. Cima, K.W. Gentle, R.L. Hickok, W.L. Li, N.C. Luhmann, Jr., W.A. Peebles, P.E. Phillips, R. Gandy, P.M. Schoch, A.J. Wootton, X.Z. Yang, C.X. Yu, "Recent Electron Cyclotron Heating Results on TEXT," Proc. of 17th European Conf. on Controlled Fusion and Plasma Heating, Amsterdam, The Netherlands, June 1990.

18. Richards, B., K.W. Gentle, D.C. Sing, P.E. Phillips, W.L. Rowan, A.J. Wootton, D.L. Brower, N.C. Luhmann, Jr., W.A. Peebles, G. Cima, "Particle Transport During ECRH on the TEXT Tokamak," Eighth Topical Conf. on Radio-Frequency Power in Plasmas, AIP Conf. Proceedings 190, ed. Roger McWilliams, pp. 72-75, Irvine, California, 1989.

TASK VIIB: PROGRESS REPORT

Microturbulence Studies on the DIII-D Tokamak Via Collective Scattering and Reflectometry

FY 1990

Principal Investigator:
W.A. Peebles

Co-Principal Investigator:
N.C. Luhmann, Jr.

SECTION I. PROGRESS REPORT FY90

Task VIIB

I. INTRODUCTION

The Task VIIB Program at UCLA is primarily directed towards identifying the role of low frequency microturbulence in various confinement regimes on the DIII-D tokamak. Advanced fluctuation and profile diagnostics have been installed over the last year and initial results have provided new insight to a variety of research topics. Emphasis, to date, has been placed on characterizing the role of edge turbulence at the L-H transition utilizing the reflectometer system. In addition, preliminary work, utilizing a heterodyne FIR laser scattering system, was performed during FY90 to search for ITGD turbulence. This will be followed in FY91 by operation of the improved carcinotron tracking receiver system which will increase signal to noise and eliminate the effects of feedback that limit the existing system.

It should be noted that Task VIIB primarily supports effort on the scattering and correlation reflectometer systems. Profile measurements using an X-mode reflectometer are primarily supported from a separate DIII-D subcontract. Development of new reflectometry techniques and the associated advanced technology is supported under Tasks IIIA & B. However, since the measurement capabilities from all these systems are utilized synergistically to optimize acquisition of physics information, all aspects of the DIII-D work will be summarized with particular emphasis on the Task VIIB supported components.

Integration of the UCLA permanent staff into the DIII-D Group is now complete. The UCLA staff operate as part of the DIII-D team and initiate physics studies of interest through the "Mini-Proposal" System and participation in various working groups. The last year has been extremely productive from both a technical and physics viewpoint. Major progress achieved in the last year is summarized below, where physics and technical achievements have been separated into two categories. Invited papers will or have been presented at the APS 1990 Topical Conference on High Temperature Plasma Diagnostics, the 1990 APS Plasma Divisional Meeting; and the 1990 IAEA Conference to be held in Washington.

A. Technical Achievements

1. Density profiles have been obtained on DIII-D in Ohmic, L and H-mode plasmas. Excellent agreement has been observed with profiles determined using Thomson scattering and chord averaged interferometry data. Profiles can presently be obtained every 2.5 ms. In the coming year it is intended to demonstrate this as a routine measurement. It is also planned to upgrade the system to further improve measurement accuracy and provide a *continuous* measure of density profile evolution.

2. Construction of the first stage of the correlation reflectometer was completed, tested in laboratory and installed on DIII-D. Preliminary data is described below. Based on the success of future measurements, the correlation reflectometer will be upgraded to provide the ability to study *both* phase and amplitude fluctuations independently. This should allow the spatial profile of density fluctuations to be determined through comparison with the density profile X-mode measurements.

3. Construction, testing and installation of the multichannel heterodyne, FIR laser scattering system was completed. Data is described below. Expected difficulties with feedback of laser radiation were found to limit the frequency resolution and wavenumber range able to be studied.

4. A carcinotron, heterodyne scattering system was constructed and recently installed on DIII-D. The system utilizes a tracking receiver to eliminate the frequency pulling effects caused by feedback. In addition, the increased power available from the carcinotron ($\sim$ 300 mW) will significantly improve signal to noise, thereby allowing access to longer wavenumbers and improved spatial resolution. The system was thoroughly tested in the laboratory prior to installation on DIII-D and met all expectations. Preliminary data is expected prior to the 1990 APS Meeting.

B. Physics Achievements

1. Rapid suppression ($\sim$ 100 μs) of edge turbulence is observed coincident with the initial drop in H_α emission. Suppression is limited to an edge spatial region which extends from the scrape-of-layer in past the separatrix $\sim$ 5 cm. Coincident with the observation of edge fluctuation suppression, a substantial increase in edge poloidal rotation and creation of sheared plasma flow is observed on DIII-D (Rich Groebner et al.). These observations are qualitatively in agreement with recent theories of the L-H transition which predict stabilization of edge turbulence by sheared poloidal flow and/or electric field effects (Refs. 3&4).

2. A two-point current scan has been performed to determine the effect on the depth of the suppression zone. Preliminary results indicate that the suppression zone increased significantly ($\sim$ a factor of two) when plasma current was increased from 0.8 to 1.6 MA. This is important information that can be directly compared to theory. Initial comparison suggests disagreement with expectations from Shiang's theory, which, from a simplistic point of view, would indicate that the suppression zone should actually decrease. However, this conclusion requires more careful assessment of both theory and experiment before any definitive statement can be made.

3. Preliminary measurements utilizing the correlation reflectometer suggest that the radial correlation length significantly reduces during H-mode operation as compared to L-mode. This is consistent with theoretical expectations for the improved confinement H-mode plasmas. However, the existing data could possibly also be consistent with a measurement of the depth of the reflection layer, which also decreases in H-mode plasmas. In order to eliminate this possibility, data has to also be taken in Ohmic plasmas where the depth of the reflecting layer *increases* compared to L-mode but the correlation length is expected to *decrease*.

4. A variety of interesting observations have been made of ELM activity in DIII-D. In particular, various forms of precursor activity have been observed which often are seen to originate spatially inside the separatrix. These quasi-coherent fluctuations then grow spatially until they reach the separatrix where they apparently trigger an ELM.

5. Preliminary attempts have been made on DIII-D to confirm observations on TEXT of density fluctuations propagating in the ion diamagnetic drift direction in the saturated Ohmic plasma regime. Difficulties with feedback of laser radiation have caused some frequency resolution

limitations in the present scattering studies which may be preventing observation of ITGD turbulence. However, the data, to data, does not confirm the TEXT observations. Fluctuations propagating in the ion diamagnetic drift direction have been observed. However, they appear to be generally consistent with modifications to drift-wave turbulence caused by plasma rotation/electric field effects.

6. Scattering measurements during L and H-mode operation indicate rapid suppression of low frequency turbulence at the L-H transition. The k_θ spectrum appears to narrow and the frequency spectrum moves to higher frequencies. The propagation of the fluctuations becomes progressively in the ion diamagnetic drift direction. This direction is consistent with modifications in the fluctuation spectrum caused by the large, beam driven toroidal rotation which increases during H-mode. However, the modifications in the spectrum often occur too rapidly compared to the toroidal rotation alone. The effects of gradient modifications on the fluctuation spectrum are now under study as a possible explanation for the observed rapid changes. In addition, the possibility of the appearance of ITGD turbulence during H-mode is also under investigation.

II. BROADBAND X – MODE SYSTEM AND PROFILE MEASUREMENTS

A 50 to 75 GHz, X-mode, broadband reflectometer system is installed and operational on DIII-D. This system was initially intended as a dedicated profile measurement system. However, the frequency tunability of the system has also enabled us to improve our density fluctuation measurement capability, as described in detail in other sections. The system was installed in March/April 1989, and has been in regular operation since last summer. Density profiles have been obtained under a wide range of operating conditions, including Ohmic, L and H-mode operation, and good agreement has been found with profiles obtained by Thomson scattering, but only with the use of fast sweeps.

As the name implies, broadband reflectometer systems employ frequency tunable BWO sources to sweep through a range of plasma critical densities, while monitoring the phase of the returning, reflected, probe beam. The measured phase data are line integrated quantities related to the density profile through the same expression as for interferometry, so the profile can be recovered through the use of numerical inversion techniques. Such broadband reflectometer systems have been used with some success on several machines (TFR, Petula, TJ-1). However, none of these systems had to deal with H-mode or high beam power L-mode discharges, such as are frequently encountered on DIII-D, nor could they be considered routine diagnostics.

A. System Description

The system utilizes a 50 to 75 GHz, V band, BWO as source and X–mode propagation. Thus, the density coverage is dependent on the toroidal field strength; at full field (2.1 T) the density coverage is $\approx 2.3 \times 10^{18}$ to 4.0×10^{19} m^{-3} in the vicinity of the plasma edge. A schematic of the microwave circuit is shown in Fig. 1. Overmoded waveguide is used to reduce attenuation, while mode conversion at bends is minimized by the use of reduced height, de Ronde bends. A bistatic horn arrangement is used, with the beams collimated using polyethylene lenses located a focal distance from the horn throats. For ease of access, all the equipment is located outside the vacuum

vessel, so the separate transmit and receive horns view the plasma through a 35 cm diameter fused quartz window and an adjustable mirror, located on the vessel horizontal centerline. This port is shared with the 7 channel O-mode fluctuation monitoring reflectometer. The system is aligned and calibration data are obtained from a translatable mirror on the machine centerline during machine vents.

The tube can be swept full band in as little as 200 μs and, allowing for the reset time of the tube, density profiles can be measured every 2.5 ms. Currently, the minimum sweep time employed is 500 μs, due to the data rates at higher sweep speeds being beyond the bandwidth of the electronics. Fringes are measured using an automated fringe detection, timing and counting system employing a zero crossing detector and a DSP model 2904 timer/counter module. Profiles are currently obtained at seven selectable times per discharge, expandable to 132 profiles per discharge. Fluctuation data can also be obtained, simply by using the tube in CW mode, and directly digitizing the mixer output.

B. Profile Inversion

The measured data, $\phi_m(f)$, the phase of the reflected signal as a function of BWO frequency, have three components; $\phi_m = \phi_v + \phi_w + \phi_p$, where ϕ_v, ϕ_w and ϕ_p are, respectively, the contributions from the air/vacuum path length, waveguide, including dispersion, and plasma density profile. The air/vacuum and waveguide contributions are determined from an in-vessel calibration, so the desired plasma contribution can be obtained by subtraction. The $\phi_p(f)$ are line integrated quantities related to the density profile through the same expression as for interferometry, viz:

$$\phi_p(f) = 2\,k_o \int_{r_a}^{r_c(f)} \mu(r,f)dr - \pi/2$$

where k_o is the wavenumber of the probing beam, μ the plasma refractive index, and r_a and r_c are the limiter and cutoff radii, respectively. For O-mode propagation, this integral can be analytically solved for the density profile using an Abel inversion. For X-mode propagation, however, no analytic solution exists and numerical methods must be used. A numerical algorithm has been developed to invert the data which is similar in outline to that given in Ref. 1. However, it does not suffer from the numerical instability problems encountered with that work.

C. Effect of Density Fluctuations

In measuring $\phi_p(f)$, and hence profiles, the largest experimental problem is the effect of the intrinsic plasma density fluctuations. These impart a random Doppler shift to the frequency of the measured fringes and can distort or entirely mask the desired profile information. While this Doppler shift is determined by the plasma conditions and cannot be modified, its effect on the measured fringes can be minimized by utilizing the fastest possible sweep time. This can be understood as follows: If the IF frequency is low, the signal voltage will be close to zero for an appreciable time during each half period. Thus, only relatively small fluctuations are necessary in order to generate additional, spurious, zero crossings, increasing the measured phase. These spurious counts can only increase the measured phase, and their number is directly proportional to t, the sweep length. If the sweep is sufficiently fast to minimize these spurious counts, the fluctuations can still modulate the counting rate by both advancing and retarding the time of the

zero crossings. In this case, using a random walk type argument, the rms deviation from what the count would be in the absence of fluctuations is proportional to $t^{1/2}$. Therefore, the influence of both forms of phase distortion can be minimized by reducing the sweep length, while the desired profile induced phase shift, ϕ_p, is independent of t.

D. Results

Using the techniques described above, good agreement has been found with profiles obtained by Thomson scattering in Ohmic, L- and H-mode discharges under a variety of conditions. Examples of reflectometer density profiles, and comparison Thomson profiles, are shown in Fig. 2. The reflectometer profiles have not been fitted with a spline smoothing function as have the Thomson data. The error in the absolute position of the profiles is due to uncertainties in calibration values ($\pm$ 1 cm), and the existence of a modelled edge profile region. The size of the latter varies with plasma conditions and can be the dominant contribution. An example of the fringe quality during an Ohmic discharge phase is shown in Fig. 3. Fringes obtained during H-mode are similar, while those for L-mode are considerably more distorted during high beam power discharge phases.

The use of this system has been affected by changes in priority within the U.S. magnetic fusion program (the transport initiative) and within General Atomics. This resulted in a decision to make use of of the frequency tunability of the system to increase the spatial resolution of our measurements of the fluctuation suppression zone created at the plasma edge during H-mode, and also to adapt the system to function as a correlation reflectometer by the addition of a second BWO and mixers. These developments occupied the run time available after the new year, and are more fully described in their respective sections, below. Thus, very encouraging results have been obtained to date within a relatively short period of time.

During the next year, attention will return to the profile measurements, with the objective of demonstrating a reliable and routine "stand alone" profile measurement capability, necessary for CIT and ITER. For example, one problem to be addressed is the unexpected observation that the plasma VSWR can change such as to affect the measurements. During H-mode, the plasma can become a very good reflector, with signal levels comparable to those of actual mirrors. Under these conditions, a spurious second harmonic signal component can be generated due to multiple reflections, which can cause distortion unless filtered out.

III. CORRELATION REFLECTOMETER

The basic principle of correlation reflectometry is that if two co-aligned reflectometer systems operate at the same probing frequency, they should reflect from the same spatial location and see identical plasma fluctuations. Thus, the fluctuation signals from the two systems will also be identical, with a coherence between the two signals of unity. If the frequency of one source is detuned from the other, the reflecting layers will no longer be coincident and the fluctuations seen by the two probe beams will no longer be identical, by an amount depending on their correlation length, so the coherence between the signals will be reduced. Thus, by varying the frequency separation of the two sources the spatial separation of the probe beams can be varied, and the radial correlation length of the fluctuations measured directly.

In order to measure a radial profile of the correlation length, *two* frequency tunable sources are necessary. Previous correlation reflectometers (JET, ATF) have been limited in this respect as they

have employed fixed frequency sources, either Gunn's alone or a combination of Gunn's and BWO's, such that only a very limited density range could be investigated. The UCLA system by contrast, employs two frequency tunable BWO's, such that the correlation length can be measured at many different plasma densities and a profile obtained. In utilizing any microwave sources for such work, the main difficulty lies in how to compensate for, or eliminate, differential frequency jitter/drift effects. While BWO tubes can be phase locked, this is both difficult and the lock bandwidth can be small. UCLA opted instead to utilize tracking receiver techniques, which eliminates the frequency stability problem by having two mixers, one with the plasma signal plus frequency jitter, and another with jitter alone, such that when these two signals are combined, in yet another mixer, the jitter is cancelled and the desired plasma signal alone remains.

This system has worked very well in practice and preliminary data have been obtained on DIII-D. As illustrated in Fig. 4, the cross-coherence between the two signals clearly decreases with increasing probe frequency separation. Also, the cross-coherencies, and hence the correlation length, clearly decrease when the plasma transitions from L to H-mode operation. This is the first measurement to show a decrease in this quantity at the L-H transition, and is in agreement with expectations. If density fluctuations are responsible for the anomalous transport observed in tokamaks, then the correlation length should decrease with the improved transport in H-mode discharges.

In summary, a novel correlation reflectometer system has been developed which is both simpler (no phase locking) and more capable (radial profiles) than alternate systems. The system seems to work well in practice and the preliminary data have provided the first measurement showing a decrease in the correlation length at the L-H transition. Significantly more data need to be taken, with the goal of understanding the temporal evolution of the radial profile of the correlation length.

IV. O – MODE REFLECTOMETER RESULTS

Within the past year, substantial progress has been made in understanding the behaviour of edge density fluctuations within DIII-D H-mode plasmas. At all L-H transitions, high frequency ($\geq$ 50 kHz) fluctuations are dramatically suppressed in a localized region near the edge of the plasma, on a timescale of $\approx 100\mu s$. This is of direct relevance for all the theories of the L-H transition, and for the existence of a transport barrier at the plasma edge. The significance of these and other related DIII-D results have been recognized by the award of an APS invited talk on this work to UCLA. In addition, several types of ELM precursors have been regularly observed.

A. System Description

The reflectometer system normally used for fluctuation studies is an O–mode, homodyne, system utilizing 7 discrete channels at 15,24,32,40,50,60 and 75 GHz, with corresponding critical densities of 2.8×10^{18} to 7.0×10^{19} m^{-3}. Radiation from each Gunn diode source is transmitted in fundamental waveguide to the machine ($\approx$ 4m). The first four channels are combined in a compact suspended stripline multiplexer and the radiation is then transmitted and received by a single horn, with a similar arrangement for the three highest frequency channels. All the equipment is located outside the vacuum vessel for ease of access, so the monostatic horn/lens arrangement views the plasma through a 35 cm diameter fused quartz window and an adjustable mirror, located on the vessel horizontal centerline. The previously described X–mode system has also been used to obtain fluctuation data. In particular, it has been used to observe density layers lying between the discrete O–mode channels, thus markedly increasing the spatial resolution of the measurements.

B. L – H Transition

The unique ability of reflectometer systems to provide radial density fluctuation measurements with high spatial resolution (of the order of $\leq$ centimeters, localized to the critical layer, Ref. 2) is ideally suited to the study of the edge plasma modifications associated with H-mode operation. In addition, DIII-D is ideally suited for such studies since it is a major device noted for its robust H-mode operation and excellent basic plasma profile diagnostic information. Thus, while several previous scattering experiments on a variety of tokamaks have shown that the relative density fluctuation level decreases during H-mode operation, the improved spatial localization associated with reflectometry has yielded significant further information: An invariable observation with the reflectometer system at all L-H transitions is that high frequency ($\geq$50 kHz) density fluctuations are dramatically suppressed in a *localized region* near the edge of the plasma. That the suppression zone is localized to the vicinity of the separatrix is demonstrated by the fact that higher density channels, reflecting from deeper into the plasma, show no change at the transition itself. With such data, and knowledge of the density profile from the Thomson scattering and broadband reflectometer systems, the depth of the region in which the fluctuations are suppressed has been estimated. The edge fluctuation suppression zone extends from the scrapeoff layer inwards to $\approx$ 5 cm. past the separatrix, or $\approx$ 2–9 poloidal ion gyroradii. As illustrated in Fig. 5, this suppression typically occurs on a fast timescale of $\approx$ 100 μs, commencing at a time coincident with the first observable change in the D_α emission.

Recently, the X-mode system has been utilized to improve the accuracy of these estimates by probing density layers lying between the narrowband channels showing a change/nochange behaviour at the transition. In general, as the X–mode reflection layer is moved inwards, it is observed to agree in both time evolution and spectral width with successive fixed frequency channels. The data obtained using this technique are as yet limited, but detailed measurements made during a two point current scan show a linear increase in the depth of the fluctuation suppression zone with current, viz 4.5 $\pm$ 1.5 cm at 0.8 MA, and 10. $\pm$ 2.0 cm at 1.6 MA. Some of the data showing the extent of the suppression zone for a 1.6 MA discharge are displayed in Fig. 6.

Coincident with the observation of this edge fluctuation suppression zone, a substantial increase in the edge poloidal rotation and the creation of a region of sheared flow is also seen on DIII-D. The theory of Biglari et al. (Ref. 3) predicts the stabilization of edge turbulence by such sheared poloidal flow. However, it would also seem that the depth of the fluctuation suppression zone exceeds that of the region in which rotation induced shear exists. Also, the linear dependence of the zone depth on plasma current is contrary to what might be inferred from Shaing's theory of the H-mode transition (Ref. 4). Thus, while the experimental data are in rough agreement with recent L-H transition theories,[3,4] discrepancies may be emerging as more detailed measurements are made.

C. ELM Activity

The behaviour of the density fluctuations during ELM activity presents a considerably more complex picture than that for the L-H transition. This is mainly due to the wide variety encountered in the amplitude, frequency, and type of ELM. However, for all ELMs, the fluctuations are observed to return to L-mode like conditions in amplitude and width in frequency space. Again, this occurs on a fast timescale, typically $\leq$300 μs, supporting the hypothesis that an ELM is a transient reverse bifurcation to L-mode. However, in contradistinction to the L-H mode transition, precursor

fluctuations of various forms have frequently been observed *before* any observable change in the D_α emission. These precursors are observed first on inner channels and then sequentially on outer channels, indicating a spatial growth towards the plasma edge. An example of such precursors showing a clear spatial growth is shown in Fig. 7. Another observation is that the maximum time before an ELM at which precursors have been seen is proportional to the time between ELMs, suggesting that when ELMs are less frequent, the relevant plasma instability limit is simply being approached more slowly.

ELM precursors have been observed on both ideal and resistive timescales and are of two distinct types. Quasi-coherent modes of $\approx$ 30 to 120 kHz are sometimes seen on timescales ranging up to 30 ms before an ELM is triggered. The other form of precursor activity is a general rise in the overall broadband fluctuation amplitude and spectral width, again on timescales of from 100 μs to several milliseconds before the ELM. Finally, in high normalized beta (β_n) discharges, a wide spectrum of high frequency coherent modes, such as those illustrated in Fig. 8, have been observed prior to the beta collapse. These modes are entirely absent in low β_n discharges and their amplitude is observed to rise with β_n, reaching a maximum at the highest beta, $\beta_n \geq 3.5$. As with the quasi-coherent ELM precursors, these modes are also observed by outboard midplane Mirnov probes, and their identification is at present under active investigation.

V. FIR SCATTERING SYSTEM

The far infrared scattering experiment on DIII-D consists in the present first stage, of a twin frequency laser system with modest beam power but a well established heterodyne detection technique. In a second planned stage, the system will be upgraded using a backward wave oscillator [BWO], high frequency radiation source (Carcinotron), delivering up to 300 mW of power at a wavelength of approximately one millimeter. Heterodyne detection will be provided using a frequency doubled klystron as local oscillator source, with the differential frequency jitter compensated using feedforward tracking techniques.

A. Current Status of FIR Laser System

Currently, the scattering system uses a 245 GHz (λ = 1.22 mm) twin frequency laser with an output power of up to 5 mW on each of the two cavities. The output of a 130 W CO_2 laser is equally split and focused into the two far infrared lasers. The cavity producing the local oscillator radiation (LO) is usually maintained at the maximum of the gain curve, providing sufficient RF drive for at least three quasi optical mixers. An intermediate frequency (IF) of 1.25 MHz between the two laser beams is achieved by slightly detuning the probe beam cavity from the maximum gain. From the laser, which is located outside the tokamak pit area, the two beams are transmitted by two overmoded circular dielectric waveguides, over a distance of about eight meters to the tokamak entry port.

Limited vertical access on DIII-D dictates the use of a radial port for the FIR scattering where an entry port assembly provides access for the probe beam and the scattered radiation (see Fig. 9). In the equatorial plane of the tokamak, the laser probe beam is directed radially into the vessel and reflects from a special carbon tile on the centerpost of DIII-D (90% reflection at λ = 1.22 mm). The laser beam enters slightly above the midplane of the tokamak and is angled downward by 1.5° in order to isolate the probe laser cavity from modulation caused by feedback laser radiation. The originally planed horizontal alignment scheme, reflecting the probe beam perpendicular from the

tile, produced an external cavity which caused strong frequency pulling in the probe beam laser. Unacceptable IF frequency shifts were observed to be strongest during inside limited discharges and were enhanced during neutral beam injection. The use of a powerful BWO radiation source in the future, together with tracking receiver techniques is expected to overcome the present limitations resulting from the changed geometry. Gaussian beam propagation locates a beam waist $w_o = 2.8$ cm in the vicinity of the reflecting tile. Scattered light from the returning probe beam is reflected out of the machine by a large metallic mirror and through two 25 cm diameter fused quartz windows. The metallic mirror is adjustable between 32° and 40°, to optimize the observable wavenumber range.

A vertically mounted optical table (see Fig. 10), close by the machine holds the optical components for the distribution and mixing of the LO- and scattered radiation into the different receiver channels. Collection mirrors (CM) reflect a selected part of the total scattered radiation to their respective detectors. The angular positions of the collection mirrors selects the chosen wavenumber, while their lateral positions determine the spatial location of the scattering volume in the plasma. Currently, three receiver channels are available to study poloidally propagating fluctuations along the entire midplane of DIII-D in the range of $0.2 \leq k_\perp \rho_\sigma \leq 2$. The system is currently limited to wavenumbers of 2.5 - 16 cm^{-1} at the outside edge, 2 - 10 cm^{-1} at the center and 2 - 7 cm^{-1} at the inside edge because of the required misalignment described above (see Fig. 11). Simultaneous measurements of different wavenumbers and or different spatial locations can be made. The beam geometry of the system dictates a wave-number resolution of $\Delta k \approx 0.7 cm^{-1}$ and a radial spatial resolution of ±20 cm at k = 10 cm^{-1}. The propagation direction of the fluctuations is determined via the use of heterodyne detection techniques. Quasi optical biconical GaAs Schottky barrier diode mixers are used for the optical mixing of the local oscillator and the scattered light. The mixed signal is amplified and digitized at a sampling rate of 5 MHz using Le Croy Model 6810 digitizers which provide a measuring time window of 100 ms per channel.

B. Experimental Observations

1. Ohmic Measurements

Density fluctuation studies were initially made in the Ohmic regime of DIII-D plasmas. At the outside edge of the plasma (R = 220 cm), measurements show strong, narrow, frequency spectra with fluctuations up to 250 kHz, predominantly at small wavenumbers in the range of 2-5 cm^{-1}. Fluctuations extend to higher wavenumbers and higher frequencies but decrease strongly in scattered power (drop of two orders of magnitude in power from k = 2.5 - 7.5 cm^{-1}). In general, the characteristics of density fluctuations in Ohmic DIII-D plasmas are in accord with observations made on other tokamaks. Frequency range and wavenumber spectra are comparable as well as the scaling of density fluctuation level with mean density ($\tilde{n}/n \sim$ constant). However, the propagation direction of fluctuations has been found to be dependent on plasma parameters and plasma shape. In the laboratory frame of reference, measurements show fluctuations propagating in the ion and/or the electron diamagnetic drift direction. In limiter plasmas, density fluctuations propagate dominantly in the electron diamagnetic drift direction for all plasma conditions, except the locked mode which shows fluctuations propagating in the ion direction. Divertor plasmas however, show fluctuations propagating in the ion or electron direction depending on magnetic field, plasma current and density. Scattering data have been contrasted with charge exchange recombination (CER) spectroscopy measurements, which in these Ohmic plasmas utilized short beam pulses. These measurements indicate that the plasma possessed large toroidal rotation velocities with strong radial

dependence (see Fig. 12). Relative changes in the propagation direction of the fluctuations follow changes of toroidal rotation consistently in both sign and magnitude. These observations are evidence for correlation between shifts in fluctuation spectra and toroidal rotation.

Ohmic fluctuation spectra measured simultaneously with three receiver channels are shown in Fig. 12. Two channels measuring wavenumbers of 3 cm^{-1} and 6 cm^{-1}, respectively, are set up in the outside edge of the plasma (R = 220 cm) while a third channel measures fluctuations at 6 cm^{-1} at the inside edge (R = 120 cm). Spectra from the outside edge show fluctuations predominantly shifted to positive frequencies which indicate fluctuations propagating downwards in the tokamak corresponding to the ion diamagnetic drift direction. The spectrum measured at the inside edge shows its main signal shifted to negative frequencies, which indicates an upwards propagation, and hence reveals the same ion diamagnetic drift direction. These measurements, demonstrating spatial resolution at 6 cm^{-1}, were made in a low density double null divertor deuterium plasma at 2.1 T and 1 MA of plasma current.

2. Measurements during L-mode, H-mode and ELMs

The narrow long frequency fluctuation spectra measured in the Ohmic regime are typically enhanced in amplitude with injected beams. During the L-mode phase preceding the H-mode, frequency spectra are slightly shifted in the ion diamagnetic drift direction. Strong low frequency turbulence is observed at low wavenumbers (k = 2 - 5 cm^{-1}) which increases with beam power and duration of the L-mode phase. At the transition into H-mode, a significant drop of the low frequency fluctuations is observed coincident with the drop in D-α light. This is followed by a gradual rise of a high frequency component clearly shifted in the ion direction. The high frequency component evolves typically in the first 10 to 50 ms of the quiescent H-mode phase before settling to a frequency several hundred kHz on the ion side. Figure 13 shows the time evolution of density fluctuations, propagating in the electron diamagnetic drift direction a), and the ion diamagnetic drift direction b), around the L- to H-mode transition. Broadband low frequency fluctuations, propagating dominantly in the ion diamagnetic drift direction, are observed during the L-mode phase preceding the L to H transition which occurs at 2236 ms. At the transition, fluctuations are suppressed and a high frequency component grows within a few milliseconds on the ion diamagnetic drift side of the spectrum. These spectra have been measured in a single null divertor plasma with a field of 2.1 T, 1.75 MA of plasma current, a density of 6 $\times$ $10^{19}m^{-3}$ and 9 MW of co-injected deuterium beams. The apparent broadening of the frequency spectra as well as the frequency shift during the L-mode phase are in reasonable quantitative agreement with the measured increase of toroidal rotation. However, at the L to H transition and during H-mode operation, the observed frequency shift often occurs on faster time scale than the development of the measured toroidal rotation. This discrepancy remains a topic of active study. ELMs basically show very similar fluctuation characteristics to those measured in L-mode, supporting the hypothesis that ELMs present a transient return to L-mode.

C. Carcinotron Scattering

The far-infrared (FIR) collective Thomson scattering system operating on DIII-D is being upgraded by the development of a carcinotron backward wave oscillator (BWO) based scattering system. The FIR laser which is currently used suffers significantly from frequency pulling due to the special radial geometry necessary to circumvent the problem of poor access to the plasma. This geometry sends the incident beam directly back to the laser after traversing the plasma. This

radiation, though weak, can pull the frequency of the laser quite significantly, as seen in Fig. 14 which illustrates the system intermediate frequency (I.F.) as a function of time. Note the large frequency pulling which is dependent upon the optical path length through the plasma which is modified by plasma turbulence. The pulling causes a time dependent broadening of the IF and, thereby, a significant deterioration in the frequency resolution.

In order to supply more power to the incident beam and eliminate the frequency pulling problem, a millimeter wave carcinotron will be substituted for the laser. The carcinotron is tunable from 260-290 GHz producing a maximum of 320 mW. This is a factor of 60 more than that of the laser so a comparable signal-to-noise ratio improvement is expected. A frequency doubled klystron at 280.2 GHz will provide the heterodyne local oscillator for the mixers.

Heterodyne measurements require extreme frequency stability of the oscillators since the signal appears as a sideband at the IF. The signals of interest for microturbulence studies are generally less than 1 MHz, but these oscillators can drift 5-10 MHz even after warming up. Furthermore, the FM noise bandwidth of the carcinotron is greater than the expected frequency shift due to plasma fluctuations. A phase lock frequency synchronizing system used to control the klystron has eliminated the FM source noise and the long term drift, but it has had trouble keeping up with frequency pulling which can be very large and relatively fast. Thus, a wide-band phase-locked loop is currently being developed to keep up with the feedback.

Previously, a feedforward tracking circuit has been proposed and used for BWO based interferometer and scattering systems.[5] The technique was employed to remove the FM noise and frequency drift. Here, the tracking system (Fig. 15) is being used to prevent frequency pulling of the sources from degrading the heterodyne signal. The feedforward tracking system eliminates common mode frequencies seen by mixers M1 and M2 while preserving the heterodyne information of the scattered signal. Thus, it is vital that the IF from M1 and M2 reaching M4 be exactly the same. The electrical delay times through the reference and signal legs of the circuit (in dotted lines) must be within about 10 ns of each other depending on how fast the sources are modulated by the feedback. The use of delay line DL1 allows the equalization of these two delay times.

The effectiveness of the tracking system at removing phase/frequency drift and frequency pulling was tested in a laboratory scattering experiment. The plasma fluctuations are simulated by a TPX acoustic cell fabricated so as to produce a single sideband on the scattered radiation. Frequency pulling is simulated by frequency modulating the carcinotron by 5 MHz at f=20 kHz (akin to frequency pulling at MHD frequencies). With no modulation, the scattered signal is as shown in Fig. 16(a) where the heterodyne resolution is seen by a stronger upshift than downshift. Under modulation, the signal has sidebands at the modulation frequency at a level determined by the relative delay time. Figure 16(b) shows the scattered signal with frequency modulation when the delay times are optimized and when they are about 20 ns different. When optimized, the parasitic sidebands are only about 1% of the already low scattered signal. Thus, even under these extreme frequency pulling conditions, the system works well, removing phase noise, frequency drift, and wideband frequency pulling.

REFERENCES

1. H. Bottollier-Curtet, and G. Ichtchenko, Rev. Sci. Inst. **58**, 539 (1987).

2. F. Simonet, Rev. Sci. Inst. **56**, 664 (1985).

3. K.C. Shaing and E.C. Crume, Jr., Phys. Rev. Lett. **63**, 2369 (1989).

4. H. Biglari et al., Phys. Fluids **B2**, 1 (1989).

5. J.L. Doane, Rev. Sci. Inst., **51**, 317, (1980).

6. Philipona, R., Doyle, E.J., Luhmann, N.C., Jr., Peebles, W.A., Rettig, C., Burrell, K.H., Groebner, R.J., Matsumoto, H., DIII-D Group, "Microturbulence Studies on DIII-D via Far Infrared Heterodyne Scattering," Proceedings of Seventeenth European Conf. on Controlled Fusion and Plasma Heating, Amsterdam, 1604, (1990).

7. Philipona, R., Doyle, E.J., Luhmann, N.C., Jr., Peebles, W.A., Rettig, C., Burrell, K.H., Groebner, R.J., Matsumoto, H., DIII-D Group, "Far Infrared Heterodyne Scattering to Study Density Fluctuations on the DIII-D Tokamak," accepted for publication in Rev. Sci. Instr. Oct. 1990.

PUBLICATIONS AND PRESENTATIONS

Publications

K.H. Burrell, S.L. Allen, G. Bramson, N.H. Brooks, R.W. Callis, T.N. Carlstrom, M.S. Chu, A.P. Colleraine, D. Content, J.C. DeBoo, R.R. Dominquez, J.R. Ferron, R.L. Freeman, P. Gohil, C.M. Greenfield, R.J. Groebner, G. Haas, W.W. Heidbrink, D.N. Hill, F.L. Hinton, R.M. Hong, W. Howl, C.L. Hsieh, G.L. Jackson, G.L. Jahns, R.A. James, A.G. Kellman, J. Kim, L.L. Lao, E.A. Lazarus, T. Lehecka, J. Lister, J. Lohr, T.C. Luce, J.L. Luxon, M.A. Mahdavi, H. Matsumoto, M. Mayberry, C.P. Moeller, Y. Neyatani, T. Ohkawa, N. Ohyabu, T. Okazaki, T.H. Osborne, D.O. Overskei, T. Ozeki, W.A. Peebles, S. Perkins, M. Perry, P.I. Petersen, T.W. Petrie, R. Philipona, J.C. Phillips, R. Pinsker, P.A. Politzer, G.D. Porter, R. Prater, M.E. Rensink, M.J. Schaffer, D.P. Schissel, J.T. Scoville, R.P. Seraydarian, M. Shimada, T.C. Simonen, R.T. Snider, G.M. Staebler, B.W. Stallard, R.D. Stambaugh, R.D. Stav, H. St. John, R.E. Stockdale, E.J. Strait, P.L. Taylor, T.S. Taylor, P.K. Trost, U. Stroth, R.E. Waltz, S.M. Wolfe, R.D. Wood, and D. Wroblewski, "Confinement Physics of H-Mode Discharges in DIII-D," Plasma Physics and Controlled Fusion 31, 1649 (1989).

K.H. Burrell, S.L. Allen, G. Bramson, N.H. Brooks, R.W. Callis, T.N. Carlstrom, M.S. Chance, M.S. Chu, A.P. Colleraine, D. Content, J.C. DeBoo, R.R. Dominquez, S. Ejima, J.R. Ferron, R.L. Freeman, H. Fukumoto, P. Gohil, N. Gottardi, C.M. Greenfield, R.J. Groebner, G. Haas, R.W. Harvey, W.W. Heidbrink, F.J. Helton, D.N. Hill, F.L. Hinton, R.M. Hong, N. Hosogane, W. Howl, C.L. Hsieh, G.L. Jackson, G.L. Jahns, R.A. James, A.G. Kellman, J. Kim, S. Kinoshita, L.L. Lao, E.A. Lazarus, P. Lee, T. Lehecka, J. Lister, J. Lohr, P.J. Lomas, T.C. Luce, J.L. Luxon, M.A. Mahdavi, K. Matsuda, H. Matsumoto, M. Mayberry, C.P. Moeller, Y. Neyatani, T. Ohkawa, N. Ohyabu, T.H. Osborne, D.O. Overskei, T. Ozeki, W.A. Peebles, S. Perkins, M. Perry, P.I. Petersen, T.W. Petrie, R. Philipona, J.C. Phillips, R. Pinsker, P.A. Politzer, G.D. Porter, R. Prater, D.B. Remsen, M.E. Rensink, K. Sakamoto, M.J. Schaffer, D.P. Schissel, J.T. Scoville, R.P. Seraydarian, M. Shimada, T.C. Simonen, R.T. Snider, G.M. Staebler, B.W. Stallard, R.D. Stambaugh, R.D. Stav, H. St. John, R.E. Stockdale, E.J. Strait, P.L. Taylor, T.S. Taylor, P.K. Trost, A. Turnball, U. Stroth, R.E. Waltz, R.D. Wood, "Energy Confinement in Auxiliary Heated Divertor and Limiter Discharges in the DIII-D Tokamak," Plasma Physics and Controlled Nuclear Fusion Research 1988, (IAEA-CN-50/A-III-4, p. 193, Vienna, 1989).

K.H. Burrell, T.N. Carlstrom, E.J. Doyle, P. Gohil, R.J. Groebner, T. Lehecka, N.C. Luhmann, Jr., H. Matsumoto, T.H. Osborne, W.A. Peebles, and R. Philipona, "Physics of the L to H Transition in the DIII-D Tokamak," Physics of Fluids B 2, 1405 1990.

R. Philipona, E.J. Doyle, N.C. Luhmann, Jr., W.A. Peebles, C. Rettig, K.H. Burrell, R.J. Groebner, H. Matsumoto, "Far-Infrared Heterodyne Scattering to Study Fluctuations on the DIII-D Tokamak," Review of Scientific Instruments 61 1990.

E.J. Doyle, T. Lehecka, N.C. Luhmann, Jr., W.A. Peebles, R. Philipona, K.H. Burrell, R.J. Groebner, H. Matsumoto, T.H. Osborne, "Reflectometer Density Fluctuation Measurements on DIII-D," Review of Scientific Instruments 61 1990.

C.L. Rettig, S. Burns, R. Philipona, W.A. Peebles, N.C. Luhmann, Jr., "Development and Operation of a Backward Wave Oscillator Based FIR Scattering System for DIII-D," Review of Scientific Instruments 61, 1990.

Conferences

T. Lehecka, E.J. Doyle, R. Philipona, N.C. Luhmann, Jr., W.A. Peebles, C.L. Hsieh, T.N. Carlstrom, R.P. Seraydarian, and the DIII-D Group, "Results from the DIII-D Millimeter-Wave Reflectometer," Proceedings of the 16th European Conference on Controlled Fusion and Plasma Physics, Venice, Italy, March 1989, Vol. 1, p. 128.

R. Philipona, C. Rettig, E.J. Doyle, T. Lehecka, N.C. Luhmann, Jr., W.A. Peebles, UCLA, K.H. Burrell, H. Matsumoto, R. Waltz, H. Biglari, P. Diamond and the DIII-D Group, General Atomics, "Density Fluctuation Measurements on DIII-D via Far-Infrared Collective Scattering," 31st Annual Meeting APS-DPP, Anaheim, Bull. Am. Phys. Soc. 34, 2115 1989.

T. Lehecka, R. Philipona, E.J. Doyle, N.C. Luhmann, Jr., W.A. Peebles, UCLA, H. Matsumoto, E.J. Strait, T.S. Taylor, K.H. Burrell and the DIII-D Group, General Atomics, "Characterization of Density Fluctuations in DIII-D," 31st Annual Meeting APS-DPP, Anaheim, Bull. Am. Phys. Soc. 34, 2116 1989.

E.J. Doyle, T. Lehecka, S. Burns, E. Olson, N.C. Luhmann, Jr., and W.A. Peebles, UCLA and the DIII-D Group, General Atomics, "X-Mode Broadband Reflectometry Results from the DIII-D Tokamak," 31st Annual Meeting APS-DPP, Anaheim, Bull. Am. Phys. Soc. 34, 2116 1989.

H. Matsumoto, T. Lehecka, R. Philipona, E.J. Doyle, N.C. Luhmann, Jr., and W.A. Peebles, UCLA, K.H. Burrell, R.J. Groebner, H. Biglari, P. Diamond, DIII-D Group, General Atomics, "Fluctuation Studies of the L-H Transition in DIII-D," 31st Annual Meeting APS-DPP, Anaheim, Bull. Am. Phys. Soc. 34, 1939 1989.

R. Philipona, E.J. Doyle, N.C. Luhmann, Jr., W.A. Peebles, and C. Rettig, K.H. Burrell, R.J. Groebner, H. Matsumoto and the DIII-D Group, General Atomics, "Far Infrared Heterodyne Scattering Studies of Density Fluctuations on the DIII-D Tokamak," 8th Topical Conference on High Temperature Plasma Diagnostics, Hyannis, MA 1990, p. 148.

C.L. Rettig, S. Burns, R. Philipona, W.A. Peebles, N.C. Luhmann, Jr., "Development and Operation of a Backward Wave Oscillator Based FIR Scattering System for DIII-D," 8th Topical Conference on High Temperature Plasma Diagnostics, Hyannis, MA 1990, p. 150.

E.J. Doyle, T. Lehecka, N.C. Luhmann, Jr., W.A. Peebles, R. Philipona, T.L. Rhodes, K.H. Burrell, R.J. Groebner, H. Matsumoto, and the DIII-D Group, "Reflectometer Density Fluctuation Measurements on DIII-D," 8th Topical Conference on High Temperature Plasma Diagnostics, Hyannis, MA 1990, p. 152.

E.J. Doyle, T. Lehecka, N.C. Luhmann, Jr., W.A. Peebles, T.L. Rhodes, and DIII-D Group, General Atomics, "Reflectometer Density Profile Measurements on DIII-D," 8th Topical Conference on High Temperature Plasma Diagnostics, Hyannis, MA 1990, p. 88.

E.J. Doyle, T. Lehecka, N.C. Luhmann, Jr., W.A. Peebles, and R. Philipona, "Density Flucutation Measurements via Reflectometry on DIII-D During L- and H-Mode Operation," Proceedings fo the 17th European Conference on Controlled Fusion and Plasma Physics, Amsterdam, June 1990, Vol. 1, p. 203.

H. Matsumoto, K.H. Burrell, T.N. Carlstrom, E.J. Doyle, P. Gohil, R.J. Groebner, T. Lehecka, N.C. Luhmann, Jr., M.A. Mahdavi, T.H. Osborne, W.A. Peebles, and R. Philipona, "Physics of the L to H Transition in DIII-D," Proceedings of the 17th European Conference on Controlled Fusion and Plasma Physics, Amsterdam, June 1990, Vol. 1, p. 279.

E.J. Doyle, T. Lehecka, N.C. Luhmann, Jr., W.A. Peebles, and the DIII-D Group, "X-Mode Broadband Reflectometric Density Profile Measurements on DIII-D," Proceedings of the 17th European Conference on Controlled Fusion and Plasma Physics, Amsterdam, June 1990, Vol. 4, p. 1596.

R. Philipona, E.J. Doyle, N.C. Luhmann, Jr., W.A. Peebles, C. Rettig, K.H. Burrell, R.J. Groebner, H. Matsumoto, and the DIII-D Group, "Microturbulence Studies on DIII-D Via Far-Infrared Heterodyne Scattering," Proceedings of the 17th European Conference on Controlled Fusion and Plasma Physics, Amsterdam, June 1990, Vol. 4, p. 1604.

FIGURE CAPTIONS

Figure 1. Schematic showing the microwave circuit of the broadband reflectometer.

Figure 2 a,b,c. A comparison of reflectometer and Thomson profiles for Ohmic, L and H-mode Discharges, respectively. The continuous curves are spline fits to the raw Thomson data, while the dashed lines are error estimates on the fit. The reflectometer profiles are represented by the unconnected "box" symbols.

Figure 3. Measured fringes from a portion of a 500μs sweep during an Ohmic discharge phase.

Figure 4. Example showing a decrease in the measured cross-coherencies with increasing probe beam frequency, and hence spatial, separation.

Figure 5. Power Spectrum showing the suppression of density fluctuations at a typical L-H transition.

Figure 6. Ratio of the fluctuation power immediately before and after an L-H transition as a function of plasma radius for a 1.6 MA discharge.

Figure 7. Spatial growth of a quasicoherent ELM precursor (signal spreads from channel to channel).

Figure 8. Wide spectrum of coherent modes observed in a high normalized Beta discharge.

Figure 9. DIII-D section at elevation 195°, with entry port assembly for the FIR scattering system.

Figure 10. Entry port assembly and vertically mounted optical table holding the components for the receiver channels. Ray tracings indicate the role of the collecting mirrors (CM) selecting a restricted part, of the total scattered radiation, for a chosen wave number and a determined spatial location.

Figure 11. Wave number range available with the present laser based scattering system in the outside edge, center and inside edge of DIII-D plasmas.

Figure 12. Density fluctuation measurements during Ohmic discharges.

Figure 13. Time evolution of density fluctuation spectra, propagating in (a) the electron diamagnetic drift direction and (b) the ion diamagnetic drift direction, around the L-to H-mode transition.

Figure 14. Spectrum of the intermediate frequency of the twin FIR laser as a function of time. Moderately low density plasma turns on at t=2000 ms which pulls the laser frequency by 300 kHz.

Figure 15. Block diagram of feedforward IF tracking system which removes broadband FM noise, and frequency drift. Delay line DL1 must equalize propagation times through signal and reference legs within 10 ns.

Figure 16. (a) Scattered signal spectrum from the acoustic cell laboratory tests (100 kHz/div.), linear scale, signal at 167 kHz). The upper sideband is from the stronger direct acoustic wave, showing propagation direction resolution capability of heterodyne technique. (b) Scattered signal from acoustic cell with frequency modulation applied to carcinotron (100 kHz/div., 10 dB/div.). The upper trace is taken with the reference delayed by 20 ns compared to the signal. The lower trace is taken with the delay line optimized.

Broadband System Components.

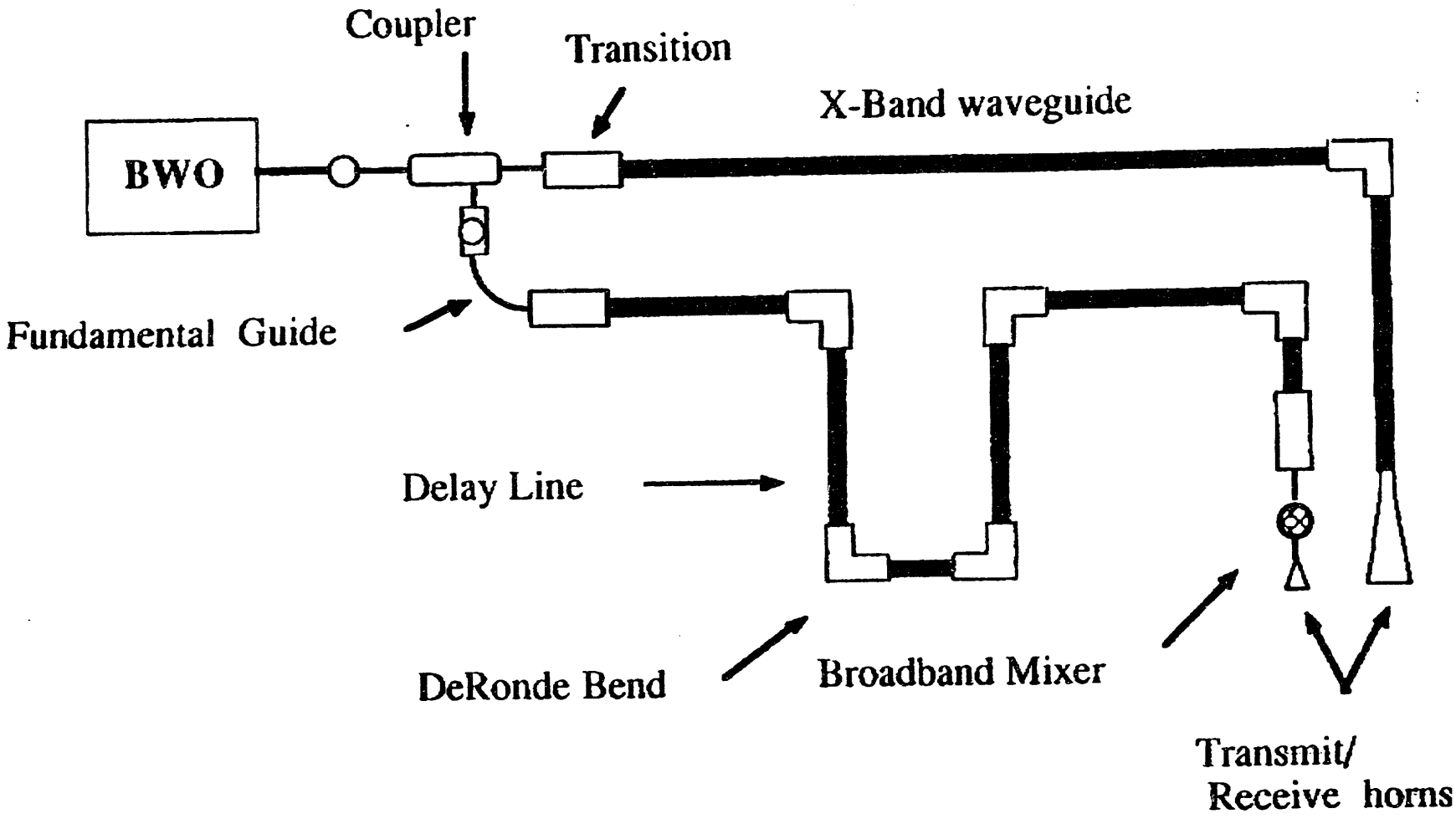

Figure 1. Schematic showing the microwave circuit of the broadband reflectometer.

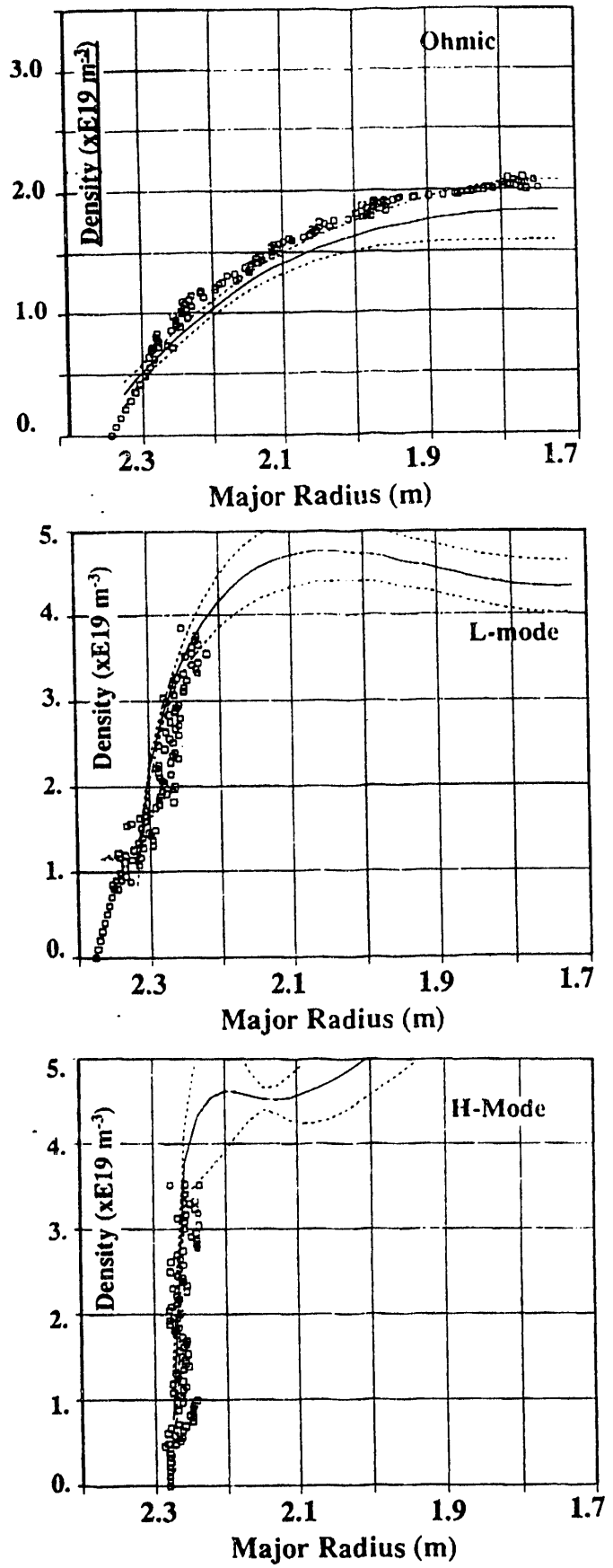

Figure 2 a,b,c. A comparison of reflectometer and Thomson profiles for Ohmic, L and H-mode Discharges, respectively. The continuous curves are spline fits to the raw Thomson data, while the dashed lines are error estimates on the fit. The reflectometer profiles are represented by the unconnected "box" symbols.

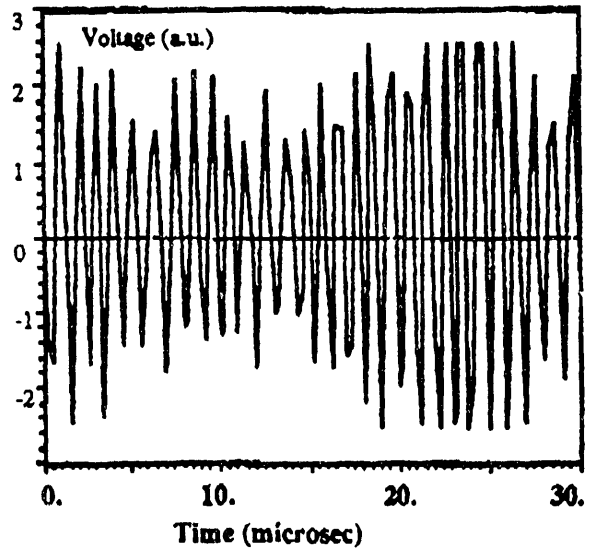

Figure 3. Measured fringes from a portion of a $500\mu s$ sweep during an Ohmic discharge phase.

Correlation Clearly Decreases with Increasing Frequency Difference

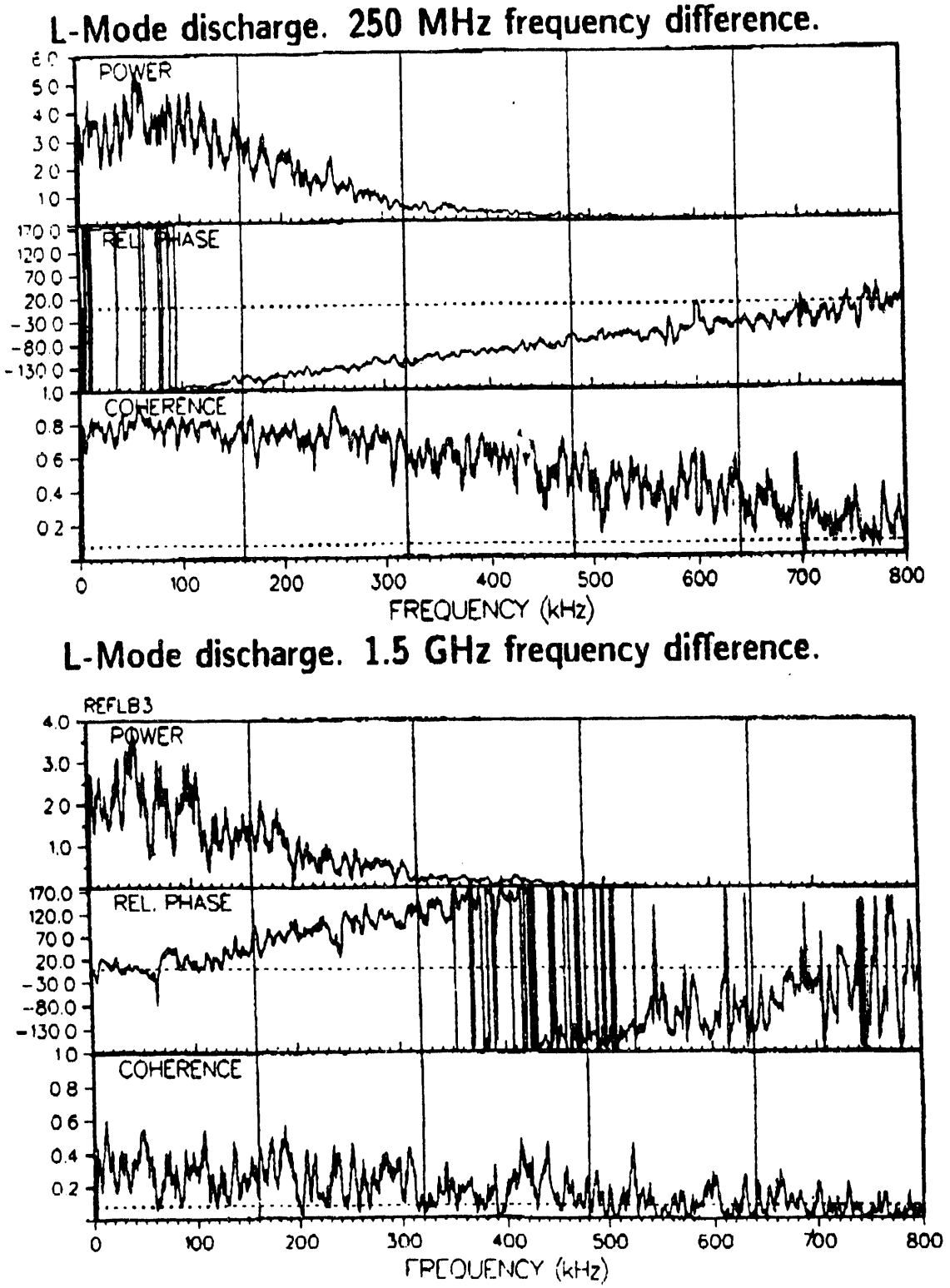

Figure 4. Example showing a decrease in the measured cross-coherencies with increasing probe beam frequency, and hence spatial, separation.

Timescale for Fluctuation Suppression at the L-H Transition

- Edge reflectometer density fluctuation signals are invariably suppressed at the L-H transition.
- Fluctuations are suppressed in $\leq 100\ \mu s$.
- Suppression occurs at a time coincident with the first drop in H_α emission.

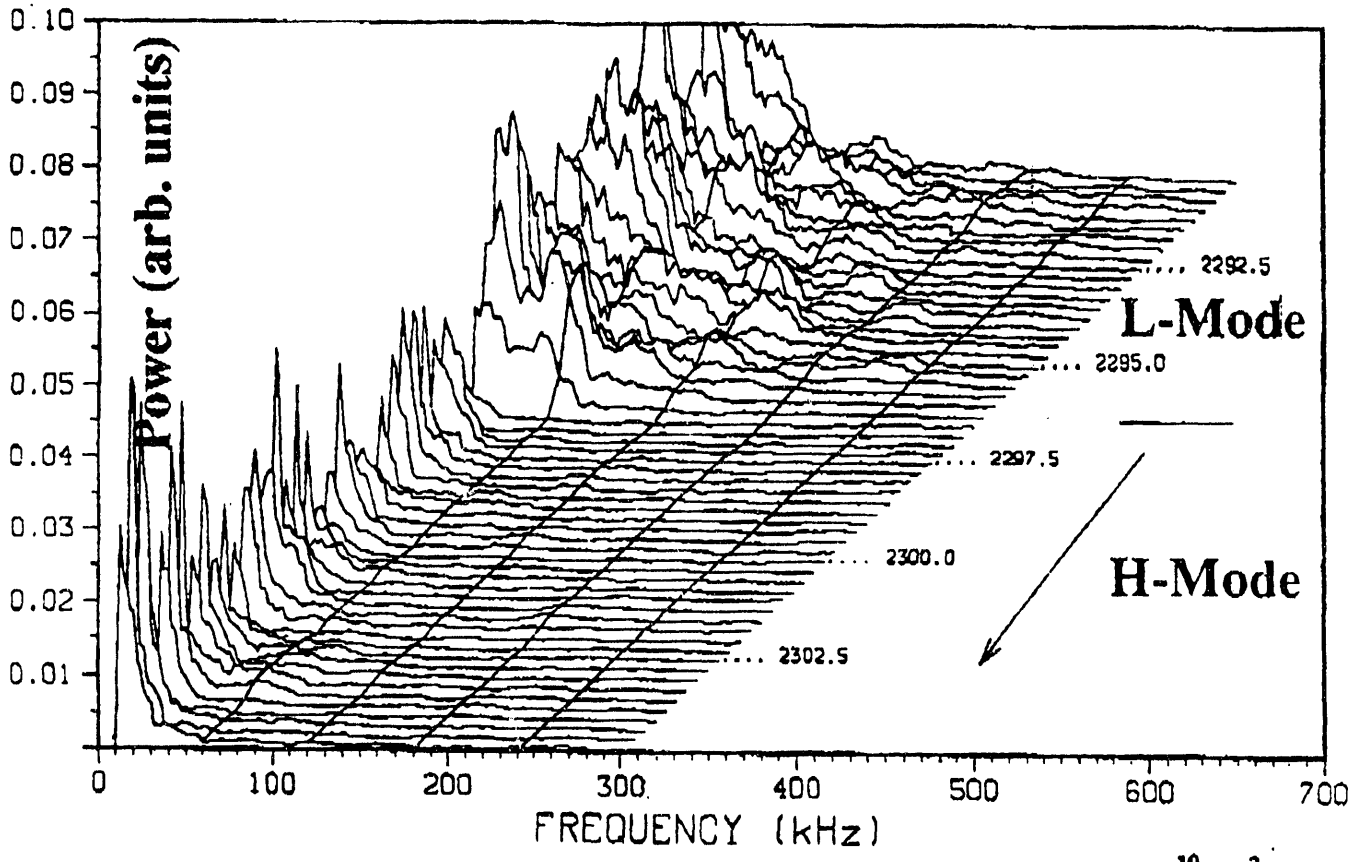

Reflectometer channel with critical density of $1.3 \times 10^{19}\ m^{-3}$

Figure 5. Power Spectrum showing the suppression of density fluctuations at a typical L-H transition.

Measured Depth of the Suppression Zone

- Plasma current 1.6 MA, 2.1 T. Depth 10. cm. Density profile and measured ratio of the fluctuations just before and after the transition. Note that the density has not yet evolved to the typical flat H-mode profile.

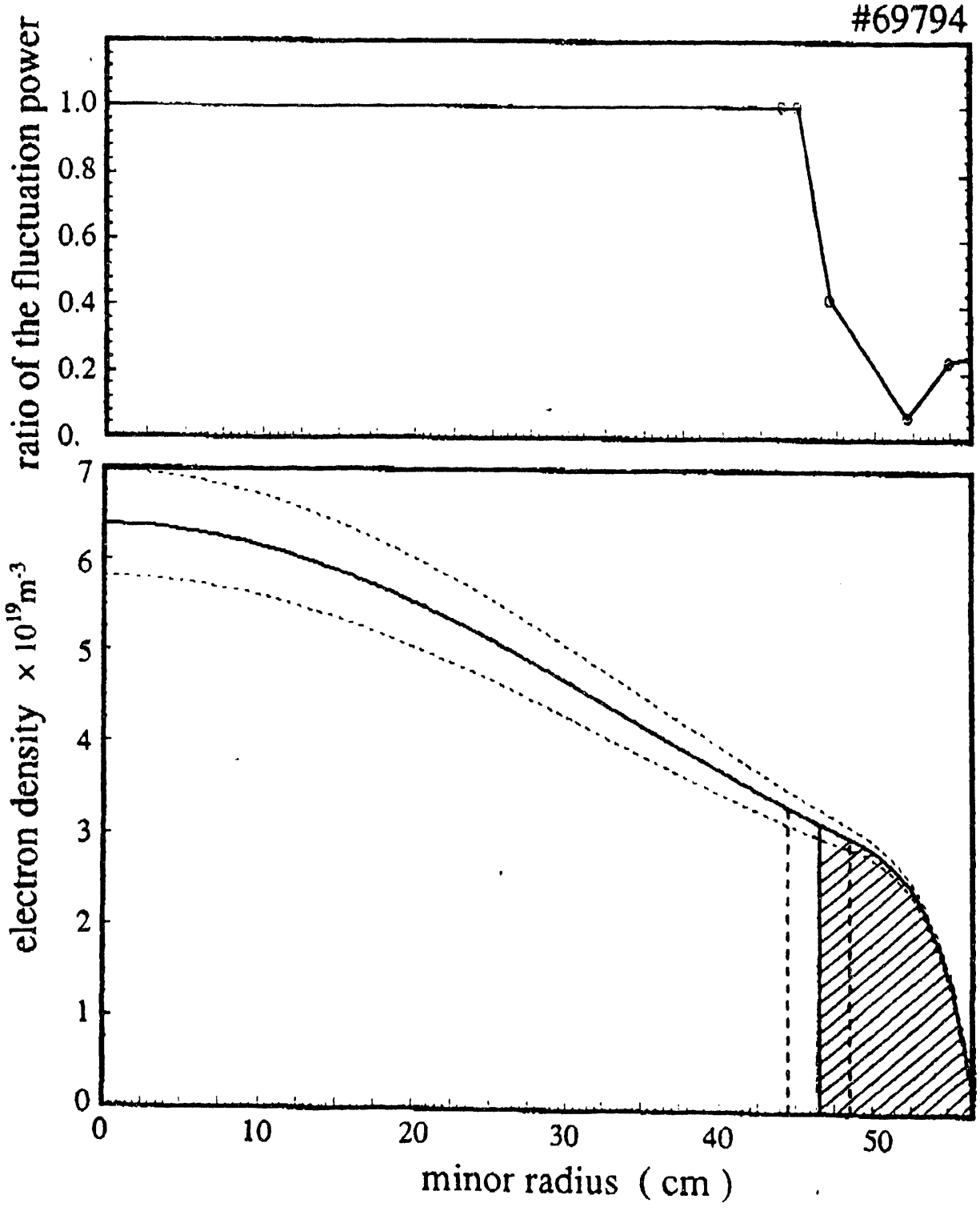

Figure 6. Ratio of the fluctuation power immediately before and after an L-H transition as a function of plasma radius for a 1.6 MA discharge.

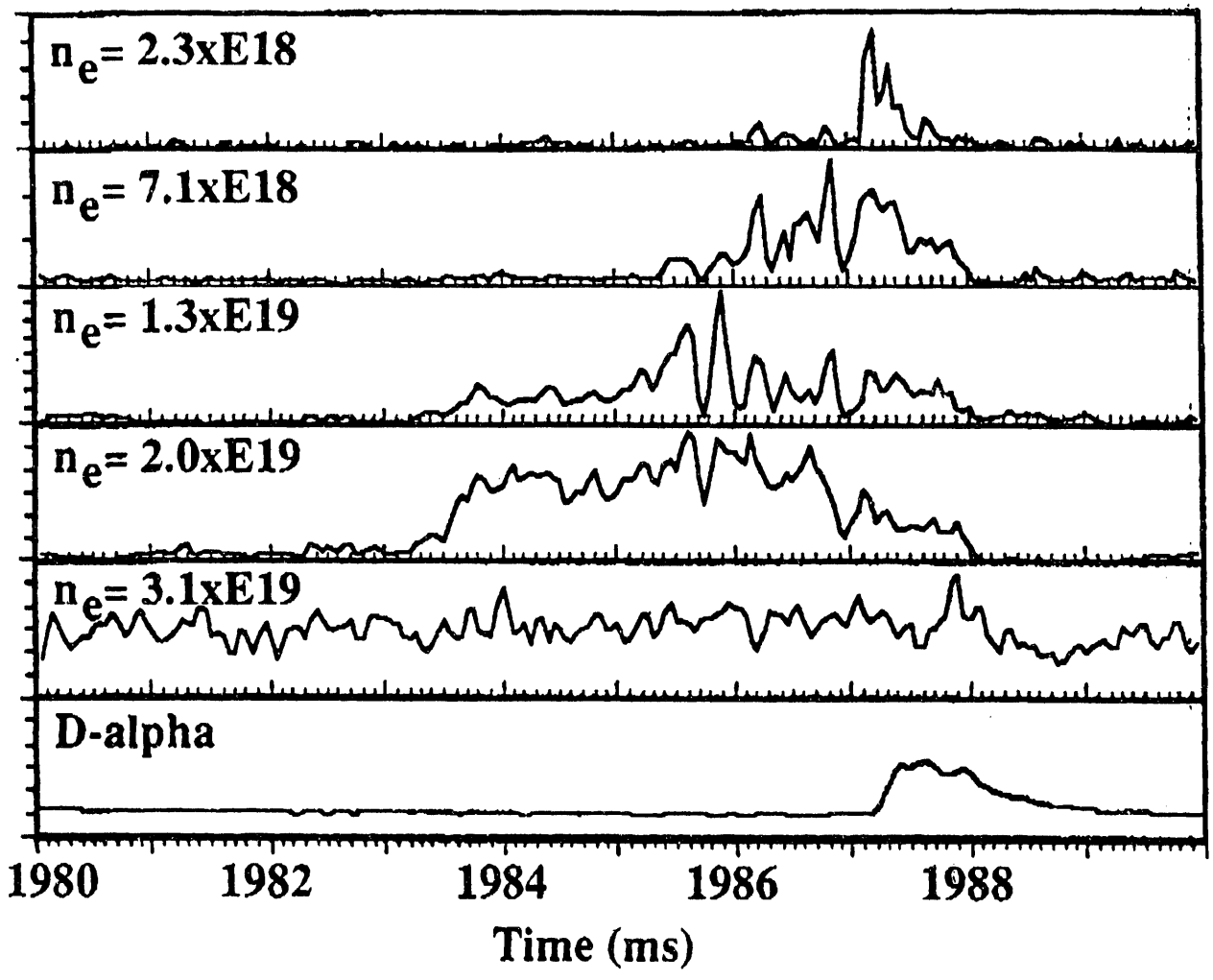

Figure 7. Spatial growth of a quasicoherent ELM precursor (signal spreads from channel to channel).

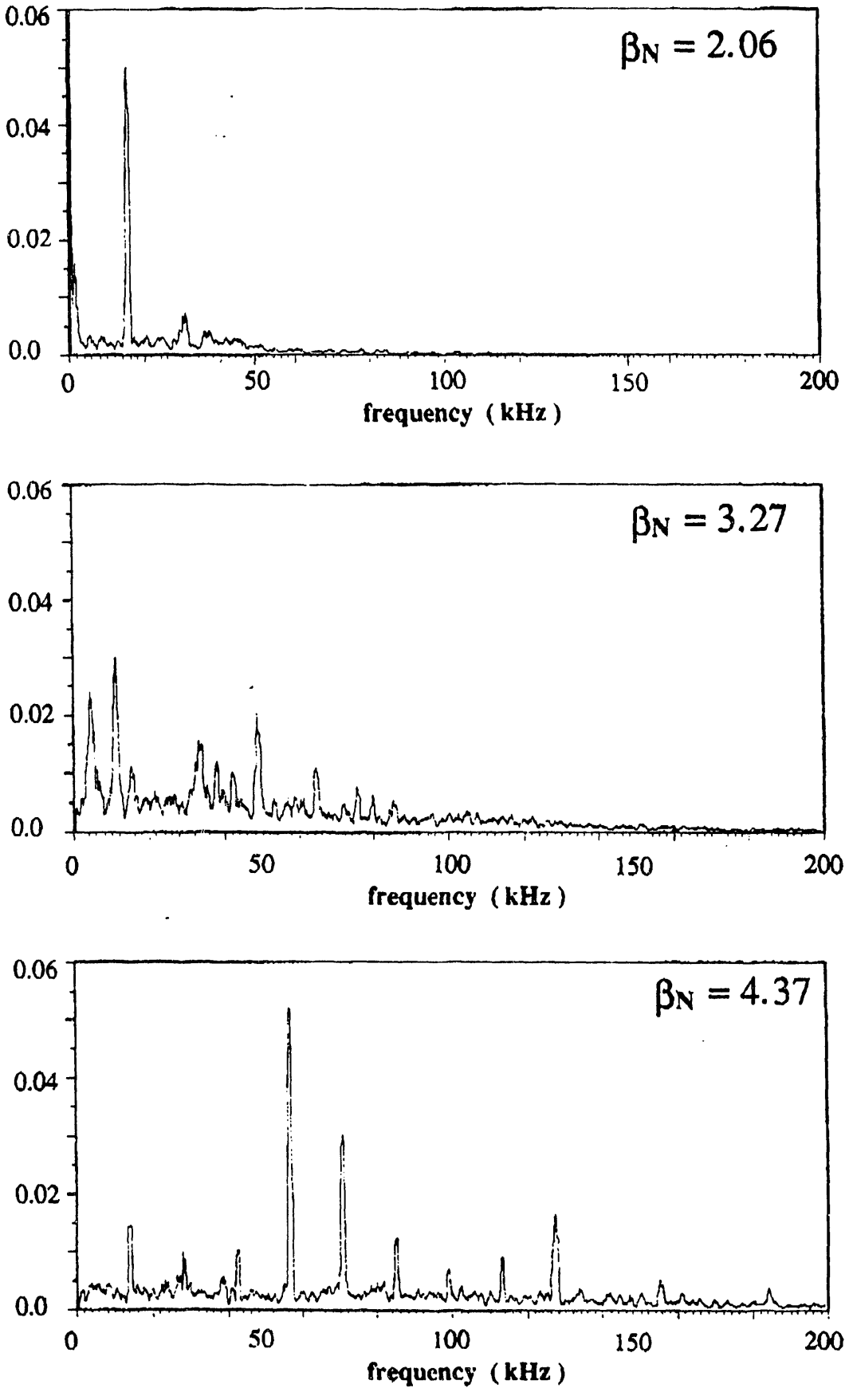

Figure 8. Wide spectrum of coherent modes observed in a high normalized Beta discharge.

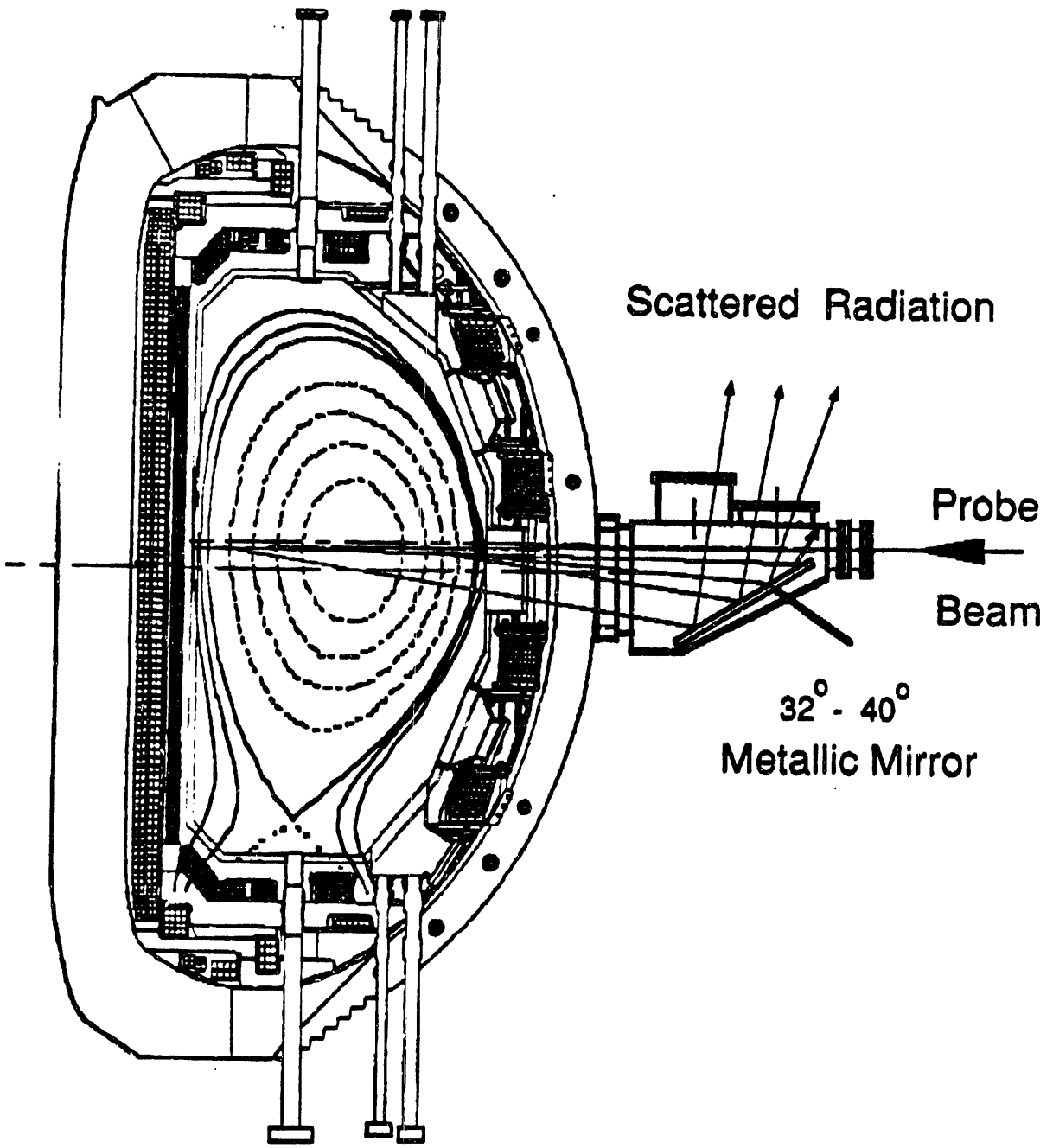

Figure 9. DIII-D section at elevation 195°, with entry port assembly for the FIR scattering system.

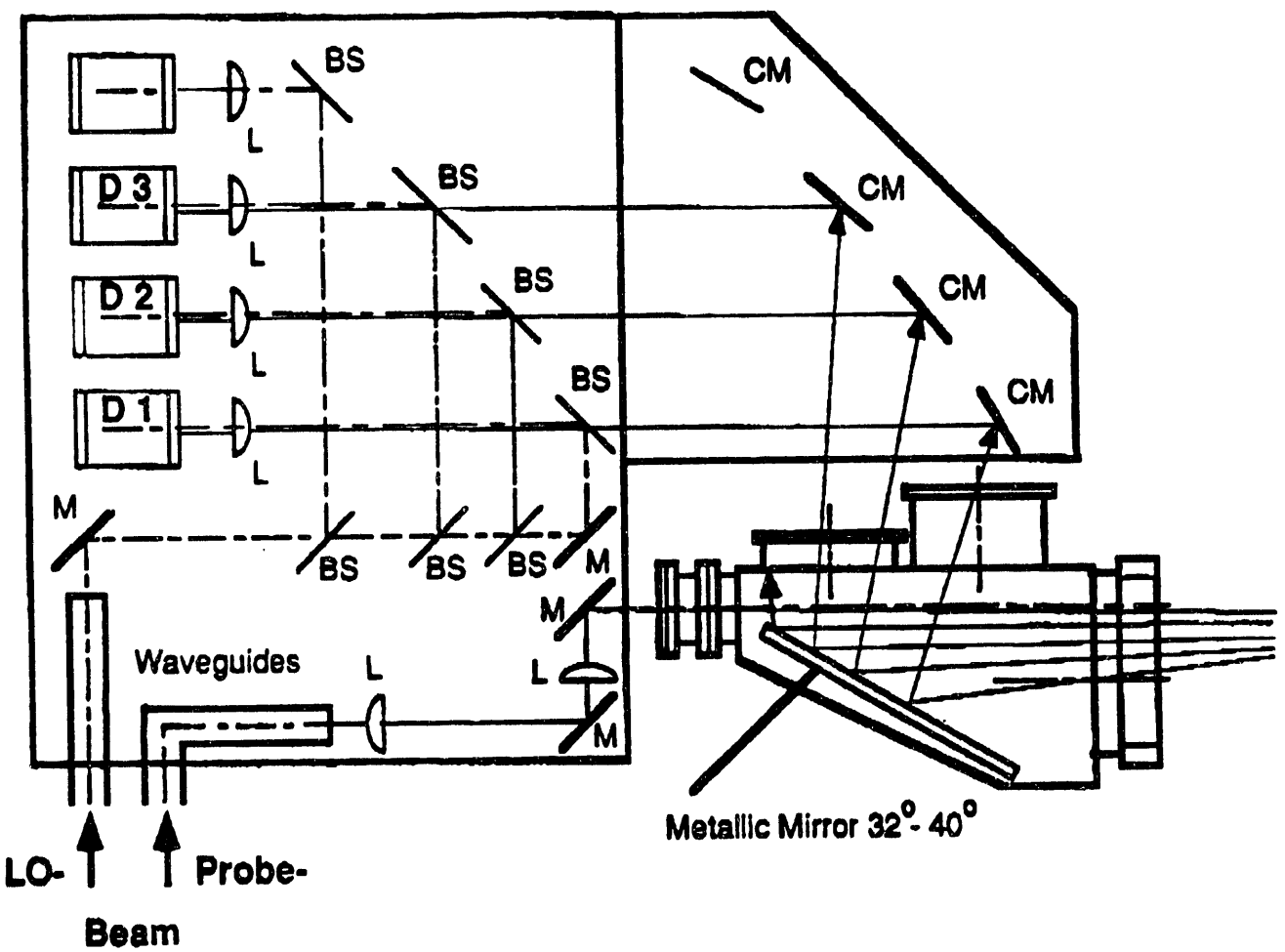

Figure 10. Entry port assembly and vertically mounted optical table holding the components for the receiver channels. Ray tracings indicate the role of the collecting mirrors (CM) selecting a restricted part, of the total scattered radiation, for a chosen wave number and a determined spatial location.

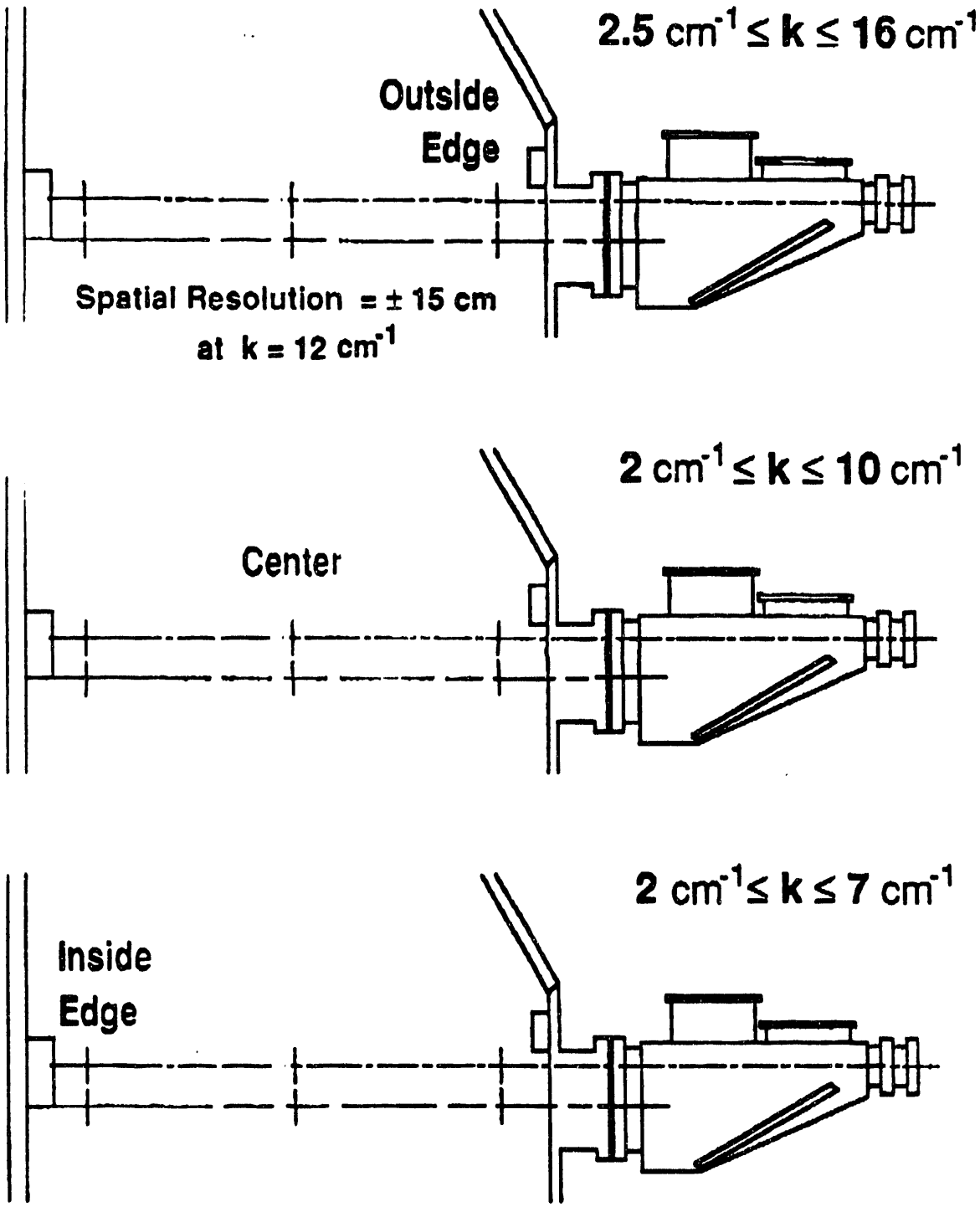

Figure 11. Wave number range available with the present laser based scattering system in the outside edge, center and inside edge of DIII-D plasmas.

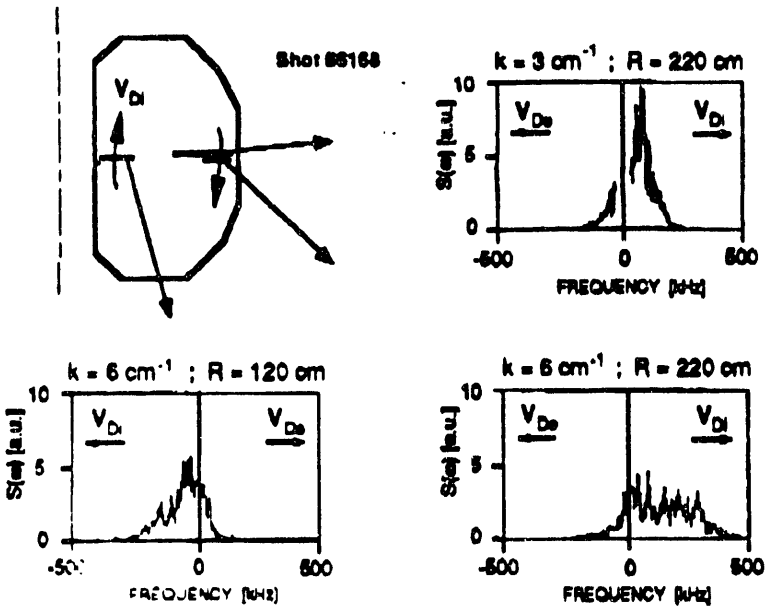

Ohmic fluctuation spectra measured simultaneously with three receiver channels to demonstrate spatial resolution at 6 cm^{-1}.

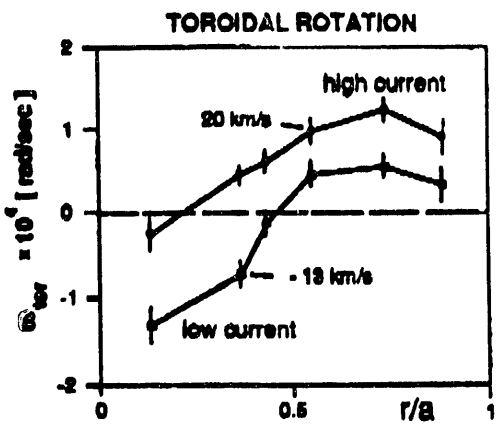

CER toroidal rotation measurements at high and low current plasmas.

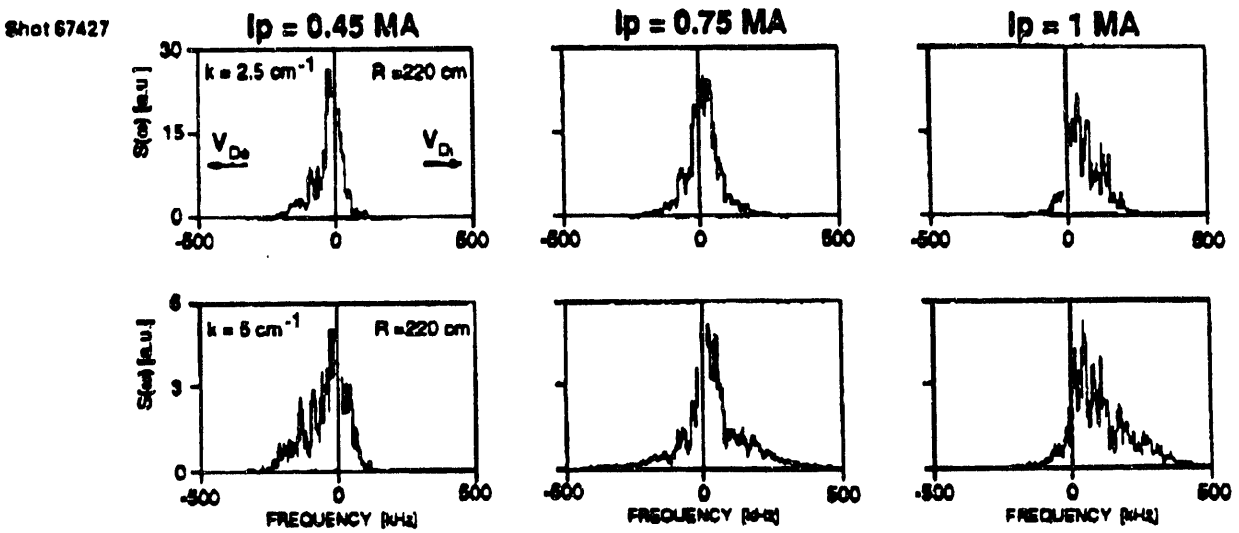

Change of propagation direction of density fluctuation during current ramp.

Figure 12. Density fluctuation measurements during Ohmic discharges.

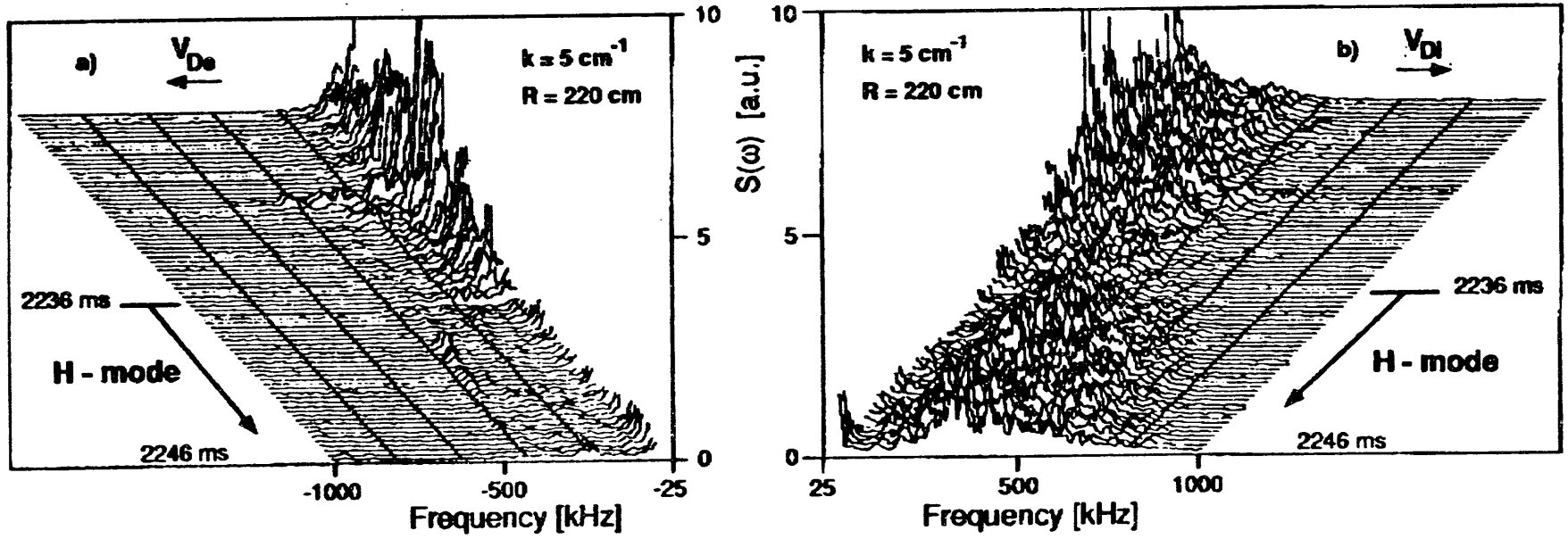

Figure 13. Time evolution of density fluctuation spectra, propagating in (a) the electron diamagnetic drift direction and (b) the ion diamagnetic drift direction, around the L-to H-mode transition.

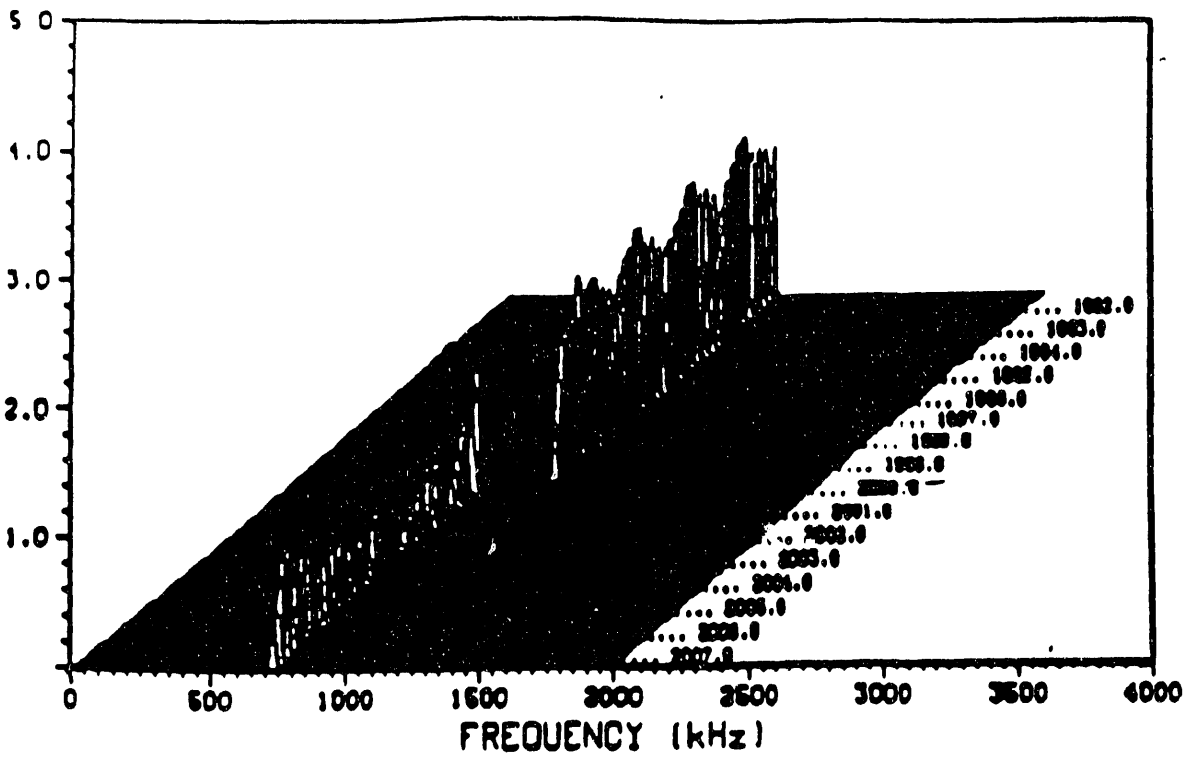

Figure 14. Spectrum of the intermediate frequency of the twin FIR laser as a function of time. Moderately low density plasma turns on at t=2000 ms which pulls the laser frequency by 300 kHz.

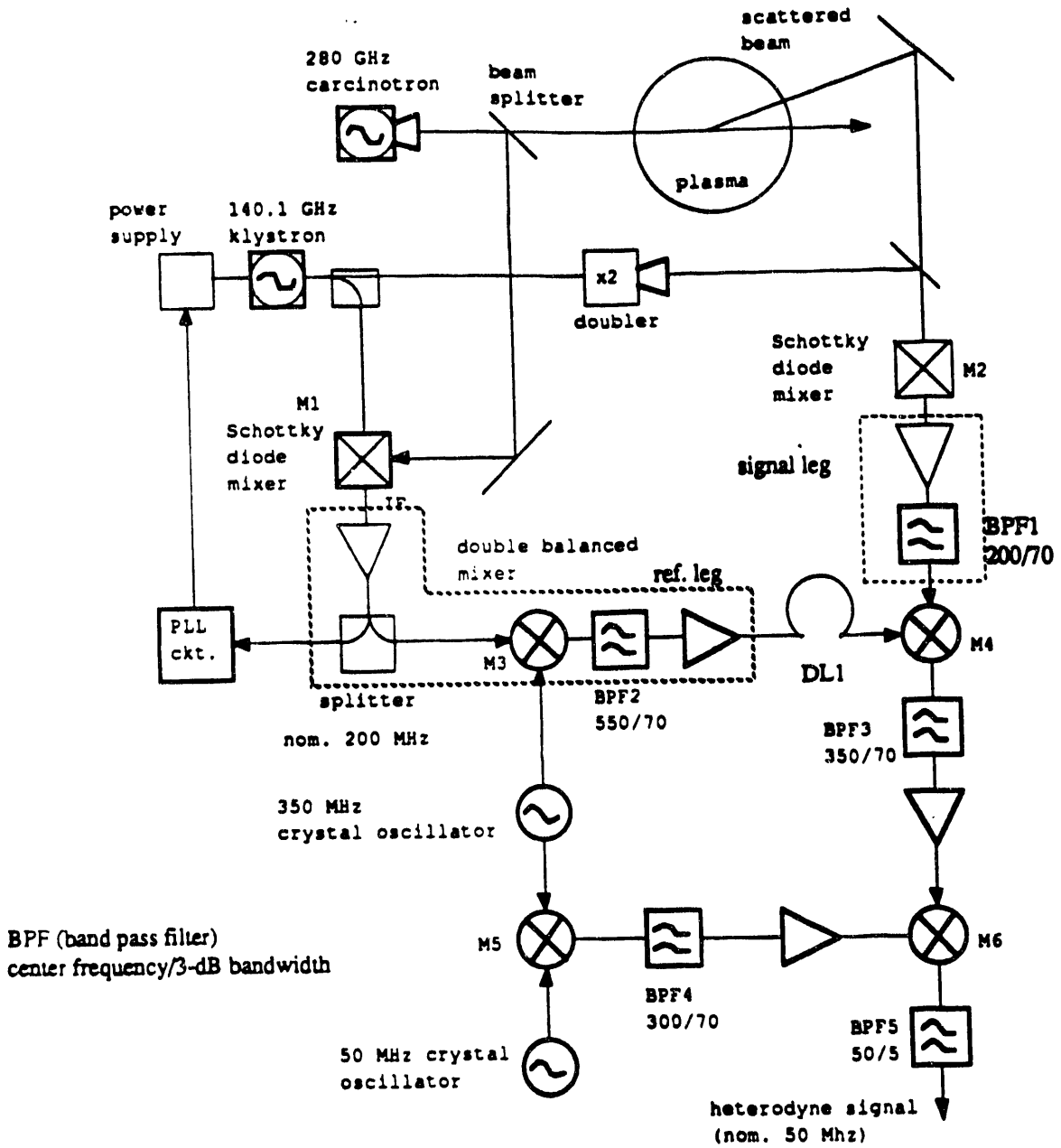

Figure 15. Block diagram of feedforward IF tracking system which removes broadband FM noise, and frequency drift. Delay line DL1 must equalize propagation times through signal and reference legs within 10 ns.

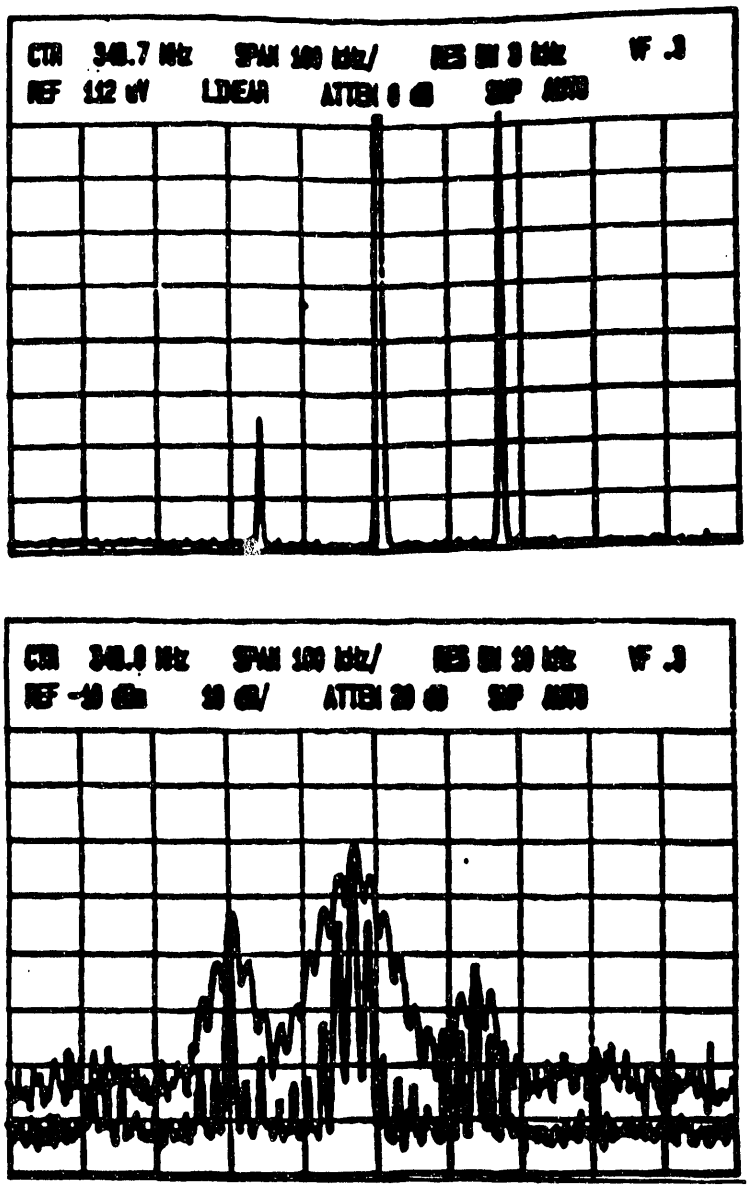

Figure 16. (a) Scattered signal spectrum from the acoustic cell laboratory tests (100 kHz/div , linear scale, signal at 167 kHz). The upper sideband is from the stronger direct acoustic wave, showing propagation direction resolution capability of heterodyne technique. (b) Scattered signal from acoustic cell with frequency modulation applied to carcinotron (100 kHz/div , 10 dB/div). The upper trace is taken with the reference delayed by 20 ns compared to the signal. The lower trace is taken with the delay line optimized.

END

DATE FILMED

12/28/92